

track-train
dynamics

Harmonic Roll Series

VOLUME **2**

70 Ton Truck Component Data
Physical Restraints
Mechanical Properties
Damping Characteristics

An International Government–Industry Research Program on Track–Train Dynamics





track-train
dynamics

Harmonic Roll Series

Volume 2

Copyright © 1974

An International Government — Industry Research Program on Track-Train Dynamics

Steering Committee for the Track Train Dynamics Project

Chairman

R. D. Spence
Vice President-Operations
Southern Pacific Transportation Company

Vice Chairman

W. J. Harris, Jr.
Vice President
Research and Test Department
Association of American Railroads

M. D. Armstrong
Chairman
Transportation Development Agency
Canadian Ministry of Transport

W. S. Autrey
Chief Engineer
Atchison, Topeka and Santa Fe Railway

D. Y. Clem
President
McConway & Torley Corporation

L. S. Crane
Executive Vice President-Operations
Southern Railway System

J. G. German
Assistant Vice President
Missouri Pacific Railroad Company

W. S. Hansen
President
A. Stucki Company

R. A. Matthews
Vice President
Railway Progress Institute

R. G. Maughan
Chairman
RAC/TDA Rail Advisory Committee

Levitte Peterson
Chief Rail Systems Division Office of
Research and Development — F.R.A.

D. V. Sartore
Chief Engineer Design
Burlington Northern Inc.

Paul Settle
President
Railway Maintenance Corporation

J. Stauffer
Director
High Speed Test Center
D.O.T.

C. Bruce Ward
President
Gunderson, Inc.

Edward J. Ward
Acting Associate Administrator for
Research and Development
F.R.A.

BACKGROUND INFORMATION
on the
TRACK-TRAIN DYNAMICS PROGRAM

The Track-Train Dynamics Program encompasses studies of the dynamic interaction of a train consist with track as affected by operating practices, terrain, and climatic conditions.

Trains cannot move without these dynamic interactions. Such interactions however, frequently manifest themselves in ways climaxing in undesirable and costly results. While often differing and sometimes necessarily so, previous efforts to reasonably control these dynamic interactions have been reflected in the operating practices of each railroad and in the design and maintenance specifications for track and equipment.

Although the matter of track-train dynamics is by no means a new phenomena, the increase in train lengths, car sizes and loadings has emphasized the need to reduce wherever possible excessive dynamic train action. This in turn requires a greater effort to achieve more control over the stability of the train as speeds have increased and railroad operations become more systematized.

The Track-Train Dynamics Program is representative of many new programs in which the railroad industry is pooling its resources for joint study and action.

A major planning effort on track-train dynamics was initiated in July 1971 by the Southern Pacific Transportation Company under contract to the AAR and carried out with AAR staff support. Completed in early 1972, this plan clearly indicated that no individual railroad had both the resources and the incentive to undertake the entire program. Therefore, AAR was authorized by its Board to proceed with the Track-Train Dynamics Program.

In the same general period, the FRA signaled its interest in vehicle dynamics by development of plans for a major test facility. The design of a track loop for train dynamic testing and the support of related research programs were also pursued by FRA.

In organizing the effort, it was recognized that a substantial body of information and competence on this problem resided in the railroad supply industry and that significant technical and financial resources were available in government.

Through the Railway Progress Institute, the supply industry coordinated its support for this program and has made available men, equipment, data from earlier proprietary studies, and monetary contributions.

Through the FRA, contractor personnel and direct financial resources have been made available.

Through the Transportation Development Agency, the Canadian Government has made a major commitment to work on this problem and to coordinate that work with the United States' effort.

Through the Office de Recherches et D'Essais, the research arm of the Union Internationale des Chemins de Fer, the basis for a full exchange of information with European groups active in this field has been arranged.

The Track-Train Dynamics Program is managed by the Research and Test Department of the Association of American Railroads under the direction of an industry-government steering committee. Railroad members were designated by elected members of the AAR's Operation-Transportation General Committee, supply industry members by the Railway Progress Institute, U. S. Government members by the Federal Railroad Administration, and Canadian Government members by the Transportation Development Agency. Appropriate task forces and advisory groups are established by the steering committee on an ad hoc basis, as necessary to pursue and resolve elements of the program.

The staff of the program comprises AAR employees, personnel contributed on a full- or part-time basis by railroads or members of the supply industry, and personnel under contract to the Federal Railroad Administration or the Transportation Development Agency.

The program plan as presented in 1972 comprised:

1) Phase I -- 1972-1974

Analysis of and interim action regarding the present dynamic aspects of track, equipment, and operations to reduce excessive train action.

2) Phase II -- 1974-1977

Development of improved track and equipment specifications and operating practices to increase dynamic stability.

3) Phase III - 1977-1982

Application of more advanced scientific principles to railroad track, equipment, and operations to improve dynamic stability.

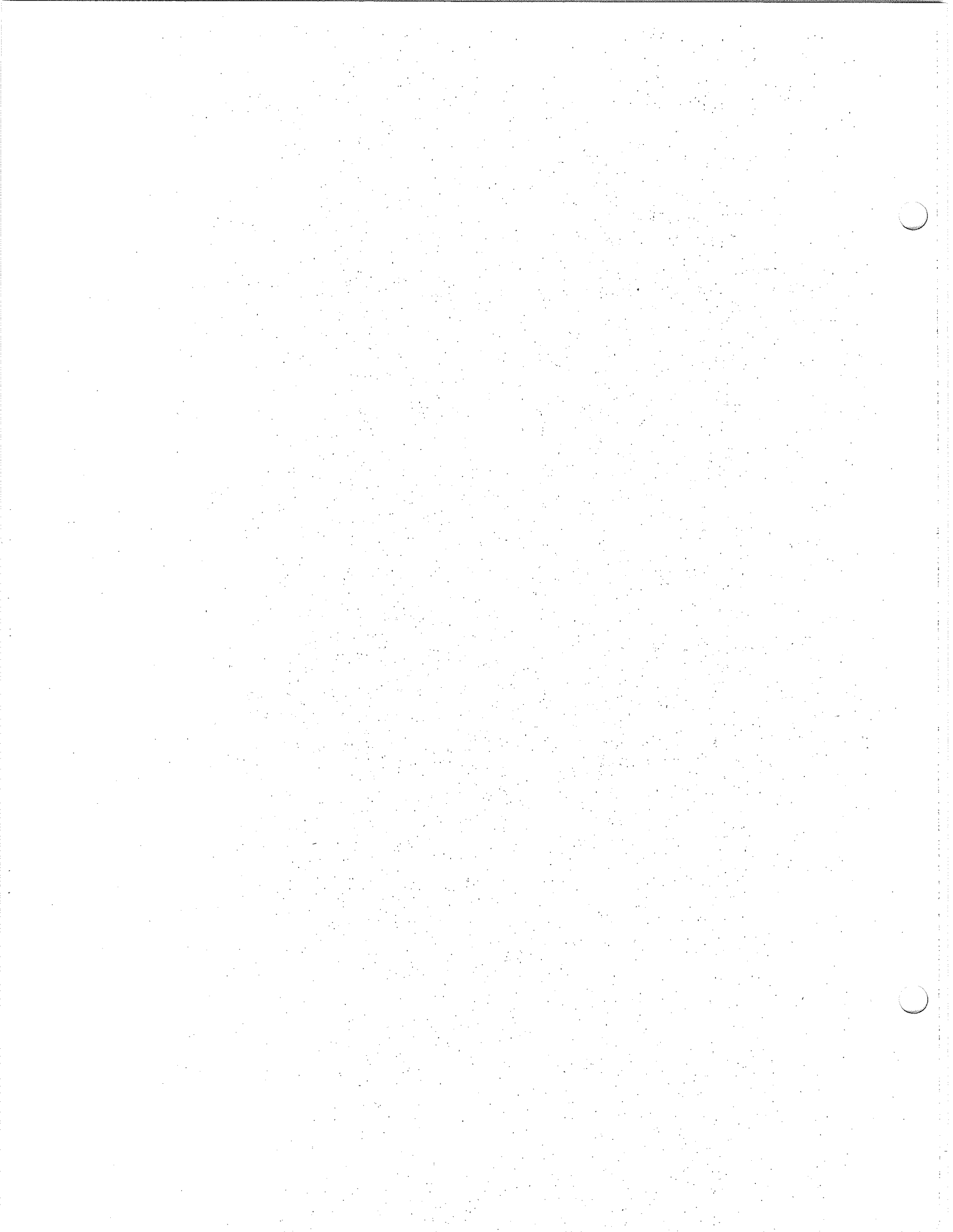
Phase I is in progress with a projected two-year budget of about \$4 million supported about 27% by FRA, 20% by RPI and its member companies, 10% by TDA, and 43% by AAR and its member railroads.

The major technical elements of Phase I include:

- a) The establishment of the dynamic characteristics of track and equipment.
- b) The development and validation of mathematical models to permit the rapid analysis of the effects on dynamic stability of modifications in design, maintenance, and use of equipment and track structures.
- c) The development of interim guidelines for train handling, makeup, track structures, and engineer training to reduce excessive train action.

The attached report presents response characteristics and physical data of the 6 x 11 Ride Control freight car truck. The report is intended to establish those parameters necessary for use in understanding the dynamic performance of the conventional three piece freight car truck related not only to the "rock and roll" problem, but to other performance problems as well.

As research on this program proceeds, reports on other elements of Phase I will be issued and existing reports updated at appropriate intervals.




ACKNOWLEDGEMENT

The following reference manual on truck component data and truck characteristics was developed as a joint effort of the Association of American Railroads, the Railway Progress Institute, the Federal Railroad Administration, and the Transportation Development Agency of Canada under the auspices of the International Government-Industry Research Program on Track-Train Dynamics. This document represents the completion of a segment of the program designated to provide insight into solving rock and roll problems.

With these thoughts in mind, the editor wishes to gratefully acknowledge American Steel Foundries who through their great generosity, provided the manpower and facilities to complete this portion of the study. In particular, Mr. Charles P. Spencer, Project Manager - Tests and Analytical, American Steel Foundries Granite City Test Engineering Dept., should be recognized for his efforts in organizing and managing the entire project. Also, Mr. Frank S. McKeown, Project Engineer, American Steel Foundries, Granite City Test Engineering Dept., should be acknowledged for his important contributions in conducting the tests and analysis.

The editor also wishes to recognize Mr. Edward F. Lind, Project Director, for his contribution to the successful completion of this manual. Finally, the editor wishes to gratefully acknowledge the Louisville and Nashville Railroad for allowing the contribution of his time to the project.



David G. Orr
Engineer - Test and Research
Louisville and Nashville
Railroad
(Task Manager - Task 13)

APPROVED:



E. F. Lind, Project Director
AAR-RPI Research Program on
Track-Train Dynamics

FOREWORD

In recent years, service demands on the railroad industry have undergone significant changes. As a result, a number of important design innovations have been introduced to the freight car fleet. The resultant has been the construction of a large number of heavy, high volume freight cars. As the utilization of this type of equipment has increased, so have the operating problems. One important problem is that of harmonic roll, most commonly referred to as "Rock and Roll."

There are several synonymous terms for harmonic roll that may be used throughout the test. They are:

Harmonic Roll - Rock and Roll
Car Rocking
Lateral Instability

In general, the rock and roll problem is related to the operation of high capacity, high center of gravity freight cars over track that has an uneven surface. The problem is most predominant on track that has surface variation due to alternately staggered joints. When operating over rough track of this nature at speeds usually between 15-25 mph, excessive carbody roll may be developed. Energy is added to the moving system with each roll cycle, and, if the car suspension does not have adequate damping, extreme carbody roll will develop, resulting in wheel lift and probable derailment.

A general solution to the rock and roll problem involves an extensive study of the entire system consisting of track, suspension, and carbody design. A study of this scope results in a better understanding of the mechanics and dynamic interactions of a freight car in its operating environment. The result can be a freight car that not only meets marketing requirements, but one that can be operated safely with minimal problems.

In order to begin investigation of track-train dynamics problems, the Southern Pacific under contract to the AAR sent a questionnaire to sixteen selected railroads in mid-1971. From the responses received, it was realized that two serious problems faced the railroads. These problems were

- (a) Rock and Roll
- (b) Sudden gage widening and rail roll-over

Keeping this in view and realizing work was needed in these areas, the planners of Phase I of the track-train dynamics research program designated Task 13, Special Projects, to

handle these areas. With respect to rock and roll, the primary objectives of Task 13 were to

- (1) Develop guidelines which could be used by individual railroads to assist them in minimizing rock and roll problems
- (2) Develop a document to be used as a reference in solving rock and roll problems
- (3) Develop a model for computer simulation of freight car dynamics
- (4) Develop characteristics of common freight car trucks and their related components
- (5) Develop a log of freight car characteristics critical in designing stable freight cars
- (6) Develop comparisons of important parameters controlling rock and roll by using existing computer simulations

By using the information developed from the primary objectives, certain secondary goals could be accomplished during Phase II of the overall research program. These goals will be to

- (1) Develop car design specifications
- (2) Develop specifications for truck design
- (3) Aid in developing laboratory procedures for evaluation of damping devices
- (4) Define the function of the freight car truck within the dynamic system as related to transfer of energy from track to carbody
- (5) Perform simulations to evaluate new car designs

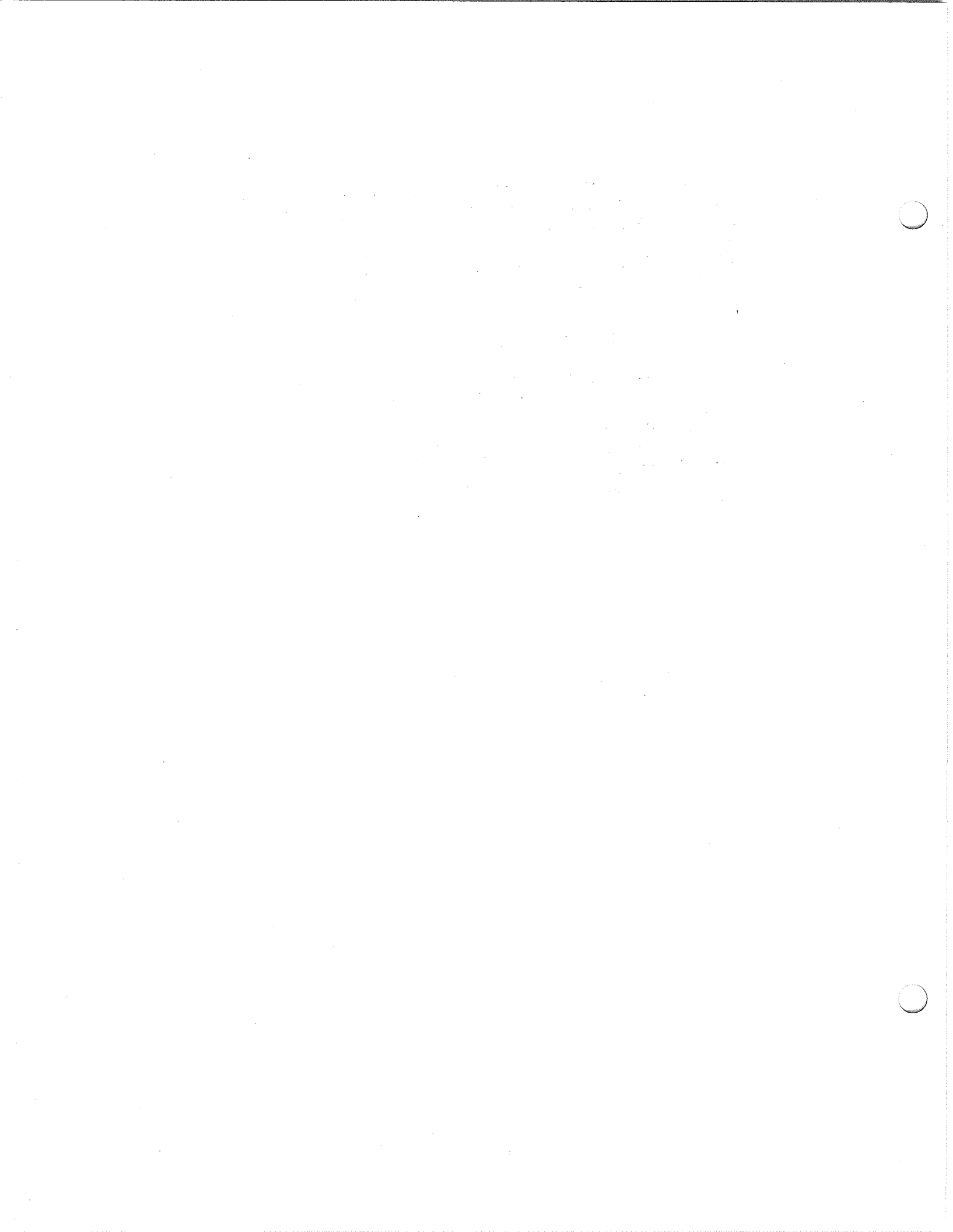
To present the findings related to the primary objectives of Task 13 outlined above, it was decided to present a series of harmonic roll related documents to the industry to be used as reference material in a similar manner as the Track-Train Dynamics Bibliography. This document, Volume II of the Harmonic Roll Series, presents important technical information on a common freight car truck. Later volumes in the Harmonic Roll Series will provide more technical information about freight car dynamics.

Report on
 American Steel Foundries Participation on
 AAR/RPI/FRA Track-Train Dynamics Program

TABLE OF CONTENTS

	Page
Foreword	ii
INTRODUCTION	1
I. FRICTIONAL DAMPING FORCES AT SIDE FRAME/TRUCK BOLSTER INTERFACE AS A FUNCTION OF DISPLACEMENT AND VELOCITY	2
Object	3
Summary	3
Test Specimens	3
Test Fixture	3
Procedure	6
Data Reduction	10
Results and Discussion	10
Vertical Damping	10
Lateral Damping	15
Vertical Damping With Imposed Lateral Force	17
Vertical Damping With Truck Out-Of-Square	19
II. VERTICAL, LATERAL, TORSIONAL AND PITCH SPRING RATES OF STANDARD TRUCK COIL GROUP	21
Object	22
Conclusions and Recommendations	22
Test Specimens	23
Test Procedure	23
Results and Discussion	30
III. DEFLECTION CHARACTERISTICS OF REPRESENTATIVE TRUCK BOLSTERS AND SIDE FRAMES, AND THE TORSIONAL RIGIDITY OF A TRUCK BOLSTER	45
Object	46
Recommendations	46
Test Specimens	46
Procedure	47
Results	52
Summary Table of Results	60
IV. TORSIONAL RESISTANCE AT A TRUCK BOLSTER/CAR BODY CENTERPLATE INTERFACE	61
Object	62
Conclusions and Recommendations	62
Test Specimens	62
Procedure and Test Fixture	62
Results and Discussion	66

	Page
V. THEORETICAL CLEARANCES AND RESULTING POSSIBLE RELATIVE MOTIONS BETWEEN TRUCK BOLSTER, SIDE FRAME AND AXLE BEARING	70
Object	71
Conclusions	71
Specimens	71
Procedure	71
Results	72
Summary Table of Results	74
VI. MASS MOMENT OF INERTIA OF SIDE FRAME (YAW AND PITCH) AND TRUCK BOLSTER (YAW AND ROCK)	87
Object	88
Recommendations	88
Test Specimens	88
Test Fixture	88
Test Procedure	89
Results	91



INTRODUCTION

The current contribution of American Steel Foundries to the AAR/RPI/FRA Track-Train Dynamics Program consists of developing the characteristics of a 70-ton Ride Control Truck.

All experimental data are a product of laboratory tests conducted in the ASF Test Engineering Department laboratory in Granite City, Ill. Total program was broken down into seven separate parts which have been reported as follows:

<u>PART NO.</u>	<u>REPORT</u>	<u>TITLE</u>
I	4-5-74	Frictional damping forces at side frame/truck bolster interface as a function of displacement and velocity.
II	3-22-74	Vertical lateral torsional and pitch spring rates of standard truck coil group.
III	2-8-74	Deflection characteristics of representative truck bolsters and side frames and the torsional rigidity of a truck bolster.
IV	2-22-74	Torsional resistance of a truck bolster/car body centerplate interface.
V	1-3-74	Theoretical clearances and resulting possible relative motions between truck bolster, side frame and axle bearing.
VI	1-4-74	Mass Moment of Inertia of side frame (yaw and pitch) and truck bolster (yaw and rock).

For the purpose of establishing investigative boundaries, the test truck was defined by the T.T.D. project as follows:

ASF A-3 Ride Control Truck
5' - 8" Wheelbase
6 x 11 Roller Bearings
33" Wheels
14" Diameter Bowl 13 3/4" Center Plate

For the purpose of establishing investigative boundaries, the test truck was defined by the T.T.D. project as follows:

ASF A-3 Ride Control Truck	Stucki Single Roller Side Bearings
5' - 8" Wheelbase	14 Outer D-5 3 11/16" travel 7791#solid
6 x 11 Roller Bearings	12 Inner D-5 3 3/4" travel 4013#solid
33" Wheels	4 Ride Control Springs 3020#Column Load
14" Diameter Bowl 13 3/4" Center Plate	AAR No. 18 Brake Beams
	H4A Composition Shoes
1 3/4" Center Pin Diameter	Approx. Wt. 8300# 5000 mls.min.wear

Test data will provide into computer-mathematical models for use in dynamic analysis of curving, hunting (also known as swivelling) and response to track irregularities. Data will be used primarily for the accomplishment of T.T.D. Tasks #8 and #13.

FRictionAL DAMPING FORCES AT SIDE FRAME/TRUCK BOLSTER
INTERFACE AS A FUNCTION OF DISPLACEMENT AND VELOCITY

Test Report - Part I

American Steel Foundries Participation In
AAR/RPI/FRA Track-Train Dynamics Program

OBJECT

Determine frictional damping forces developed by a 6" x 11" Ride Control truck bolster/friction shoe/side frame system. For a column load of 3020 lb., evaluate friction characteristics as a function of relative bolster-to-side frame motion and velocity.

SUMMARY

As is expectable from dry friction systems, damping forces were essentially independent of position and velocity of motion. Vertical and lateral damping are most easily described by statement of their average effective coefficients of friction (sliding), .5 and .37, respectively, regardless of direction of motion. Data scatter relating to these figures was relatively moderate, but specific data events were seen to be dependent on immediate history of motion. For example, vertical damping forces approached a galled surface state without combination lateral motion, and lateral damping increased quite linearly (to a maximum) with continued lateral-only input.

With imposition of steady lateral loads acting through the bolster gib/side frame column interface, vertical damping forces increased by a factor of .46 (the interface sliding coefficient of friction) times the lateral load. Vertical damping forces were seen to be negligibly effected by truck out-of-square condition except for the maximum case in which gib/column contact occurred.

TEST SPECIMENS

The following components comprised the subject damping system.

	<u>Drawing No.</u>	<u>Pattern No.</u>
1 Truck Bolster	74455-B	21732-DA
1 Side Frame	72965-H	21850-N
2 Friction Shoes	71808-P	17742
2 Outer Damping Coils	53998-H	3025
2 Inner Damping Coils	53999-G	3026

All but the bolster (which was acquired solely for the Track-Train Dynamics program) were on-hand items used in previous road test applications. The specified side frame was a substitution for the requested Patt. 21850-R side frame, but the two are identical for these test purposes.

TEST FIXTURE

Desired data were derived from application of the

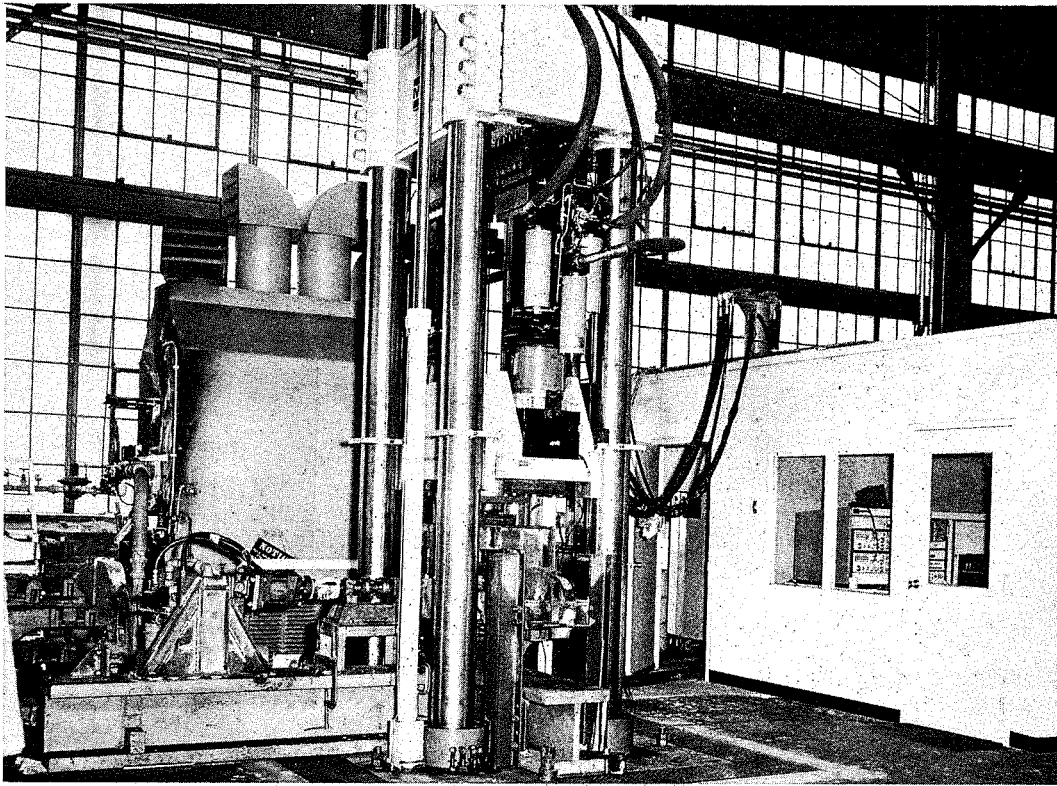


Fig. 1

TEST FIXTURE

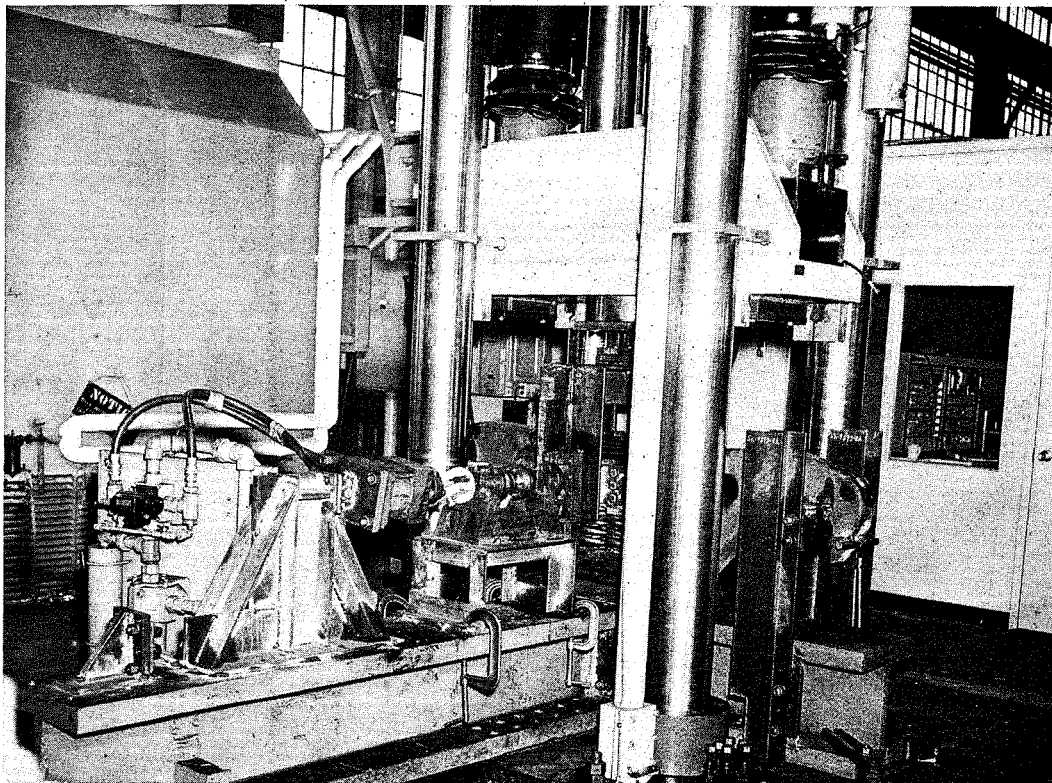


Fig. 2

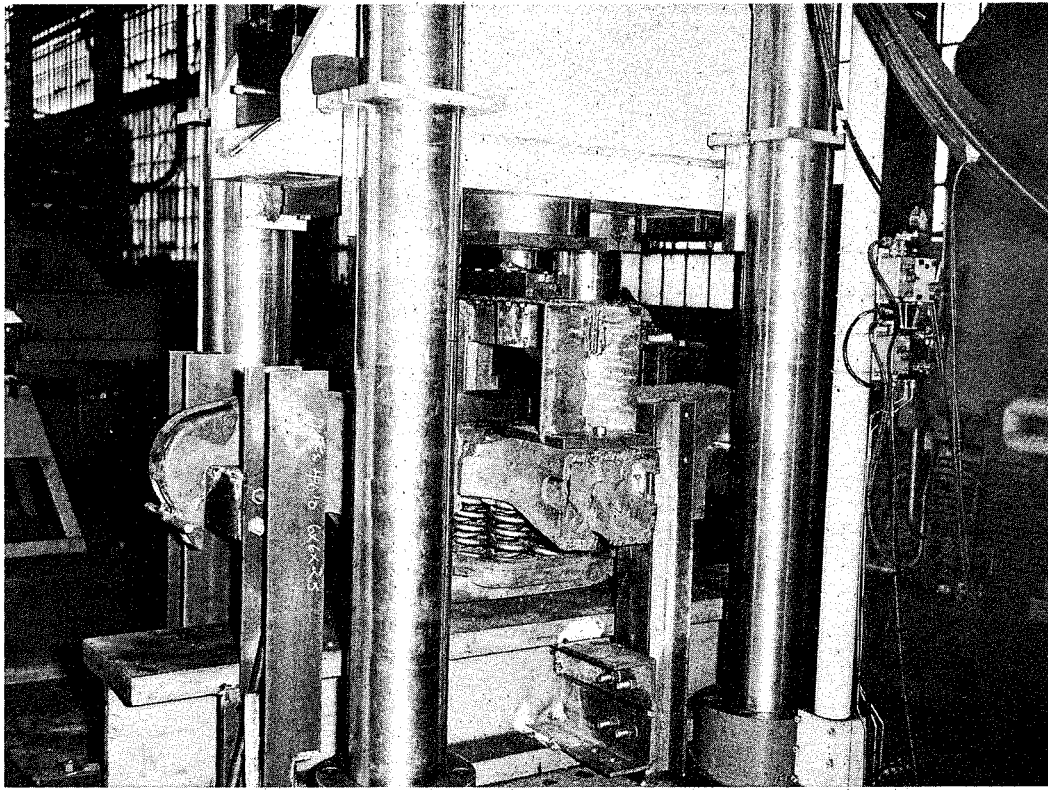


Fig. 3

TEST FIXTURE

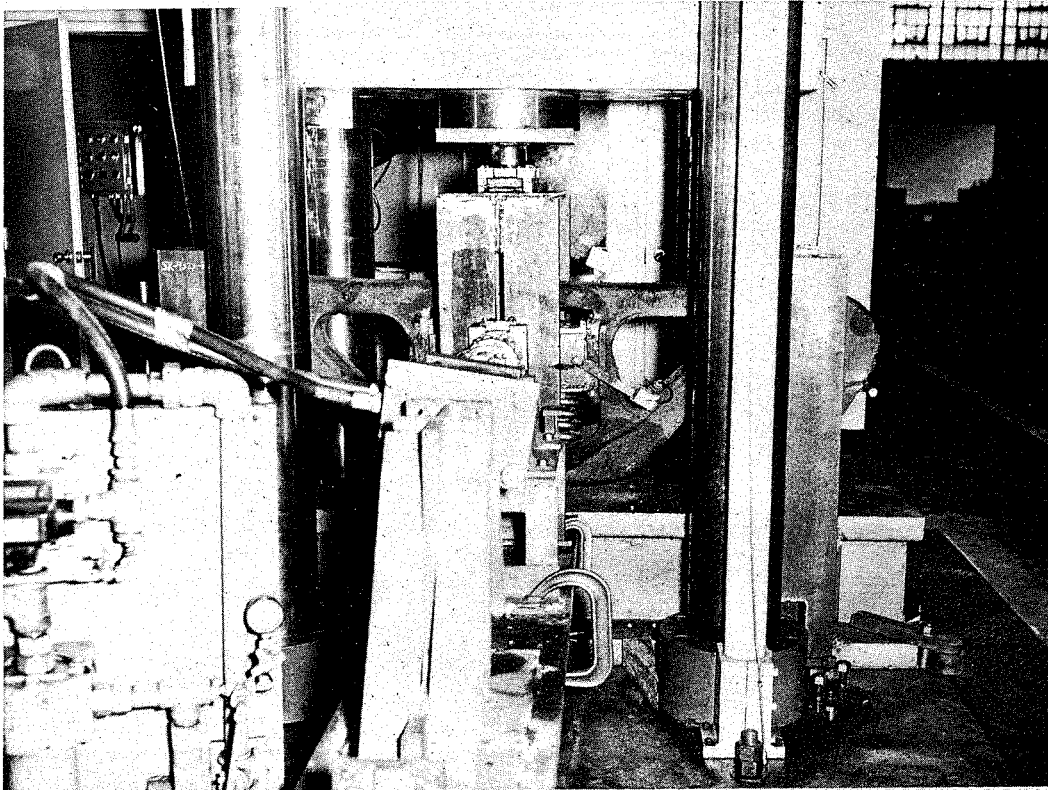


Fig. 4

specimens to the fixture illustrated by Figures 1-5. As shown, the test fixture accepted a bolster end (burned from the test specimen), the friction components and the entire side frame, which collectively represent one-half of a truck's damping system. The basic function of the apparatus was to simulate coil motion by hydraulically imparting vertical and/or lateral bolster displacements relative to the retained (welded in place) side frame. The indicated slides afford desired one or two dimensional bolster motion.

Vertical and lateral bolster movements were controlled by separate but similarly-operating electro-hydraulic closed-loop systems, which were generally programmed for sinusoidal motion for this test. Appropriate adaptations allowed use of the MTS Systems Corp'n. test machine (which is normally used for bolster fatigue testing) for controlling the vertical bolster parameters. A scratch-built system yielded necessary lateral inputs.

Data acquisition took form in oscillograph recordings of the vertical and lateral motions and loads in resistance to the motions. Force-displacement oscilloscope photographs were also taken of specific events to provide better presentations of the damping characteristics. For the vertical case the load and displacement transducers were "built-ins" of the hydraulic actuator trains. Since there were two vertical-acting actuators, the load signals were electronically summed and the motion signals averaged for application to the oscillograph. The single load cell and displacement beam transducer signals were applied directly for the lateral case. Figure 6 presents an example of an oscillograph recording in illustration of the four monitored signals.

PROCEDURE

Since the tests were to simulate service damping conditions, wear-in of the specimen components was necessary. This involved imparting roughly 25,000 cycles each of vertical and lateral bolster motion over the range of positions slated for use during the data events. The side frame column friction plates had been renewed prior to wear-in, but the described cyclic inputs generated roughly 80% friction shoe/plate bearing and the red powder associated with the components' wear. Post wear-in column load was set at 3020 lb. through appropriate damping coil shimming (accurate to within \pm 25 lb.). One final point concerns use of load coils during the wear-in (as illustrated in the set-up photographs) to help return the bolster to the upper position of a cycle. While this helped relieve strain of the lateral slide for the extended wear-in period, load springs were not used for the actual test events.

The test itself was divided into four basic phases, but the general procedure was similar for all. That is, various displacements and frequencies were used within definition of the basic phase to satisfy the objective of determining the friction characteristics as a function of displacement and velocity. A given test event consisted of a reasonable number of motion cycles with a specific peak-to-peak displacement and cyclic frequency. Within limitations of the test apparatus, the amplitude and frequency variations were directed toward encompassing typical service phenomenon. Taken individually, the four phases were:

1. Vertical Damping

As the name implies, the subject phase involved only frictional forces generated by vertical bolster movements. With a center position corresponding to a load coil spring height of 8-1/4" (chosen because it is a rough median to the range of possible coil heights), vertical bolster displacements were varied in even increments from 1/4" to 3.0" peak-to-peak, each displacement having been used in conjunction with a frequency range of "very slow" (down to .1 hz) to the maximum capable from the hydraulic actuating system for the amplitude involved (up to 3.0 hz). A lateral movement of 1/8" @ 1 hz. was combined with the vertical motion to prevent galling of the shoe or friction plate surfaces, but this lateral input was removed for oscillograph recording of the vertical events.

2. Lateral Damping

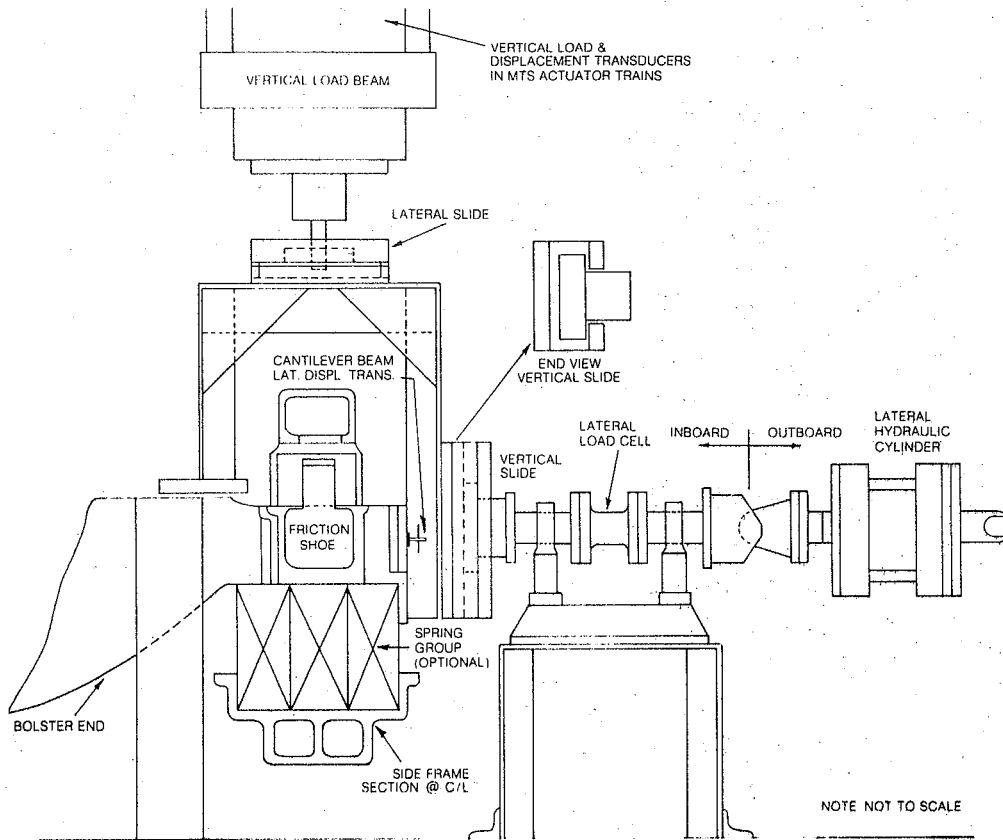
A sequel to the vertical damping test, the subject phase used lateral inputs ranging from 1/8" to 1/2" peak-to-peak at frequencies from .25 to 3.0 hz. The side frame columns centered within the bolster gibs served as the center of the lateral movements. Similar to the previous phase, a vertical motion (.5" peak-peak @ .25 hz) was added to the lateral during event set-up, but was removed for lateral event recording.

3. Vertical Damping With Superimposed Constant Lateral Force

The subject phase was conducted to test for the increased frictional effect of bolster gib side/frame column contact during vertical motions. The lateral cylinder (under load control) was used to apply steady lateral loads against the side frame while the vertical motions were imparted in the usual manner. Lateral loads were varied from zero to

Fig. 5

FRICITIONAL DAMPING TEST FIXTURE



30,000 lb. in 5,000 lb. increments and vertical motions of .5" @ .5 Hz, 1.0" @ .5 Hz and 2" @ .2 Hz were used for each of the lateral loads.

4. Vertical Damping With Truck Out-Of-Square

This final test phase simulated the rail conditions, self-explanatory in its title, by pivoting the side frame with respect to its center in a yaw motion. The angular position was maintained by welding the side frame at the pedestal supports and the bolster was laterally centered in its usual "square position" and maintained by appropriate cylinder input and the stop illustrated in the photographs. With the bolster and side frame positioned as described, vertical bolster motions were induced with variation of stroke amplitude and frequency similar to that of the phase 3 test.

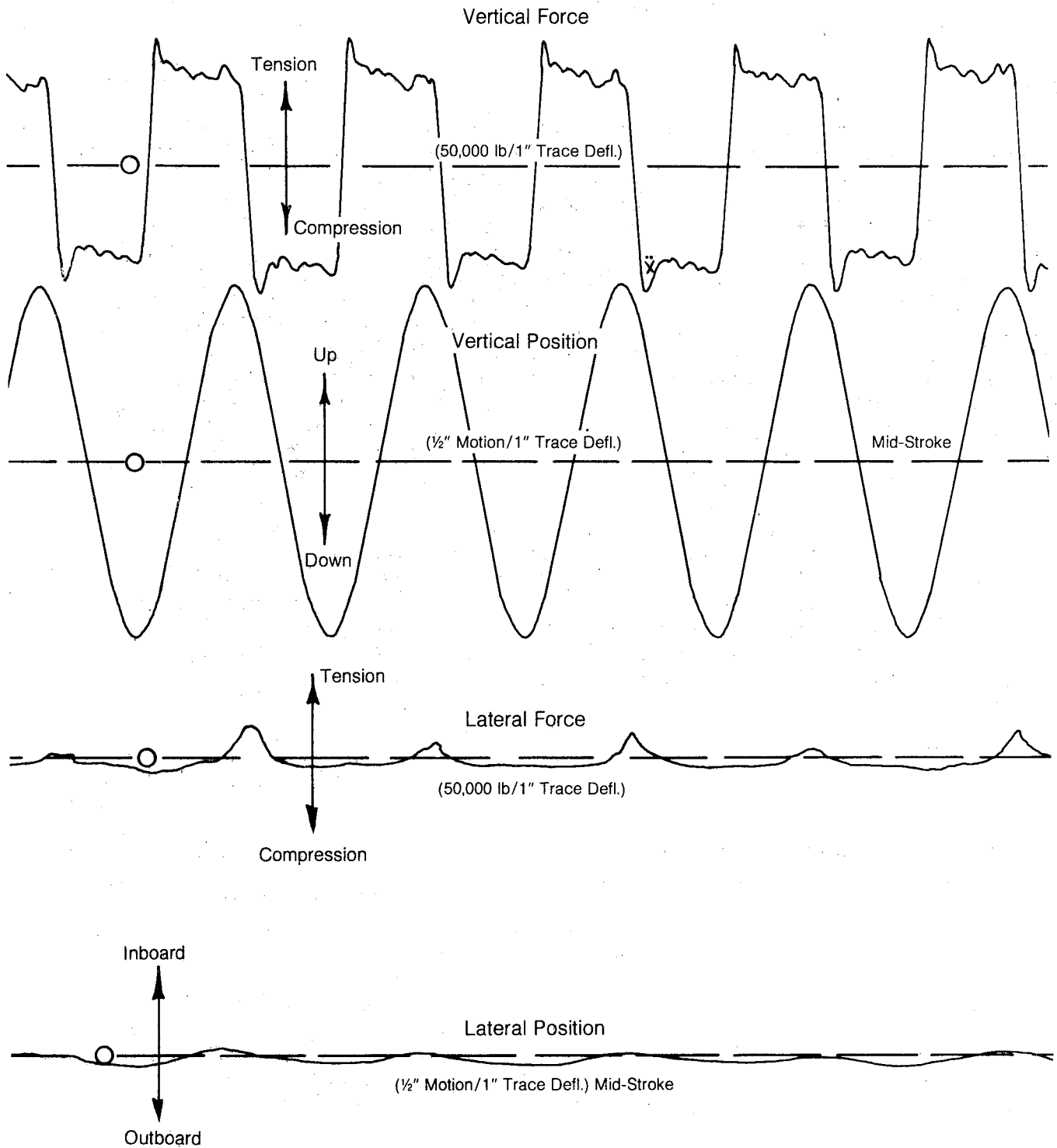
Two angular side frame positions were tested in addition to the standard square orientation. The first was attained

Fig. 6
OSCILLOGRAPH RECORDING

PART I TTD PROGRAM

FRICITIONAL DAMPING FORCES

R.C. 3020 Col. Ld.



PHASE 1, VERTICAL DAMPING EVENT

by manually yawing the bolster until physical interaction, such as gib/column contact, would permit no more. This resulted in a yaw motion approximately 1.5 degrees. The second position was achieved by simply reducing the first by .5 deg. to yield a one degree out-of-square condition. This smaller yawed position did not involve any direct bolster/side frame contact.

DATA REDUCTION

Data procurement generally consisted of straightforward measurement of the oscillograph traces at appropriate locations, yet certain data corrections were required to account for signal error induced by the apparatus slide friction and inertia effect of the moved bolster assembly. Slide friction was simply subtracted from the measured loads based on pre-test, calibration with the friction shoes pinned. Inertial forces, however, presented a more complex problem. Calculations disclosed that for the lateral and lower frequency/lower amplitude vertical motions, inertial force bias in the load signals was negligible and was treated as such. The inertial forces of the more rigorous vertical movements were significant though (up to roughly 10% of the damping force), but the motion variant load, being unlike the constant slide friction error, essentially prescribed its own correction by permitting load reading at motion midstroke, the point at which inertia effects are zero. While this worked satisfactorily for analysis of sliding friction forces, derivation of break-away (static) friction loads was hindered by its roughly simultaneous presence with the peak of the inertial load at the start of a stroke motion. For this reason, break-away study was directed primarily to those amplitude/frequency combinations for which inertial forces were negligible.

RESULTS AND DISCUSSION

1. Vertical Damping

Figures 7 and 8 initiate the subject discussion since they best illustrate the general damping characteristics associated with this test phase. Comparison of the two force/displacement oscilloscope photographs leads to the fact that the load magnitudes are roughly equal.

Since the two cases represent different amplitude/frequency combinations, it follows that vertical damping force is independent of both amplitude and velocity. Although in light of known friction laws the stated independence is not surprising, establishment at this point simplifies

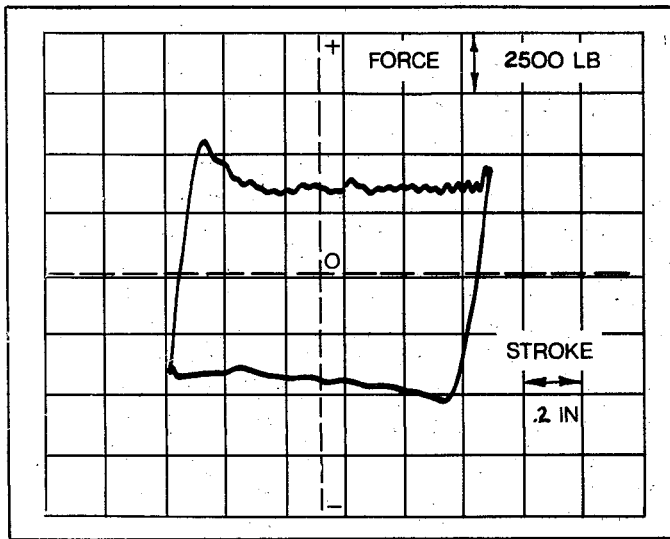


Fig. 7
 Vertical Damping Cycle
 1.0" PK-PK Stroke
 @ .25 Hz
 7400 In-Lb
 Energy Dissipation Per Cycle

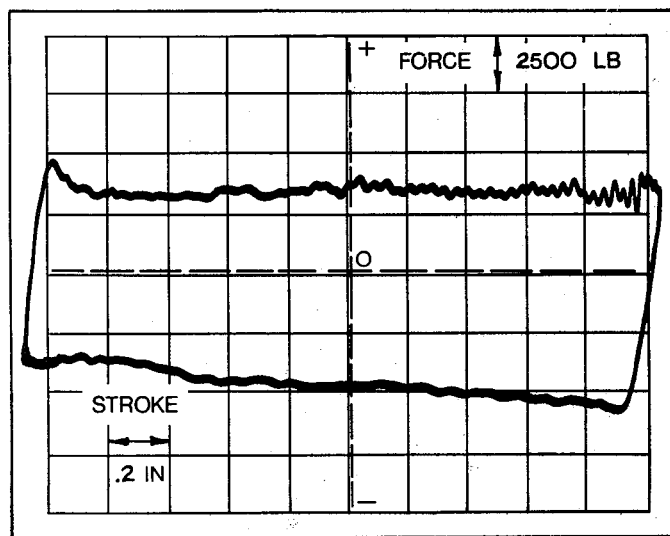
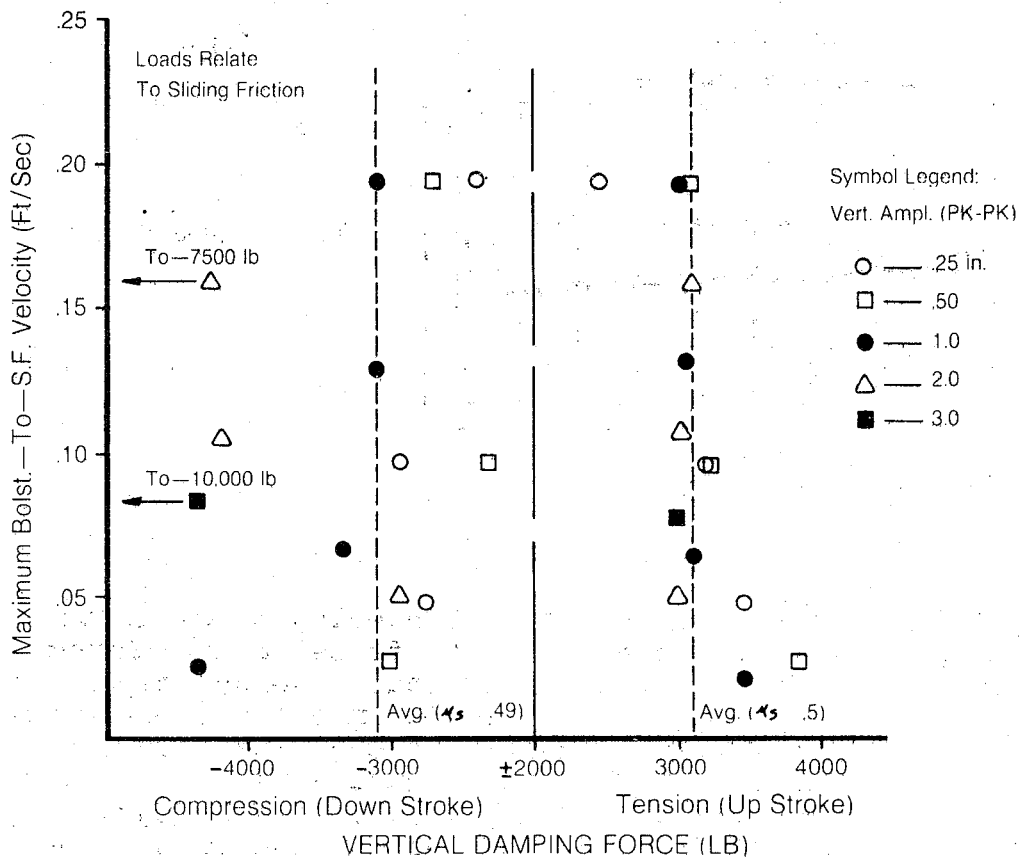


Fig. 8
 Vertical Damping Cycle
 2.0" PK-PK Stroke
 @ .1 Hz
 15,300 In-Lb
 Energy Dissipation Per Cycle

energy modeling of purely vertical damping since it may now be based on a constant friction force acting through some given distance. Indeed, expended energy comparison for Figure 7 and 8, derived from planimeter area determination, relates them almost exactly through ratio of their amplitudes of motion. That is, Figure 8 with a two inch peak-peak stroke displayed roughly twice the energy absorption as the Figure 7 diagram with a one inch stroke.

With acceptance of the previous paragraph it becomes necessary to define the constant friction force (or ensuing effective coefficient of friction). Enter Figure 9, which was developed from the many events relating to the various combinations of motion amplitude and frequency. Loads are plotted as a function of calculated maximum velocity to support the non-dependence of load on same. Here it is seen that while loads over the gamut of events were not as constant as implied by Figures 7 and 8, variation was not too extensive in most cases. Besides, the departures from the average lines (developed through simple numerical averaging of the loads defined by the horizontal portions of their load traces) generate no obvious trend, which actually forces use of the averages from a practical standpoint. Therefore, the given averages, 3100# ($\mu_s = .49$) and 3140# ($\mu_s = .5$) for the down-and up-strokes, respectively, are offered as the vertical damping characteristics of the used system. The effective μ_s values are based on the 3020 lb. column load, but should reasonably hold for others as well. Of course a sole $\mu_s = .5$ could accurately serve for both directions of motion.

Fig. 9



Use of the preceding for vertical damping modeling seems straight-forward, yet some conditions of nature could render this simplified approach appreciably inaccurate in various service instances. The first of these complications, break-away friction force, at first appears considerable, but from an energy absorption analysis may be accurately neglected in most cases. This stems from the fact that the static break-away peaks averaged 4300 lb. ($\mu = .68$) and 3800 lb. ($\mu = .6$) for the up-and down-strokes, respectively (which are roughly 25% greater than the steady sliding figures), but provided only a small percentage of the energy damping of a cycle, the percentage decreasing to negligible with large amplitude motions. As a specific example Figure 7 is cited. Here, of the 7400 in-lb total damping energy represented by the load/displacement rectangle, only 200 in-lb (2.7%) was attributable to break-away friction (downstroke break-away was negligible for this particular event). Assuming a 200 in-lb down-and up-stroke break-away peak, this would still only amount to slightly over 5% of the total damping energy. Check of break-away characteristics for events of other amplitudes revealed that the 5% figure held down to displacements of .25" peak-peak, but diminished to about 2.5% at a 2" stroke. These percentages could be applied to the average sliding energy determinations if accounting of the small break-away energy is desired in the modeling situations.

Another factor tending to complicate vertical damping modeling is well illustrated by the previously discussed Figure 9. The point made here relates to the damping force scatter illustrated by both up-and down-stroke data, but primarily by the latter. Although the average force recommended for modeling of the average situations should provide adequate realism in most situations, the noted scatter in this controlled test makes it obvious that certain rail occurrences will not be explained by this method. Furthermore, test execution made it apparent that the scattered points, or any for that matter, can be greatly influenced by the history of previous motion insofar as the activity effects the condition of the contacting friction surfaces. For example, the two up-stroke data points, indicated as being off the scale in the Figure 9 plot, resulted from data events previous to which little or no gall-eliminating lateral motion was applied during vertical motion set-up. Hence, the lack of lateral motion allowed a tremendous increase in the vertical coefficient of friction. While this was a departure from usual procedure it served to illustrate a dramatic problem involved with modeling of

damping forces, and since motion history in service is generally random, such variation in damping force is likely, but difficult to accommodate in modeling situations.

A logical progression from this service-complicating situation leads to the possible variation in truck fabrication which could markedly effect damping forces. The primary violations in this regard are simple variation of column load due to spring, friction shoe, etc., inconsistencies and non-parallelism of the side frame column friction plates. While the variation in column load could be easily handled through use of the given effective coefficient of friction, the friction plate problem can alter effective coefficient of friction through change in the self-energizing characteristics of the wedge friction shoe system, primarily on the downstroke. Also, the vertical out-of-parallelism can yield damping forces which are dependent on stroke, due to change in column load with position. ASF has witnessed instances in which friction plate irregularities have been the apparent cause of shoe chatter, which would yield an oscillating damping force curve, but in all it is felt that the mentioned problems in this paragraph do not match the damping load variations possible with the previously-discussed friction plate/shoe galling type of damping, which was seen to depend on motion history.

One further area was investigated to help qualify the vertical damping characteristics offered for modeling use. It pertains to the range of tested motions in comparison with those possible in service. Considering that vertical motions of roughly 3.0" peak-peak @ 3-4 Hz (which calculates to a maximum velocity of about 3 ft/sec) may be expected in service under some rough track conditions, the used velocities of the test, at about .2 ft/sec maximum, seem insufficient. But research into published dry friction tests has indicated that the implied difference between test and possible service velocities is not nearly sufficient to expect an appreciable change in friction characteristics. Aside from the velocity aspect, the vigorous service motion mentioned, through inertia effect of the 18 lb. friction shoes, can yield column load variations of about ± 60 lb. This too, however, at only $\pm 2\%$ effect on static column load, appears insufficient to warrant great concern for modeling purposes, assuming lack of unknown dynamic effects. Hence, the range of test conditions should have provided data sufficiently descriptive of the entire range of service vertical motions.

In summary to vertical damping, the use of a $\mu_s = .5$ figure should provide satisfactory modeling of a fixed column load system such as the Ride Control tested. Additions to

damping energy due to break-away forces may be made by using the small percentage given. The other conditions discussed which tend to detract from this simple modeling approach are mentioned to provide possible qualitative correction to those modeling situations in poor correlation with service phenomenon.

2. Lateral Damping

Lateral damping characteristics generally resembled those of the vertical phase as the oscillograph photographs, Figures 10 and 11, are quick to illustrate. Again, the constancy of damping force level within an event and in comparison with events of differing motion indicate an independence from amplitude and velocity. Furthermore, the damping energies displayed by Figures 10 and 11 are related through ratio of their amplitudes of motion. With this established, derivation of a good average damping force (or effective μ_s) for multiplication with given stroke will provide the simple model for simulation of lateral damping energy.

The average lateral damping level is provided through Figure 12, which is a plot of the in-and out-board motion damping forces as a function of maximum velocity of the appropriate amplitude/frequency combination. As seen, the inboard force at 2190 lb. ($\mu_s = .36$) and the outboard level at 2275 lb. ($\mu_s = .38$) are similar enough to define with an effective μ_s of .37 acting with the 3020 lb. column load. This μ_s is immediately recognized as being less (about 25%) than the .5 figure generated by the vertical damping phase. The self-energizing effect of the vertical system may provide explanation for this difference, but the effect of pre-event motion history rates concern, as will be seen.

Vertical damping forces had been observed as being quite constant for cycles within a given event (see Figure 6). On the other hand, lateral loads within a given event exhibited an increasing nature in almost linear relation with the number of cycles elapsed during the event. (Loads also displayed some scatter from event to event but did not show the range of the vertical case). The lateral loads given in Figure 12 were taken from the first lateral-only motion cycle after stopping of the anti-galling vertical motion used during lateral set-up. However, maximum lateral damping forces were not developed until an average of 30 cycles later, at which point damping forces had more than doubled from the initial cycle level.

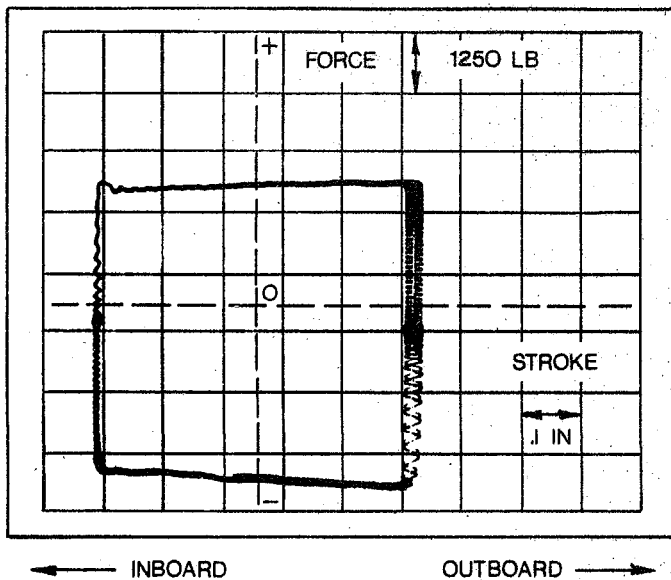


Fig. 10
 Lateral Damping Cycle
 .5" PK-PK Stroke
 @ .5 Hz
 3025 In-Lb
 Energy Dissipation Per Cycle

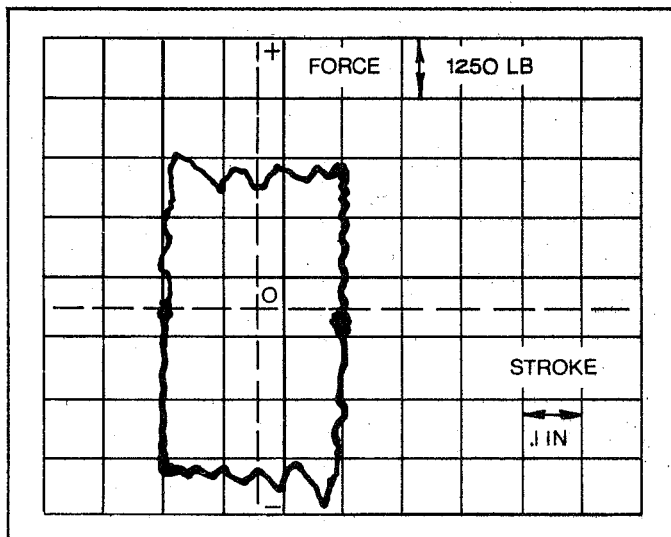
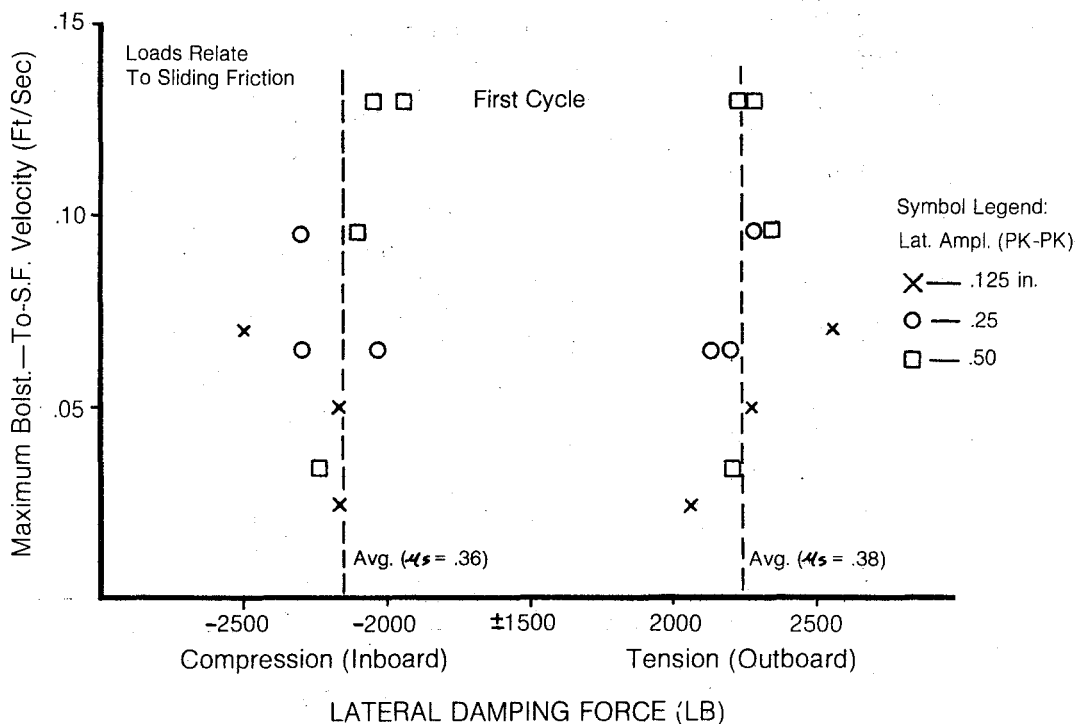


Fig. 11
 Lateral Damping Cycle
 .3" PK-PK Stroke
 @ 2.0 Hz
 1720 In-Lb
 Energy Dissipation Per Cycle

Figure 13 was constructed to describe the nature of the lateral load build-up since, having occurred diligently for each standard lateral event, the characteristic is assumed valid. Note that the lateral damping forces portrayed in this figure were averaged from the individual in-and out-board forces of the various amplitude/frequency events for the particular elapsed cycle.

Fig. 12



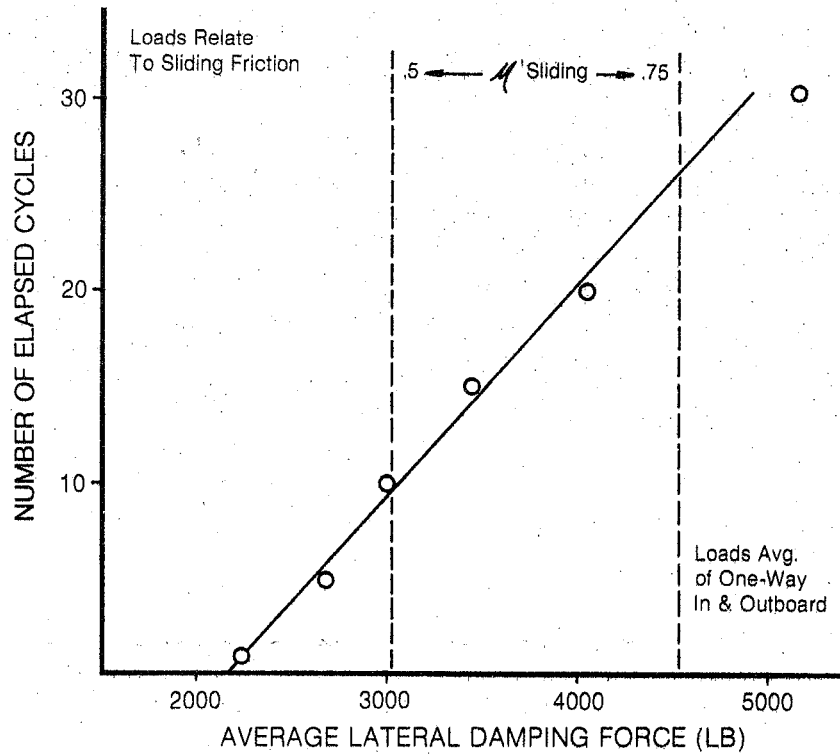
While the described lateral force build-up is definitely mysterious, it is apparently related to the pre-event motion history since lateral events recorded back-to-back, that is, without vertical motion used in between for anti-galling purposes, displayed roughly continuous lateral forces without appreciable drop-off or build-up. Hence, use of the Figure 13 data is assumed mandatory for accurate modeling of lateral energy damping.

As illustrated in Figure 11, lateral break-away loads were usually no greater than the sliding forces. Occasionally peaks of a few hundred additional pounds were noted, but the effect on damping energy was so miniscule that modeling for the lateral case need not consider it.

3. Vertical Damping With Superimposed Constant Lateral Force

The subject test phase generated straightforward results

Fig. 13

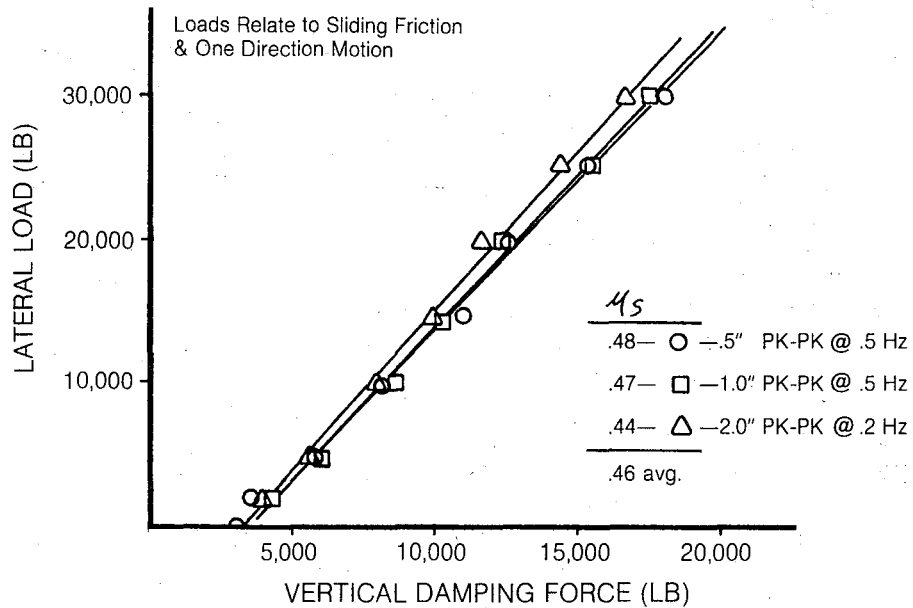


as depicted in the Figure 14 plot. Here, data appeared to follow elementary friction laws as vertical forces increased linearly with imposed lateral force at an average ratio of .46:1, which effectively describes the sliding friction coefficient at the bolster gib/side frame column interface. (Data were corrected for slide friction as of function of applied lateral load).

Note that the plot offset to the right of origin resulted from the normal friction shoe damping forces. To model the subject situation under average conditions all that is required is to add vertical damping of a .46 x lateral force to the standard friction shoe damping term.

Study of break-away friction forces for the phase at hand revealed, as with the vertical friction shoe-only tests, that the static forces contributed very minutely

Fig. 14



to the energy damping of the system. In this case the break-away forces averaged about 13% greater than the given sliding friction forces, but being essentially instantaneous and occurring at the start of a motion, at which point velocity is a minimum, the break-away loads provided no appreciable gain with regard to energy absorption.

4. Vertical Damping With Truck Out-Of-Square

The following table summarizes sliding friction results applicable to this section.

Side Frame Yaw (deg.)	One Way Average Vertical Load (LB)	
	<u>.5" ampl. @ .5 Hz</u>	<u>1.0" ampl. @ .5 Hz</u>
1.0	2800	2900
1.5	3900	3800

Recalling from Figure 7 that the average "square" truck damping force was around 3100 lb., it appears that the slight 1° yaw had little, if any (considering scatter of friction forces) effect on the damping characteristics of the

friction shoe apparatus. On the other count, however, the maximum side frame yaw angle presented greater friction resistance; but, considering that bolster gib/side frame column contact was maintained at two points during this test, it is felt that the supplementary friction force resulted therefrom. Thus, for simulating purposes it is concluded that through yaw angles just short of the maximum tested (this condition eliminating possibility of supplementary metal contact), friction shoe damping will be negligibly effected by an out-of-square condition. For yawed circumstances involving gib/column contact, a supplementary damping term could be added to the friction shoe effect based on a sliding friction coefficient of .46 (borrowed from the superimposed lateral force phase, #3). This should adequately consider the supplementary friction effects if the yawing input load can be determined.

In qualifying the stated conclusions, the "Clearance" report Part V is considered. The maximum yaw angle achieved for this test, at 1.5° , is sufficiently close to the maximum achievable from appropriate tolerance combinations, about 2.5° , that included results should cover the majority of service conditions, excessively worn situations excepted.

VERTICAL, LATERAL, TORSIONAL AND
PITCH SPRING RATES OF STANDARD TRUCK COIL GROUP

Test Report - Part II

American Steel Foundries Participation In
AAR/RPI/FRA Track-Train Dynamics Program

OBJECT

Determine the Vertical
Lateral
Torsional
and Pitch (including Rock)

spring rates for the subject 70-ton Ride Control truck coil group over the range of possible coil heights.

CONCLUSIONS AND RECOMMENDATIONS

The following table summarizes the instantaneous spring rates coincident with a vertical spring height of 8".

<u>Loading</u>	<u>Rate</u>
Vertical	22,150 lb/in
Lateral	9,300 lb/in
Torsional	5,760 in-lb/deg.
Pitch	1,720 lb/deg.
Rock	1,520 lb/deg.

A second table presents the approximate rate of spring rate change within the given range of vertical heights.

<u>Loading</u>	<u>Rate of Rate Change</u>	<u>Application Spring Height Range (in.)</u>
Vertical	None	7 - 9-3/4
Lateral	+3,260 lb/in/in. vert.defl.	7 - 9-1/2
Torsional	+1,064 in-lb/deg/ in.vert.defl.	7 - 9-1/2
Pitch	+ 147 lb/deg/in.vert.defl	7 - 9-1/2
Rock	+ 214 lb/deg/in.vert.defl.	7-1/4 - 9-1/2

As seen, the vertical rate remained constant throughout the noted range, whereas the other rates displayed a general tendency to increase with spring deflection.

With nominal solid and free heights of 6-9/16" and 10-5/16", respectively, the presented information should handle most situations. However, the significant increases in rate of rate change for spring heights beyond the given ranges require recognition for accurate modeling throughout the spring heights in service use. Specific data are supplied in the Results covering the entire coil height range.

Orientation of spring tangs (coil ends) had no significant effect on the various spring rates.

TEST SPECIMENS

Test spring grouping, a 70-ton Ride Control Configuration, was composed of 7 outer (ASF Drg. 31081-003) and 6 inner (ASF Drg. 32506-129) D-5 coils taken at random from a stock of coils previously used for road test purposes. The specimens should be good representations of "average" service coils, having experienced initial settling but affording design load support. Test set-up illustrations to be discussed show arrangement of the coil group.

TEST PROCEDURE

Data acquisition basically involved imposition of appropriate group loading (corresponding to the four loading forms stated in the Object) and measurement of resulting group deflection. This yielded data in the form of load vs deflection for graphical determination of the load rates.

Spring tang orientations were varied for most loading configurations to test for possible effect on rate. To aid organization, the spring group was arbitrarily assigned to the BR corner of a rail car. Tang orientation "outboard" is self-explanatory. Orientations "A" and "B" indicate tangs facing the A and B car ends, respectively, and perpendicular to the outboard orientation. For a given orientation, all tangs for inner and outer springs faced the same direction.

Common to all but the vertical rate test, the load and deflection signals were recorded on oscillograph paper for convenient reduction. Loads were measured with an axial load cell and displacements with a linear transducer. Therefore, geometric transformations of the recorded data were needed in some cases to yield data applicable to the load rate desired. Although the displacement-measuring linkages and corresponding transformations may be inaccurate for large displacements, the small motions concerned with this report are well with the good practice small angle assumptions used.

At this point the peculiarities of the four loading modes are discussed separately.

Vertical Spring Rate

The simplest of all, this test consisted of vertically deflecting the coil group through its range of travel, while simultaneously noting load and deflection at convenient height increments. It was performed in a standard static test machine, from which load measurements were taken.

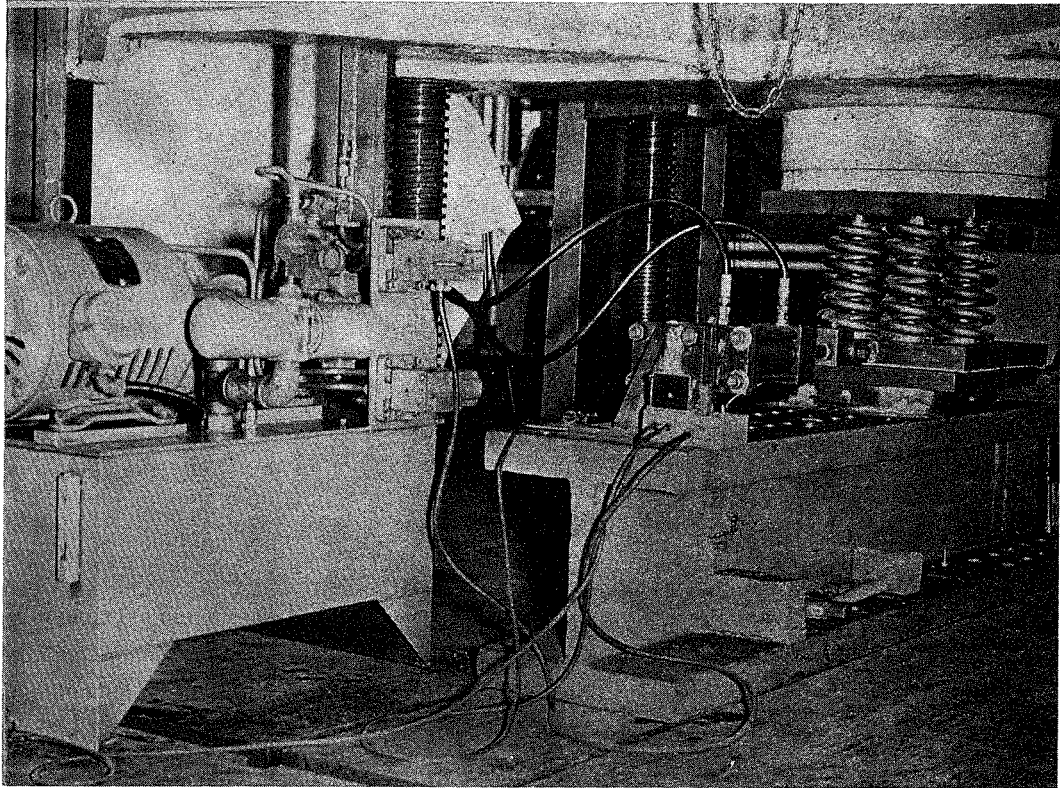


Fig. 15

LATERAL SPRING RATE TEST SET-UP

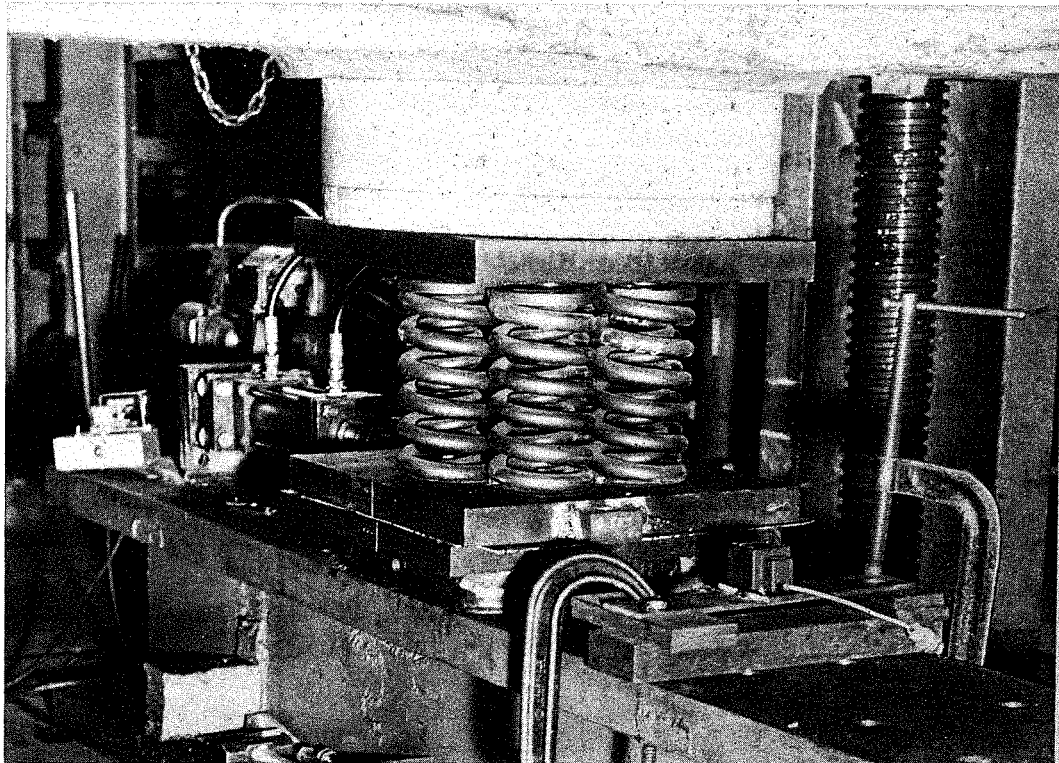


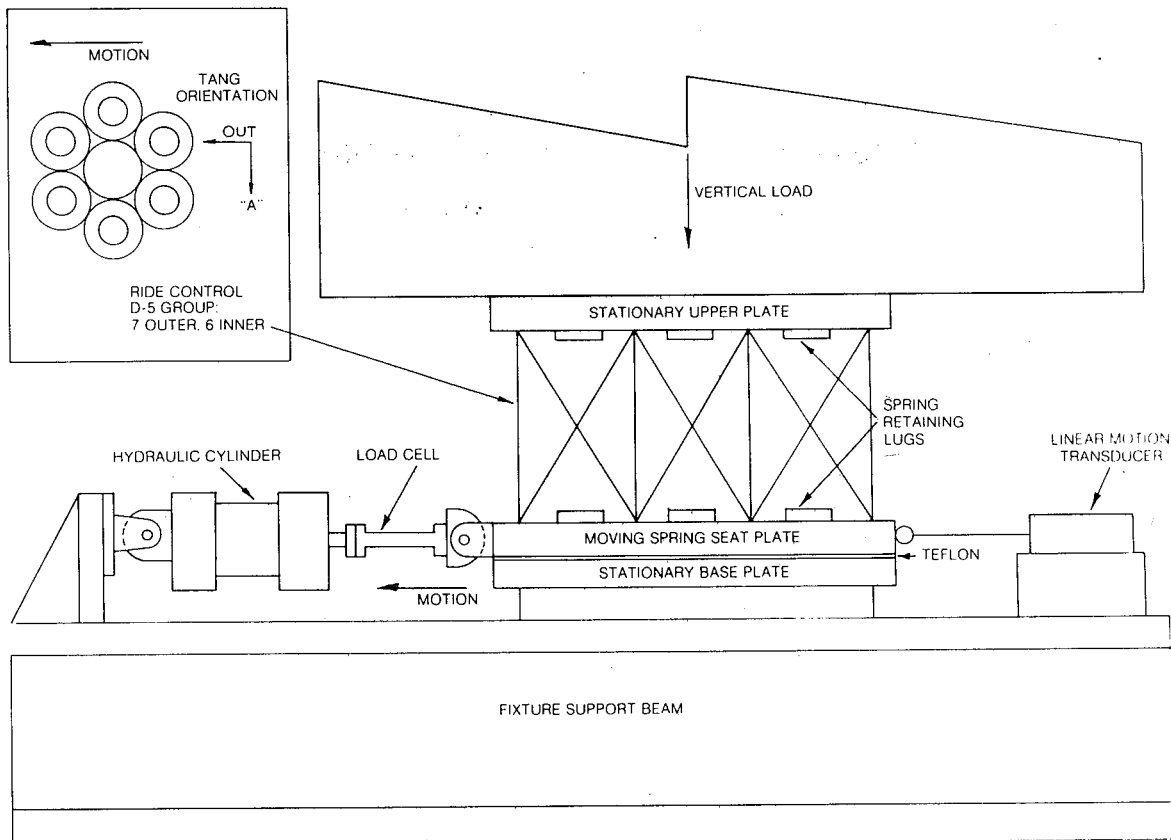
Fig. 16

Resulting data provided rate in units of lb. vertical load per in. vertical deflection. Deflections were scale measured. Random tang orientation was used since no tang effect could even be imagined for this type of loading.

Lateral Rate

Figure 15 & 17 illustrate the utilized lateral rate set-up. Test method consisted of laterally zeroing the movable spring seat bottom plate, setting the desired vertical height by applying necessary static machine load, and then activating the hydraulic cylinder, which pulled the bottom plate from its datum position. The noted displacement transducer measured the relative motion between top and bottom of the springs. Figure 18 presents an oscillograph example of a lateral rate test event for a specific spring height. A similar recording was attained for each in the gamut of spring heights and tang orientations. Rate information developed from the load/deflection data took the form of lb. lateral load per in. lateral deflection of the bottom spring seat.

Fig. 17
LATERAL SPRING RATE TEST SET-UP



NOTE NOT TO SCALE

Fig. 18

LATERAL SPRING RATE RECORDING

D-5 Coils
RC Group
7 out, 6 in

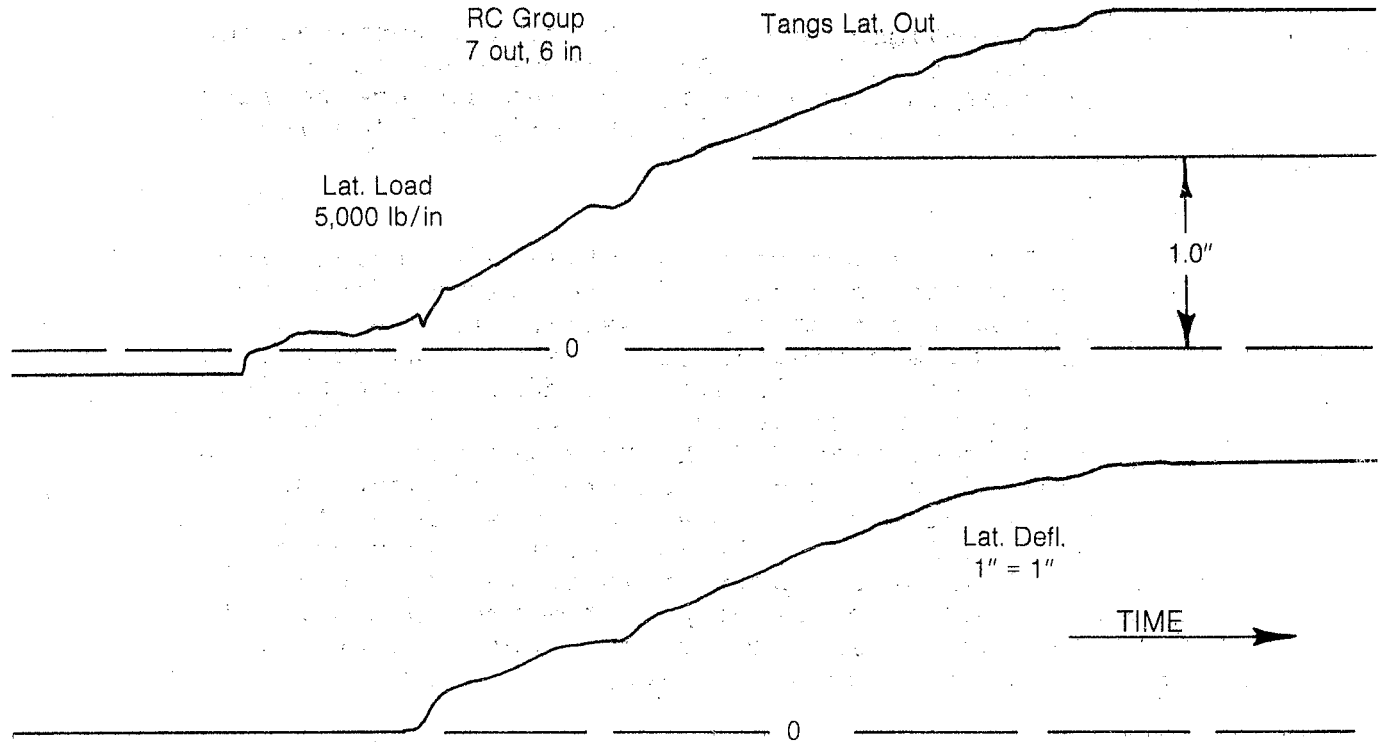
9" Coil Ht.
Tangs Lat. Out

Lat. Load
5,000 lb/in

Lat. Defl.
1" = 1"

TIME

1.0"



TORSIONAL SPRING RATE RECORDING

D-5 Coils
RC Group
7 out, 6 in

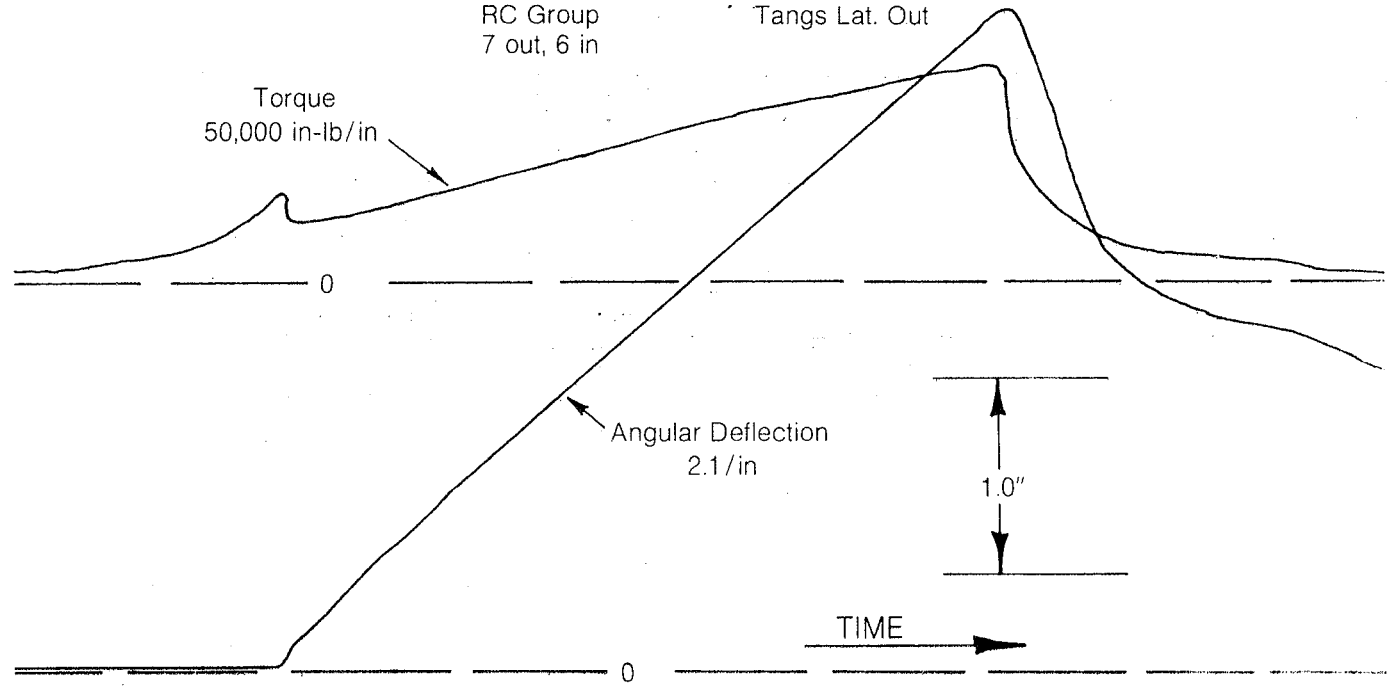
7¹¹/₁₆" Coil Ht.
Tangs Lat. Out

Torque
50,000 in-lb/in

Angular Deflection
2.1/in

TIME

1.0"



The lateral rate test was done primarily with the tangs outboard (in direction of the lateral deflection) and secondarily with the tangs in the "A" orientation, perpendicular to the deflection. The degree of lateral deflection imposed was guided by the maximum possible bolster-to-side frame lateral motion, 23/32", derived from Part V of this report.

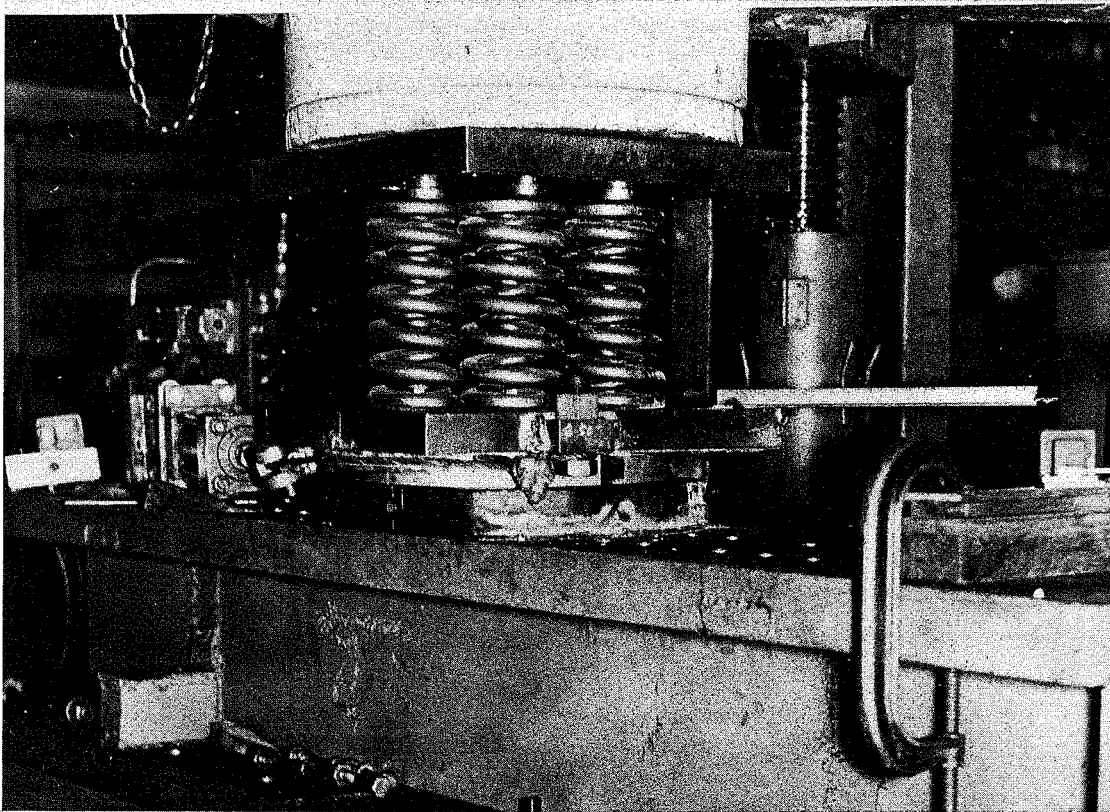
The greased teflon sheet in the set-up illustration, while enabling ease of slip between the bottom spring seat plate and stationary base plate, was nevertheless not completely friction-free. The force required to overcome this friction did not, however, complicate lateral rate determination since it merely acted to shift the load/deflection data curve upward, without altering its slope. (Of course for math model use the slope-developed spring rates are assumed to initiate from the zero load/zero deflection origin). Comparisons of vertical load with the springs in the laterally deflected position to the vertical load for the zero position (negligible difference) verified the constant teflon friction component throughout the lateral travel of a test event.

Torsional Rate

Figure 19 & 20 illustrate the subject fixture, which is a variation of the lateral rate fixture just discussed. In this case, however, motion was imparted by the hydraulic cylinder acting through a wire cable/partial sheave assembly to twist the bottom spring seat plate relative to the top plate. In addition to the greased teflon bearing beneath the bottom spring seat plate, a center radial bearing was required to serve as the center pivot.

The axial load measured in turning the spring seat plate was multiplied by the sheave radius to yield torque. The linear bottom-to-top spring seat motion measured by the noted transducer was transformed to arcuate motion through appropriate trigonometry. The resulting torque/angular deflection relation yielded graphical slope (rate) determination in the form of in-lb torque per degree of spring seat rotation. As with the lateral test, bearing

Fig. 19
TORSIONAL SPRING RATE TEST SET-UP



friction was neglected in the rate determinations. Figure 18 presents an oscillograph example of a torsion test, single height event.

Tang orientations used include outboard as primary and "A" as check. Angular deflections were guided by the maximum possible bolster-to-side frame yaw (2.46° - one direction from datum) found

Pitch Rate (Including Rock Rate)

Pitch and rock rate are discussed coincidentally because the test fixture required was the same for both, as illustrated by Figures 21 & 22. Variations between the two loading modes result from the orientation and placement

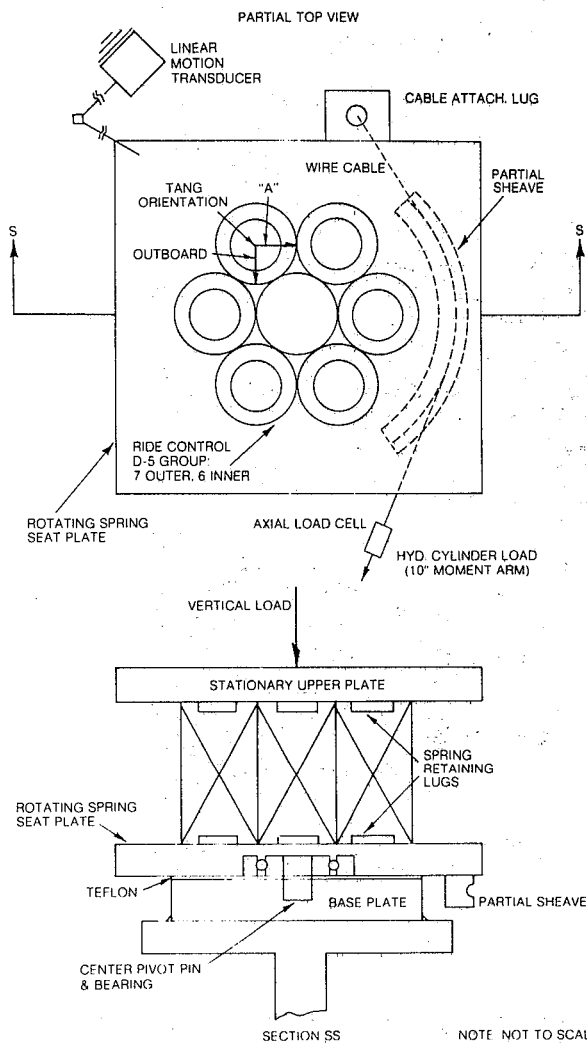


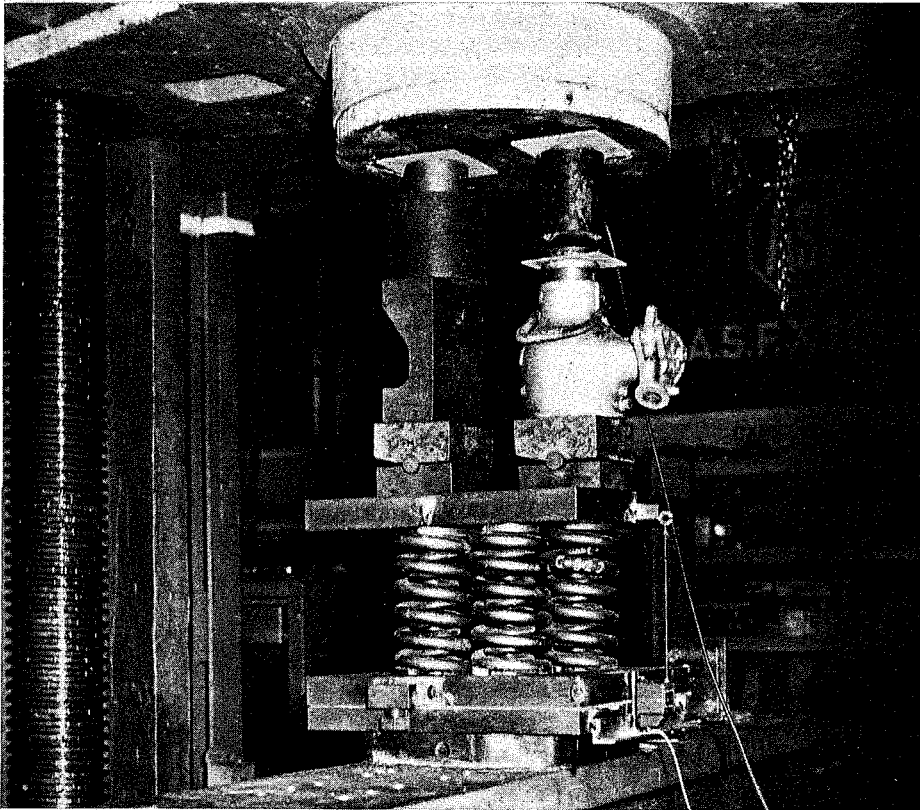
Fig. 20
TORSIONAL SPRING RATE
TEST SET-UP

of the indicated load blocks. (Figure 21 shows pitch set-up.)

Test method consisted of setting desired vertical height and applying jack load to one side of the coil group until sufficient deflection was attained. For application to the load/displacement plot, the load data were used as recorded, whereas the deflection data were adjusted to indicate arcuate displacement about the top, center of the spring beneath the solid load block (opposite the jack). Ensuing rates took units of lb. jack load per degree of upper spring seat deflection. Innate fixture friction was effectively zeroed-out by the graphical procedure as in the previous lateral and torsional rate determinations.

Pitch and rock rates were figured for tang orientation outboard, primarily, but also for "A" and "B" thoroughly. From the Part V clearance report, maximum side frame pitch possible (4.75° one direction) was used to limit that loading. Maximum side frame rock relative to the bolster,

Fig. 21
PITCH SPRING RATE TEST SET-UP



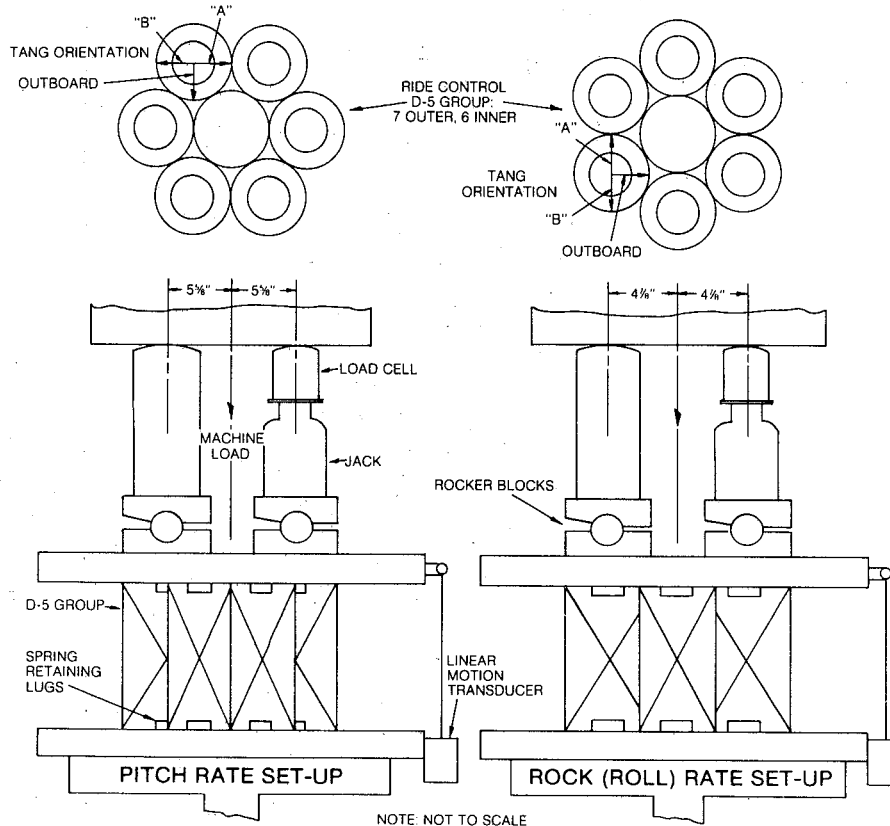
at almost 15° , was too great to achieve with the used fixture, so deflections were limited by factors of test safety and accuracy. Still, inputs achieved were sufficient to develop satisfactory rate data which should stand for most situations achievable in service. As with all other test loadings, the spring group was unloaded and zeroed before each test event.

RESULTS AND DISCUSSION

General

Figures 23 - 30 present the load vs deflection plots from which the load rates were determined for the four basic load set-ups. Not shown on these plots are the repeat data events used to verify accuracy of the primary events. The summarizing tables presented in the Conclusions provide a "handle" on rates expectable within range of most coil heights. However for most loading cases, accuracy of

Fig. 22
 PITCH AND ROCK SPRING RATE TEST SET-UPS



rate throughout spring travel requires departure from the approximate rates given, primarily due to the tendency for drastic rate increase for heights approaching solid and rate decrease for spring lengths approaching free height. When appropriate, plots of rate as a function of coil height are presented with the individual loading discussions to enable accurate computer modeling throughout the range of possible coil heights.

Vertical Rate

The simplest of the rate tests also produced the most straightforward results, as the vertical calibration of Figure 31 indicates. Here, the vertical load/spring height plot was almost perfectly linear between spring heights of 9-3/4" and 7", with a corresponding constant rate of 22,150 lb/in (22,207 lb/in theoretical design). Since

Fig. 23
LATERAL SPRING RATE DETERMINATION

Ride Control 70-Ton Spring Group
 D-5: 7 outer, 6 inner

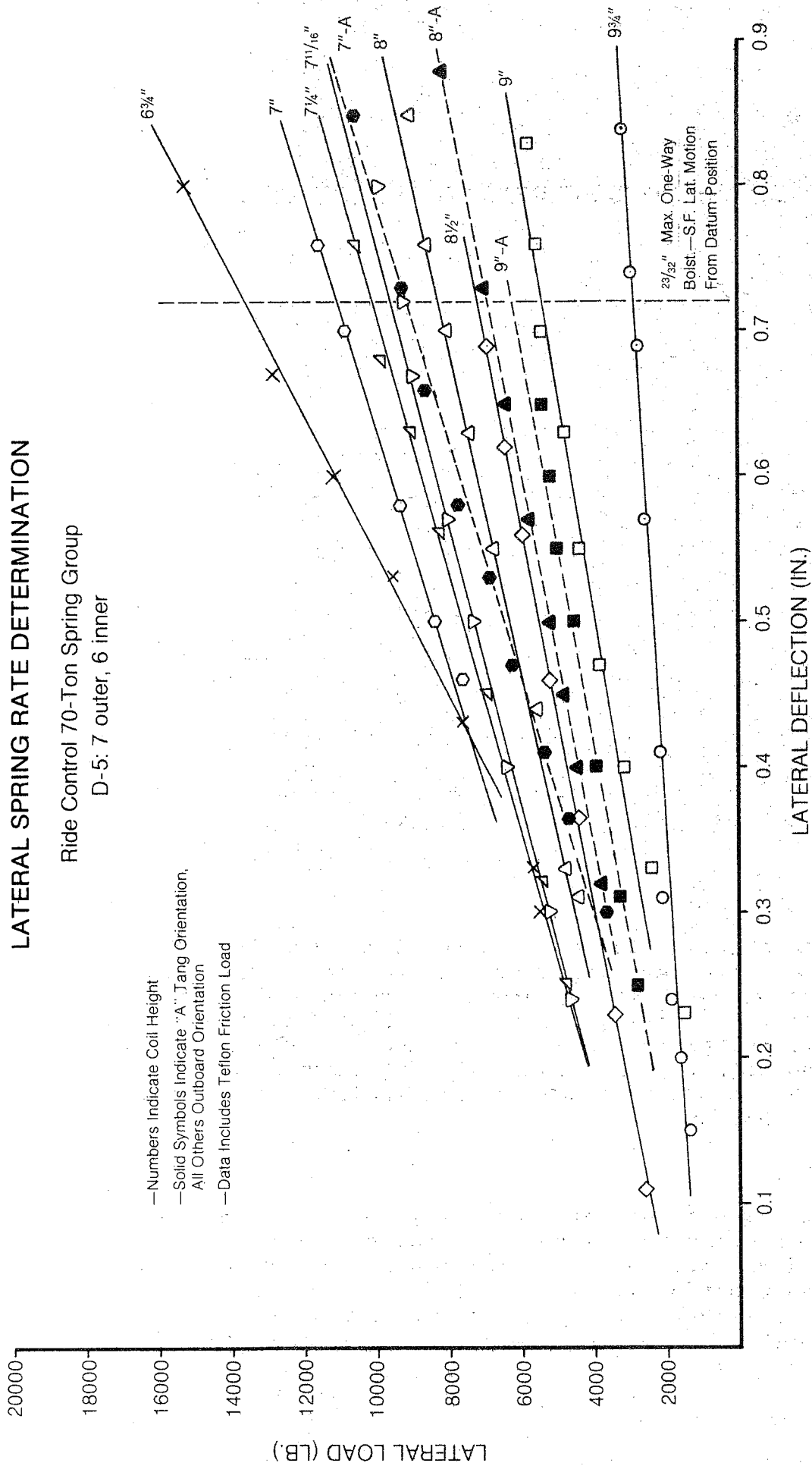


Fig. 24

TORSIONAL SPRING RATE DETERMINATION

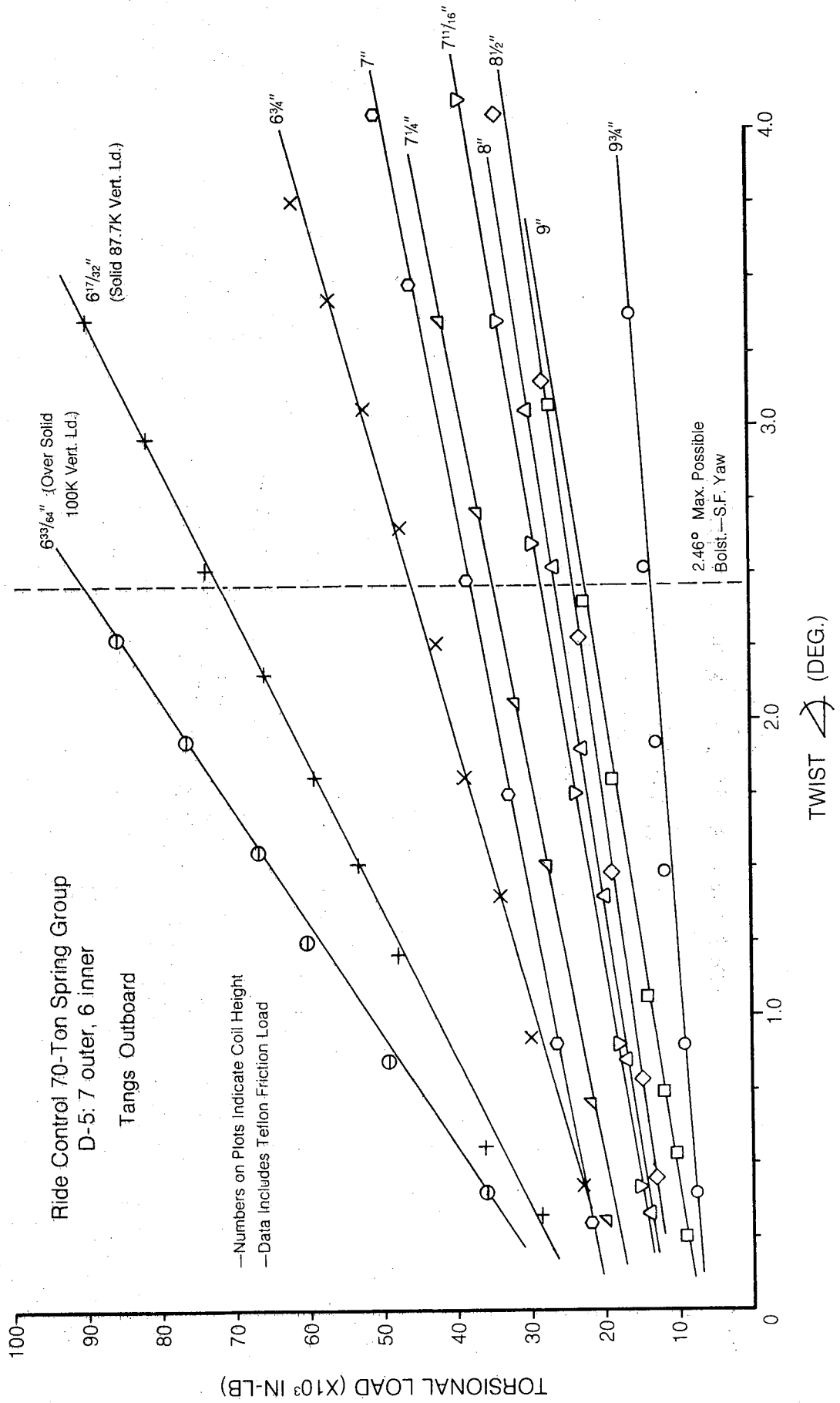
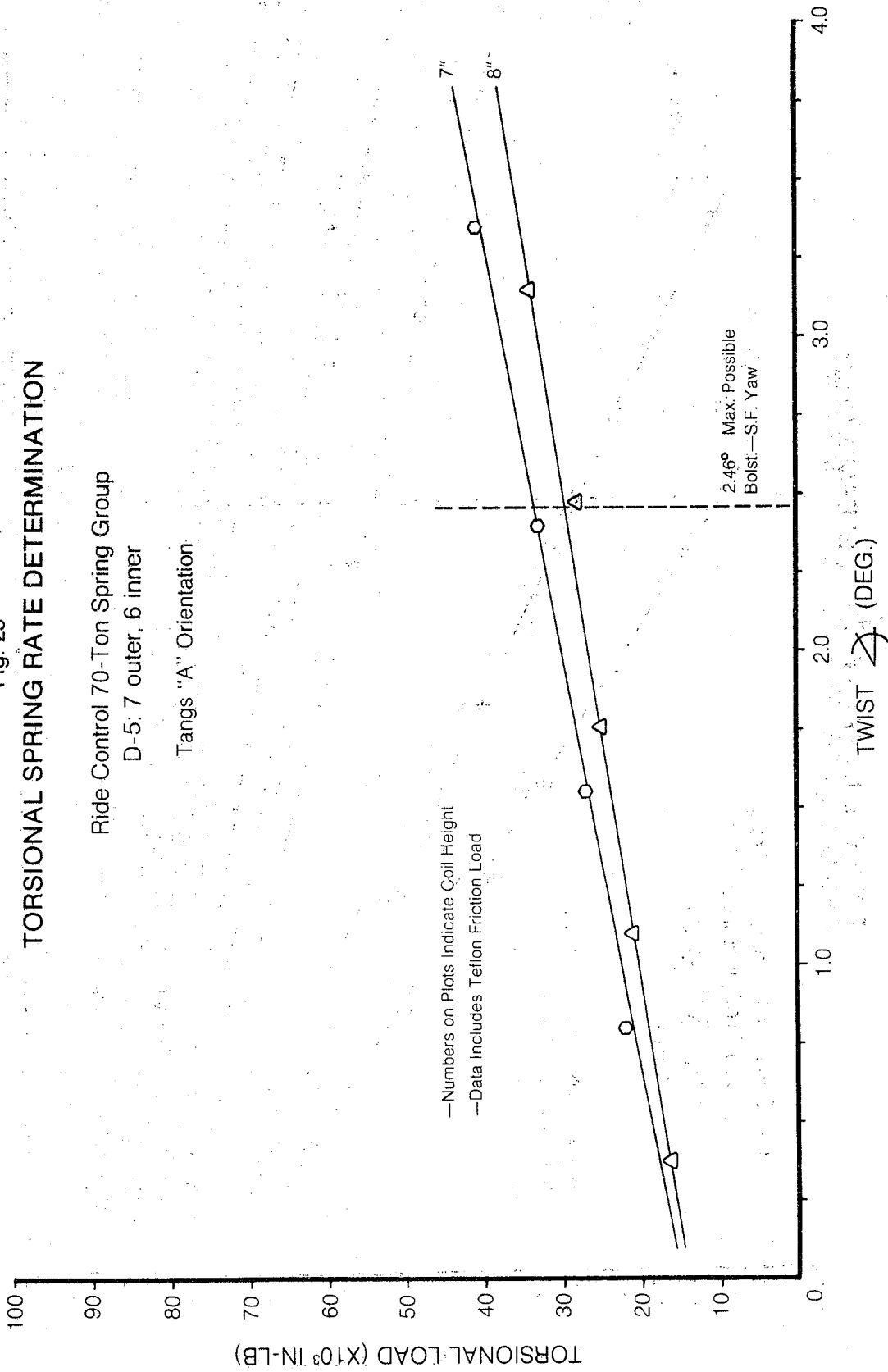
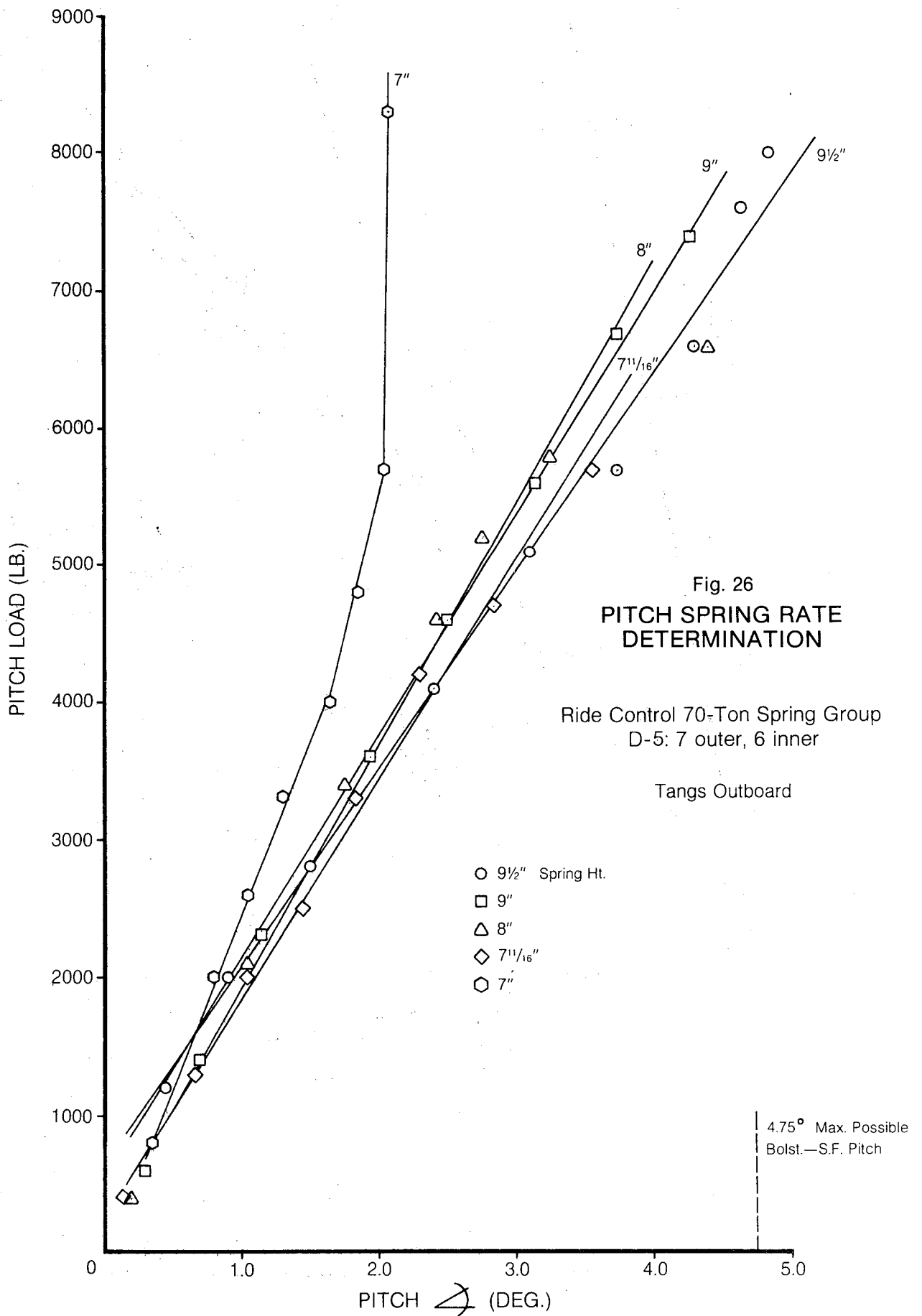


Fig. 25
TORSIONAL SPRING RATE DETERMINATION

Ride Control 70-Ton Spring Group
 D-5: 7 outer, 6 inner
 Tangs "A" Orientation





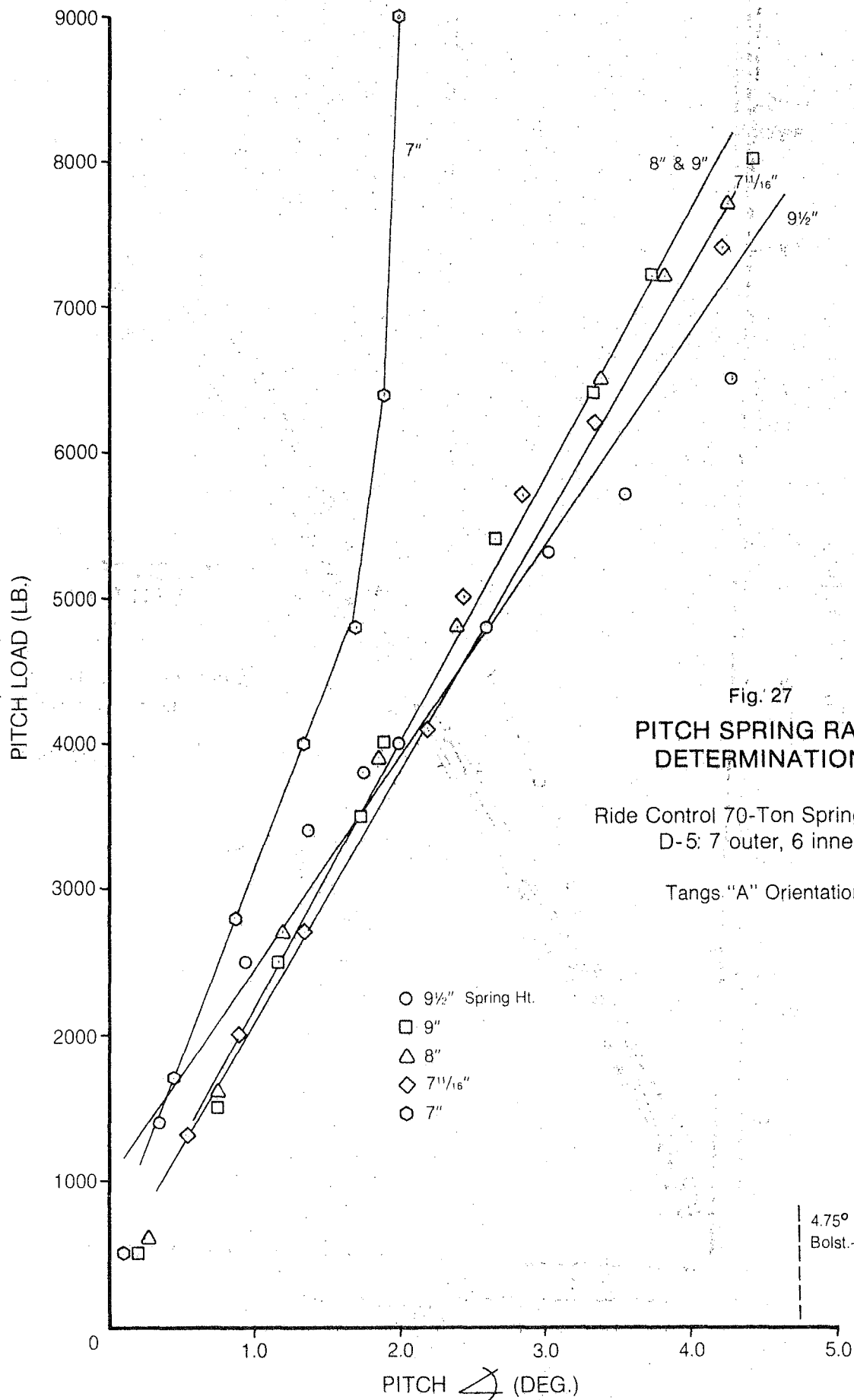
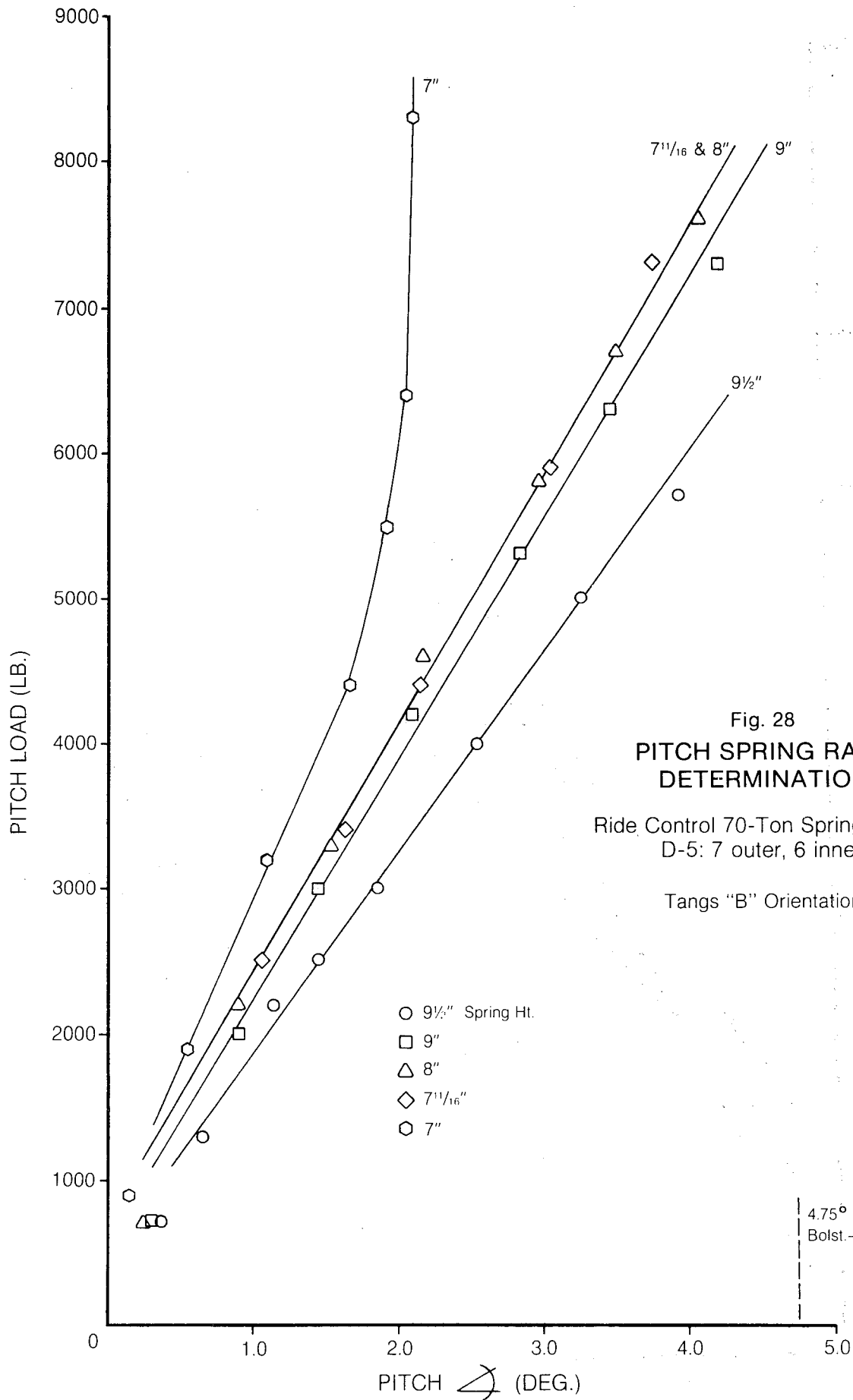


Fig. 27
**PITCH SPRING RATE
 DETERMINATION**

Ride Control 70-Ton Spring Group
 D-5: 7 outer, 6 inner

Tangs "A" Orientation



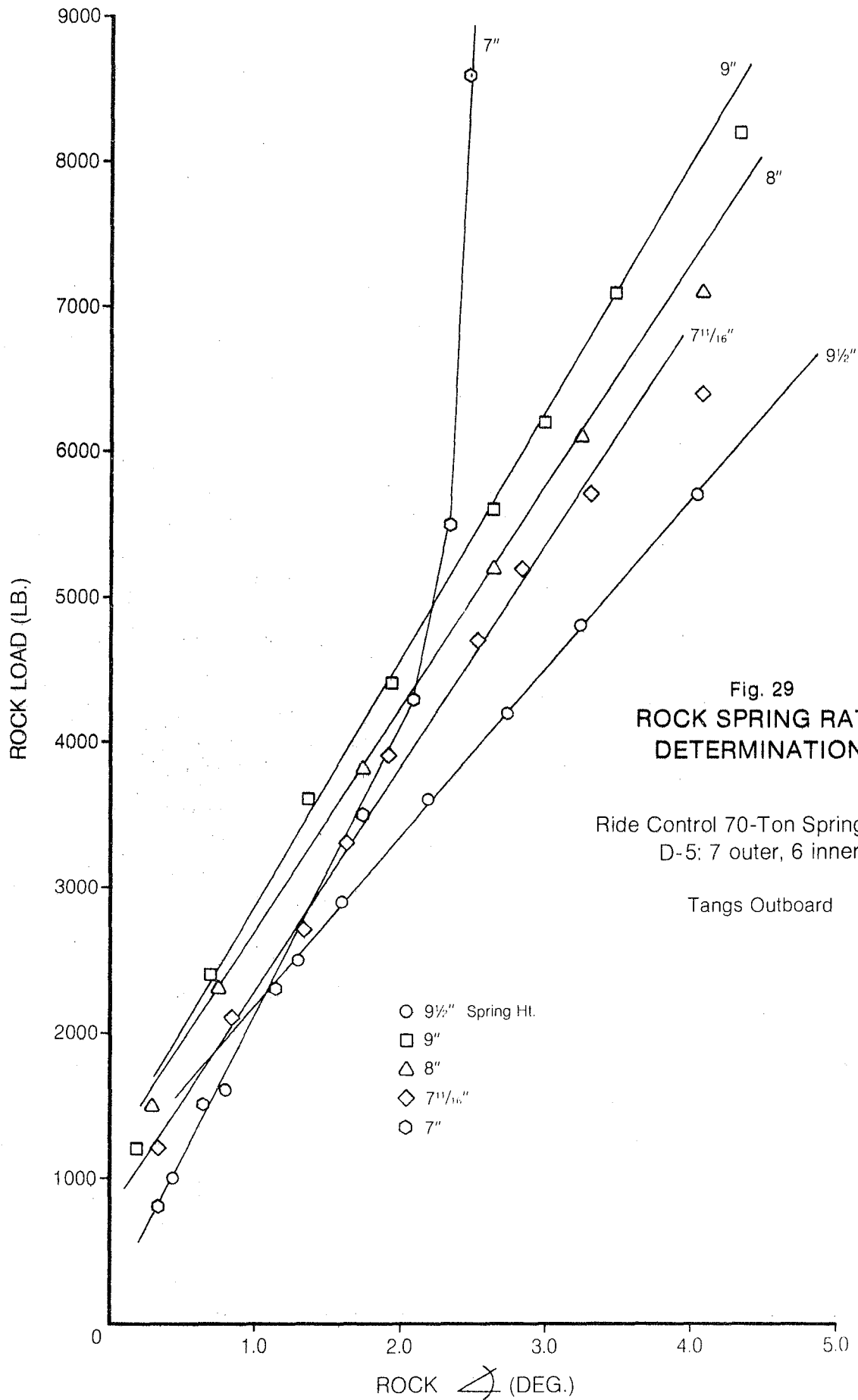


Fig. 29
**ROCK SPRING RATE
 DETERMINATION**

Ride Control 70-Ton Spring Group
 D-5: 7 outer, 6 inner

Tangs Outboard

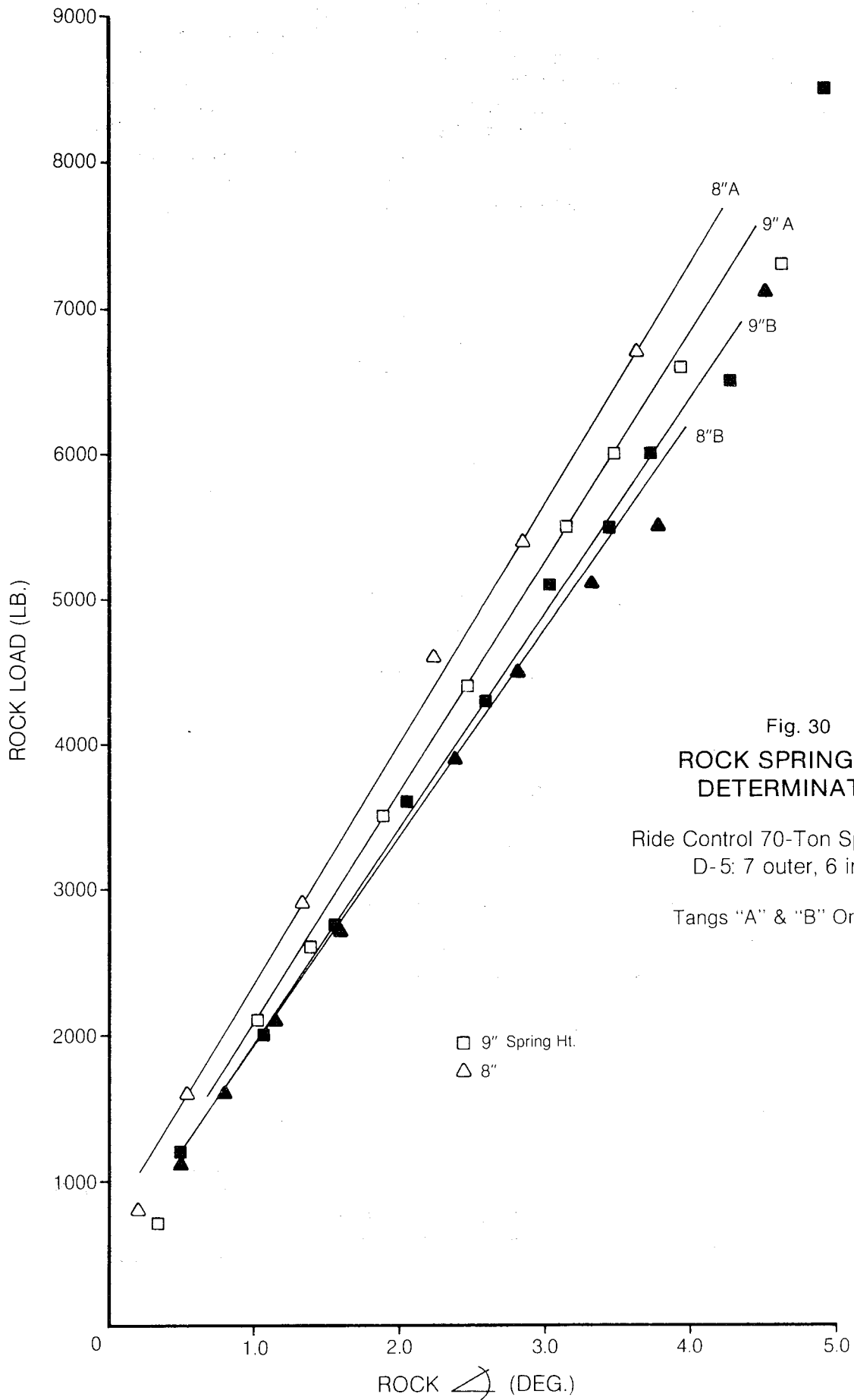
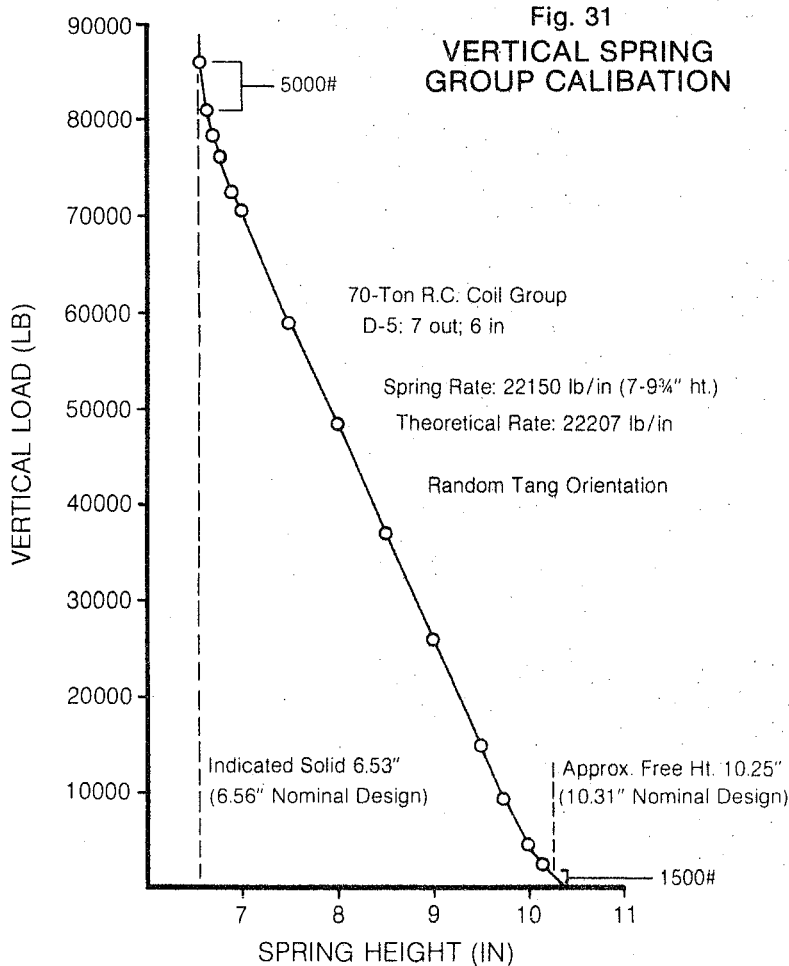


Fig. 30
**ROCK SPRING RATE
 DETERMINATION**

Ride Control 70-Ton Spring Group
 D-5: 7 outer, 6 inner

Tangs "A" & "B" Orientation

the given rate span nearly covers the range of possible coil height (10-1/4" to 6-9/16"), and the deviations from linearity are not too extensive, the 22,150 lb/ in. figure could reasonably satisfy modeling use for the entire range of vertical heights. By linearly extrapolating the straight line portion of the load/height plot, errors of only 5,000 lb. (6% low) at solid and about 1,500 lb. (also low) at free height are indicated for the linear approximation. Of course, complete accuracy could be achieved by programming the entire data plot.

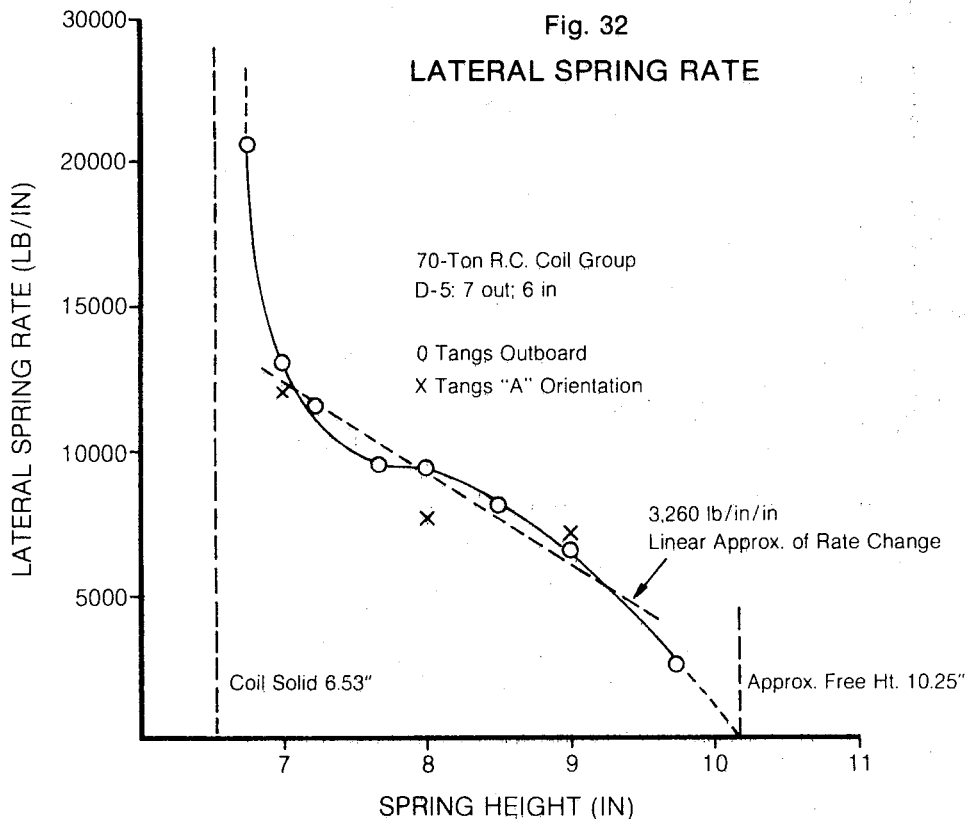


The rate deviations mentioned are further discussed at this point since similar behavior, though more pronounced, was noted for the other three loading modes in this test. Specifically, spring rate decreased as coil heights approached free conditions from some compressed state. On the other end, rate increased with approach of solid height. The reasons for this behavior, at least for the vertical loading,

probably lie in the variations of the individual springs in that different free heights and end square variations could cause the reduced rates near free height, and random inter-coil contact could result in the increased rates near solid height.

Lateral Rate

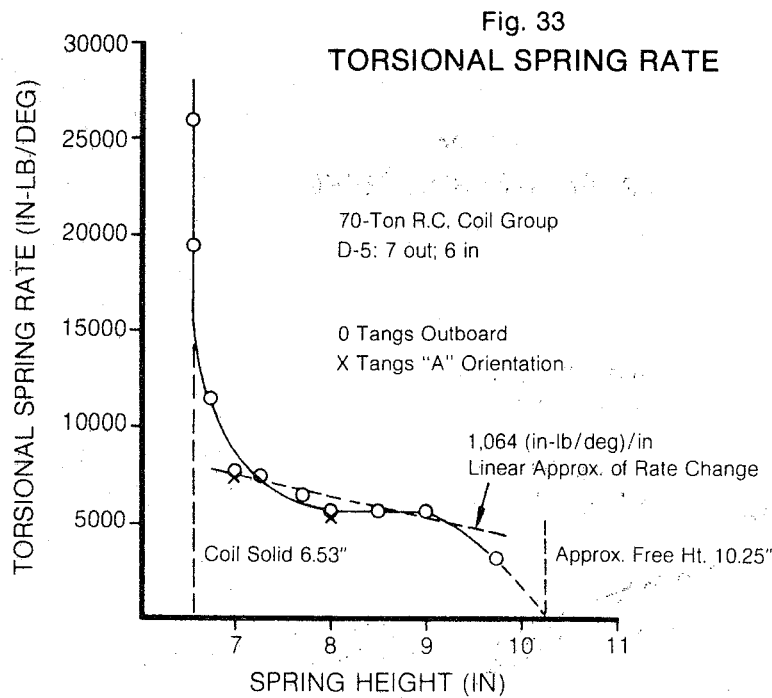
The Figure 32 lateral rate plot demonstrates an obvious tendency for rate increase with increased coil deflection. While this characteristic is similar to those portions of the vertical calibration showing rate variation, the lateral data formed only a very narrow plateau of constant rate, noted at the 8" spring height position. Still, the data formed a rather smooth curve with programming capability for accurate modeling over the range of spring heights. (35,000 lb/in is offered as a rate estimation for the solid spring height). The noted linear approximation line, as given in the Conclusions as 3,260 lb/in per inch of vertical height, is within 15% of the data curve in the 7" to 9-1/2" range and could offer convenient use if it fits a particular modeling situation.



The "A" tang orientation data points in Figure 32, while hinting at a slightly lower rate than the outboard orientation, are not sufficiently different to warrant consideration, particularly in view of the relative sensitivity of the graphical slope technique for rate determination. The indicated "outboard" curve should provide satisfactory model usage and be within about 1,500 lb/in of an average serviceable spring group through the height range.

Torsion Rate

The Figure 33 torsion rate plot displays rate change behavior similar to the lateral results, yet the subject plot possesses a much broader plateau of relatively constant rate, spanning the 7-3/4" to 9" heights.

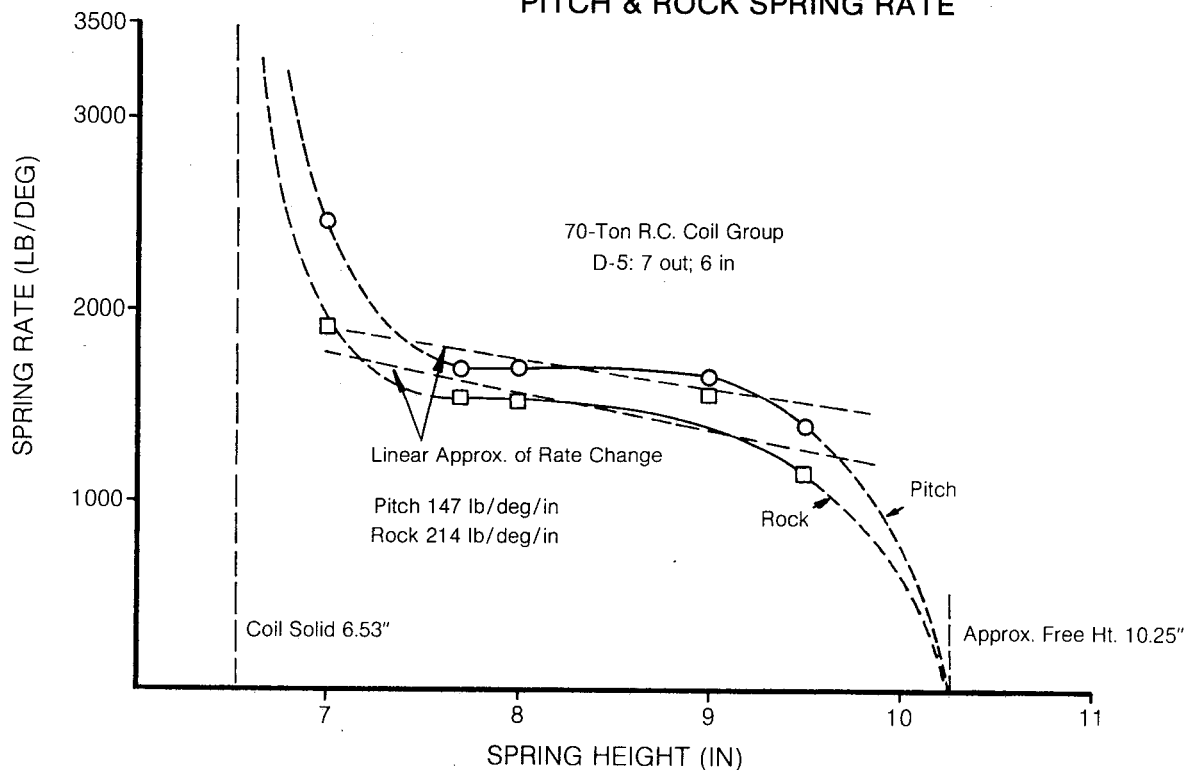


As with the lateral rate plot, entire curve programming should be considered for full range accuracy.

A quick look at the "A" tang orientation data points dispels any concern for possible tang effects on torsional rate.

Fig. 34

PITCH & ROCK SPRING RATE



Pitch And Rock Rate

The subject rates, presented in Figure 34, portray characteristics in direct mimic of the forgone lateral and torsional loadings, except that they afford the greatest height range (7-1/2" to 9") in possession of a reasonably constant load rate. Since tang orientations were so thoroughly investigated for these loadings, the plotted rate points represent average rates from orientations outboard, A, and B for all pitch points and the 8" and 9" heights of the rock curve. The plots also indicate range of rate for a specific height and loading, generated by the three tang orientations. As seen, all ranges were within the dimensions of the plotting symbols except for the 7" pitch rate and the two averaged rock points. This allows the conclusion that tang orientation is immaterial to the subject rate levels.

As with the other load rates, the linear approximation of the rate plot could be used for convenience within the intermediate spring height range, but full curve programming is required to handle situations including free and solid heights. 6,000 and 5,000 lb/deg. are offered for the respective pitch and rock curves as reasonable approximations for rate at spring height infinitesimally greater than solid.

DEFLECTION CHARACTERISTICS OF
REPRESENTATIVE TRUCK BOLSTERS AND SIDE FRAMES,
AND THE TORSIONAL RIGIDITY OF A TRUCK BOLSTER

Test Report - Part III

American Steel Foundries Participation In
AAR/RPI/FRA Track-Train Dynamics Program

OBJECT

Determine the deflection characteristics of the subject castings under the following loading conditions:

1. Truck Bolster.

- a) Vertical Centerplate
- b) Vertical Side Bearing
- c) Transverse
- d) Torsional

2. Side Frame.

- a) Vertical (Full spring seat)
- b) Transverse (At columns)

RECOMMENDATIONS

The succeeding table presents average load rates recommended for general description of 6"x11" Ride Control truck components with rod-under brake configurations and 5'-8" truck wheel base. "Results" section of the report presents values for specific casting patterns, which were generally seen to be within roughly 10% of the listed averages.

1. Truck Bolster.

	<u>Average Load Rate</u>
a) Vertical Centerplate	2.12 x 10 ⁶ lb/in.
b) Vertical Side Bearing	3.58 " "
c) Transverse	1.95 " "
d) Torsional (single specimen)	1.72 " in-lb/deg.

2. Side Frame.

a) Vertical	3.21 x 10 ⁶ lb/in.
b) Transverse	.71 " "

TEST SPECIMENS

Although the general plan for data acquisition in the Track Train Dynamics series of laboratory testing centered about bolster Patt. 21732-DA and side frame Patt. 21850-R, various other patterns (in addition to 1732-DS) - were used for this particular test phase since appropriate vertical and transverse test data were already available, and, in justification of their use, they represent only minor variations to the primary pattern designs. Too, use of the numerous patterns provides insight to the possible range of deflection rates within the realm of similar casting design. The list of

utilized patterns is presented below.

	<u>Patt. No.</u>	<u>Drg. No.</u>	<u>Serial No.</u>
Truck Bolsters	21732-AJ	77108-B	102,103 (Except Torsion Test)
	21732-AW	71888-B	102,103 (Except Torsion Test)
	21732-CE	74455-B	4731, 4732
	21732-DA	74455-B	1887 (Torsion Test Only)
Side Frames	21850	70635-B	63, 65
	21907-A	71224-B	9, 10
	21974	71739-B	6, 7

As seen, the Patt. 21732-DA bolster was used only for the torsion loading, whereas the other three bolsters' use applied to the vertical and transverse loadings. All castings were of 6" x 11" Ride Control design (5'-8" wheel base) with a rod-under brake rigging configuration (Patt. 21732-CE bolster uses ABSCO-type brakes).

PROCEDURE

Procedure for acquisition of all but bolster torsion data resorted to simple file research into records of previous AAR static deflection tests, which are standard for certification of new casting designs. Related vertical and transverse loading test set-ups and methods are those of AAR specifications M-202-67 and M-203-65 for bolsters and side frames, respectively. (Copies of test set-ups, as illustrated in the AAR manual, are included as Figure 35a, 35b and 35c. Basically, the deflection tests consists of loading specimens in set increments while monitoring corresponding deflection with dial gages. Casting set (indication of yield) is determined by noting dial gage offset from zero datum after release of a specific load. A 5,000 lb. zero datum load is standard for all AAR loading conditions to "settle" twist of non-uniform loading of the specimens.

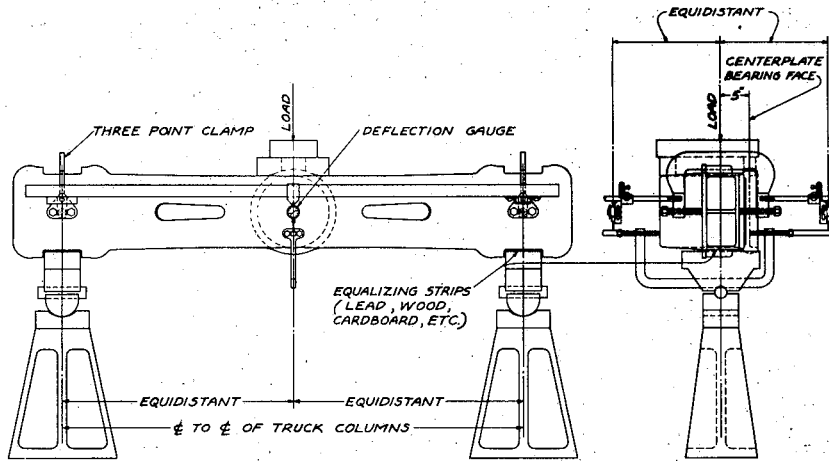
Typical AAR test loading sequence for a specific specimen restricts gross yielding until the final load set-ups, namely "vertical centerplate" for the bolster and "vertical" for the side frame. This procedure, while importantly ensuring good elastic deflection data for all loadings on a given specimen, limits yield point study for all but the noted loading set-ups. (Some tests, due to variations in procedure over the years, never grossly yielded the specimens; e.g. Patts. 21732-AW & CE bolsters).

AAR static certification tests require that two specimens of each pattern be subjected to the loadings, thereby providing

Fig. 35a

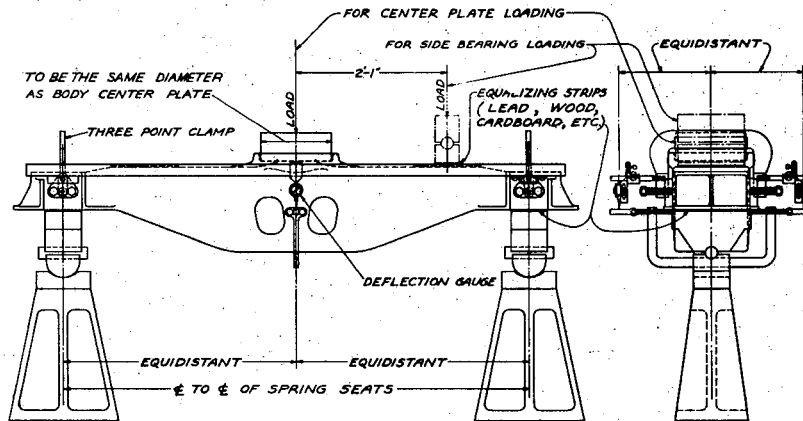
M-202-66
4

Association of American Railroads



NOTE:
SETUP IS TYPICAL; VARIATIONS ARE PERMITTED IN DESIGN OF APPARATUS, ALSO TO SUIT DESIGN OF BOLSTER, PROVIDED TEST RESULTS ARE NOT AFFECTED.

Fig. I

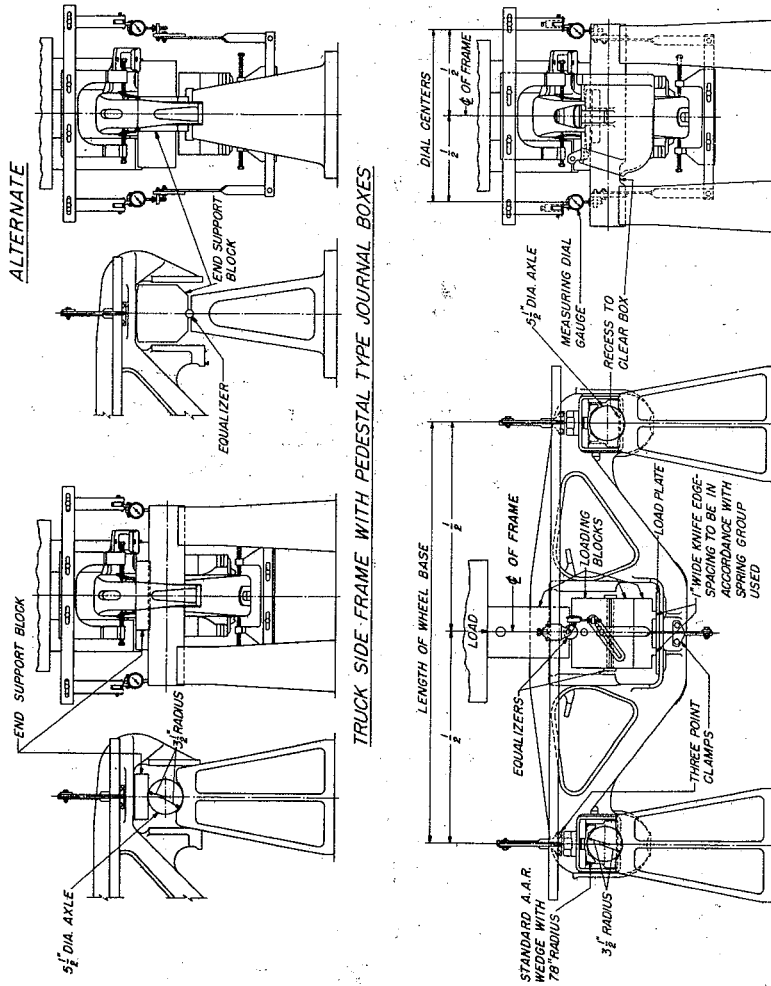


NOTE:
SETUP IS TYPICAL; VARIATIONS ARE PERMITTED IN DESIGN OF APPARATUS, ALSO TO SUIT DESIGN OF BOLSTER, PROVIDED TEST RESULTS ARE NOT AFFECTED.

Fig. II

A-1968

Fig. 35c



NOTE: SETUPS ARE TYPICAL; VARIATIONS ARE PERMITTED IN DESIGN OF APPARATUS, ALSO TO SUIT DESIGN OF SIDE FRAME, PROVIDED TEST RESULTS ARE NOT AFFECTED.

Fig. II

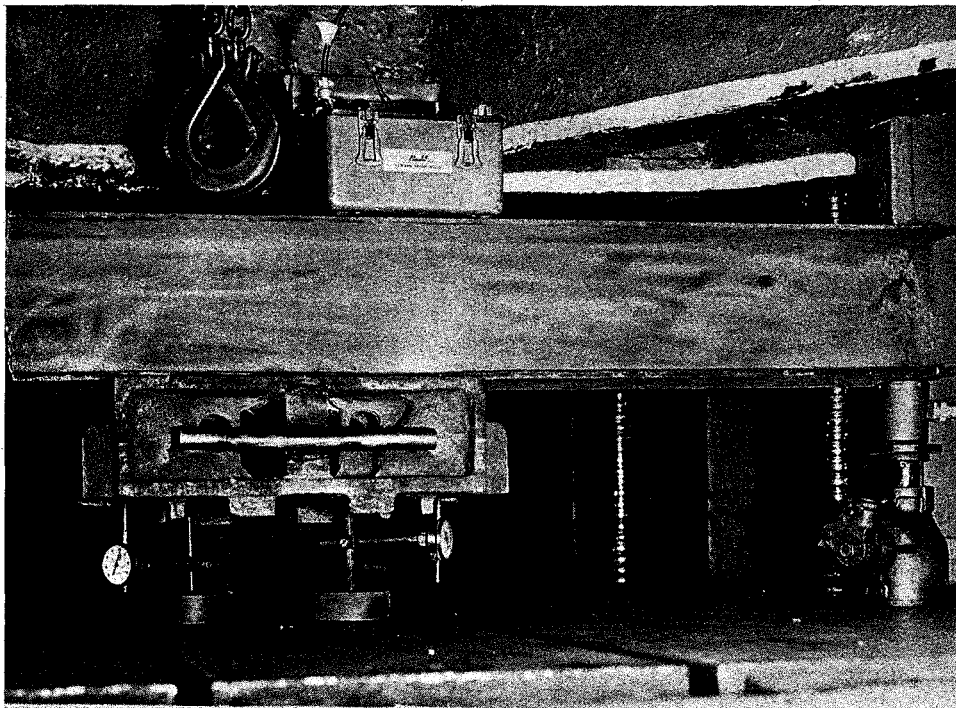
A-1962

a more statistically valid test and, in turn, providing two sets of data for appropriate averaging in this report. This should ensure development of reasonably representative deflection characteristics.

Bolster torsional deflection data were determined from application of the single Patt. 21732-DA specimen to the test set-up illustrated in Figure 36. With the casting "clamped" by the test machine at its centerplate, twist was imposed by the measured jack load acting through the known moment arm, resulting in a corresponding torque input. Dial gages located at the extremes of the spring seat provided "differential" twist measurements to comply with the imposed torque. For the small angles involved, the lineal dial gage motions were taken as arcuate displacement in calculation of twist angles.

Fig. 36

BOLSTER TORSIONAL LOAD RATE TEST SET-UP



Two vertical clamping loads (50,000 and 100,000 lb), were used to test for possible effect. The degree of angular deflection imposed was limited by the strength of the torque arm beam, which had been chosen to provide sufficient input, based on estimation of the torsional load rate.

As with the vertical and transverse deflection situations, the torsional data were applied in the form of load vs. deflection plots for graphical (slope) determination of the desired load rates. Torsional inputs were not sufficient to inflict set, but set data, where available from the vertical and transverse loadings, were also plotted on the deflection plots for convenient evaluation.

RESULTS

The load vs. deflection (and set, where appropriate) plots are presented in Figures 37 - 42. Summarizing deflection rate, set and yield point information are provided on page 60.

Vertical and Transverse Loadings

Generally, vertical and transverse load results are straightforward and require little comment. The load-deflection plots closely parallel typical stress-strain curves, thereby displaying characteristic linearity in the elastic range and increased deflection rate after yield point attainment (where applicable).

Recalling that a 5,000 lb. zero datum load was used for these tests, it is not surprising to see that the load-deflection plots intersect the ordinate axes in the neighborhood of this load level. The most consistent violation of this characteristic was displayed by the Patt. 21732-AW bolster plots which intersect the ordinate (with extrapolation) notably above the 5,000 lb. level for all of the three load set-ups. Explanation of the discrepancy appears to lie in a slight non-linear condition at the lower end of the deflection range which is not well defined by the relatively few data points. The given Patt. 21732-AW plots neglect the lower scale non-linearity, but should still be sufficiently accurate for most mathematical model situations.

Note that all individual castings displayed good deflection correlation with their "partner" specimen for all loading conditions. This implies that, not only are the given load rates reasonably accurate, but that specimens of a specific pattern display very similar and repeatable deflection characteristics. Furthermore, castings of similar general design have very similar load rates, as evident by the given individual rates being within 15% of average of the comparable patterns.

Bolster Torsion

The bolster torsional rigidity plot, Figure 40, illustrates a very linear load-deflection relation within the range

Fig. 37

BOLSTER RIGIDITY
— TRANSVERSE —

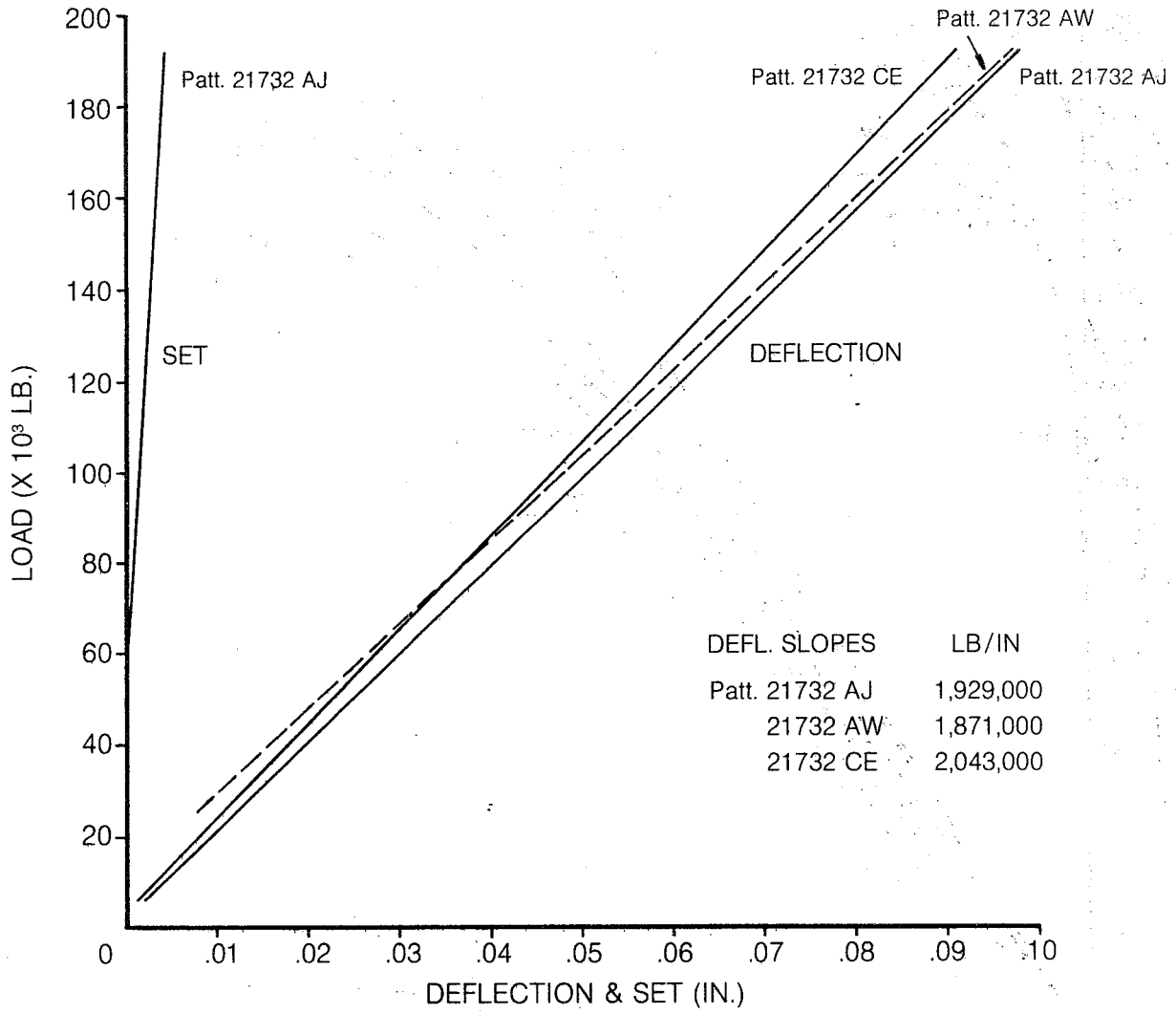


Fig. 38

BOLSTER RIGIDITY
— VERTICAL SIDE BEARING —

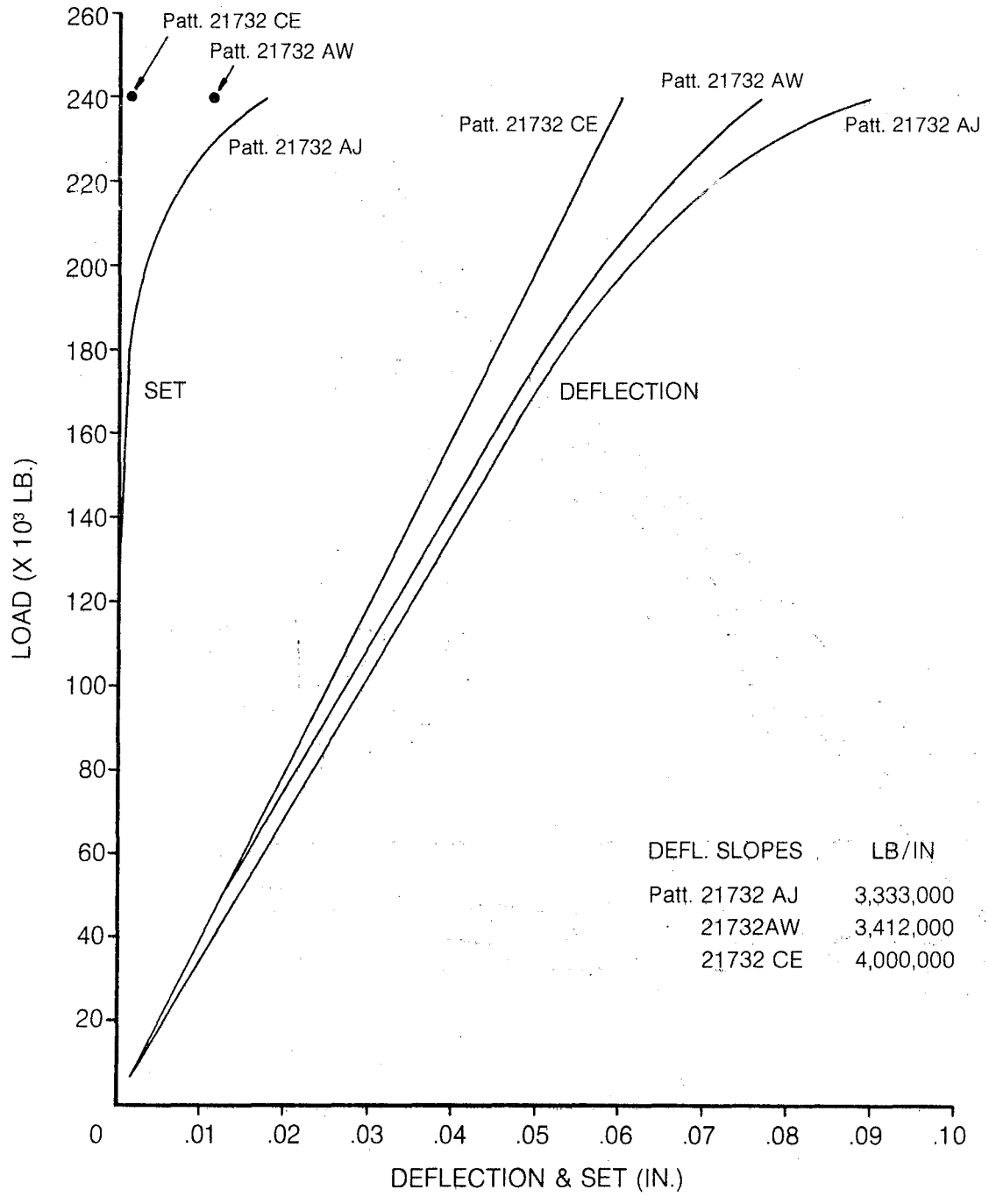


Fig. 39

BOLSTER RIGIDITY
— VERTICAL CENTERPLATE —

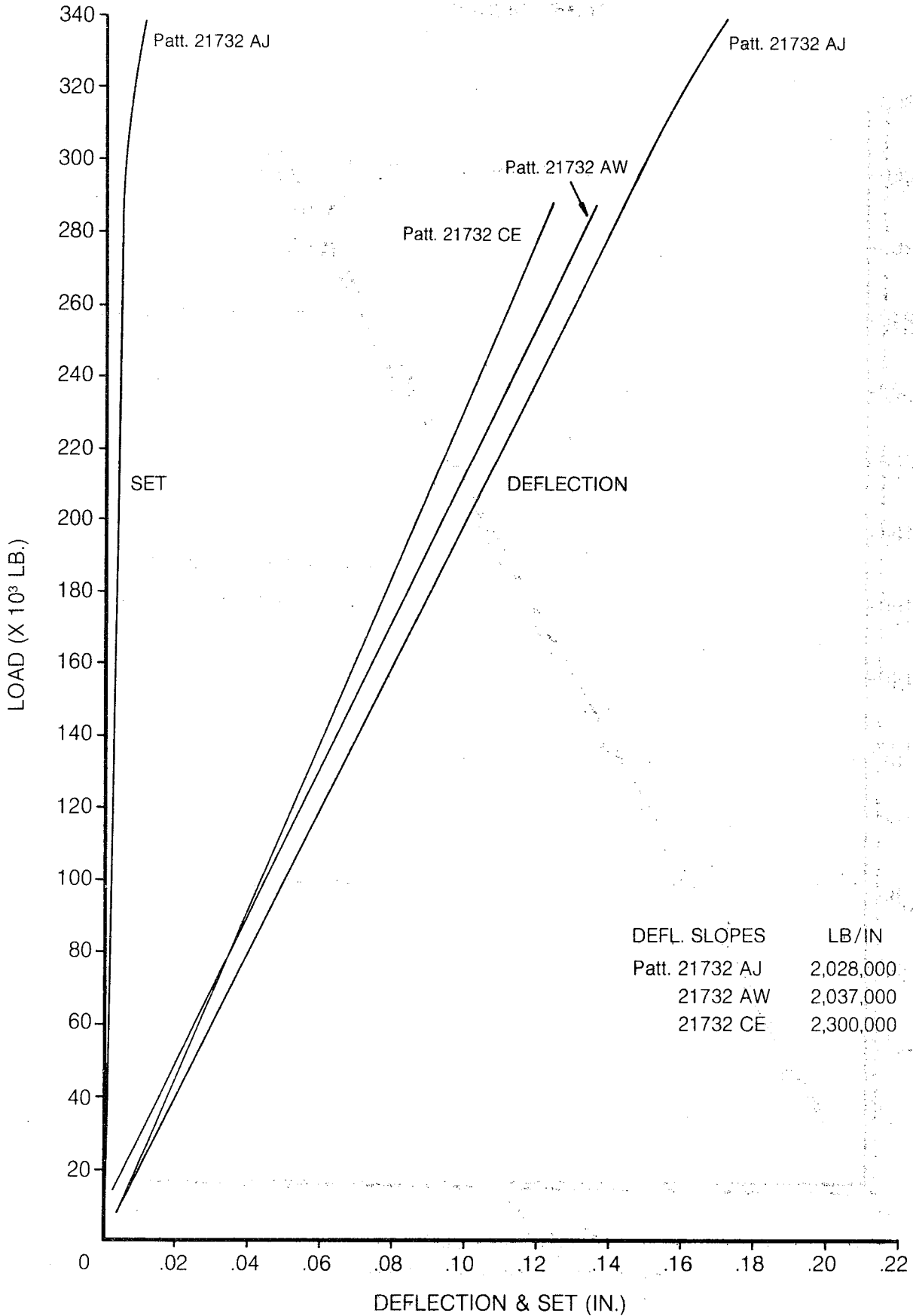


Fig. 40

BOLSTER RIGIDITY
— TORSIONAL —

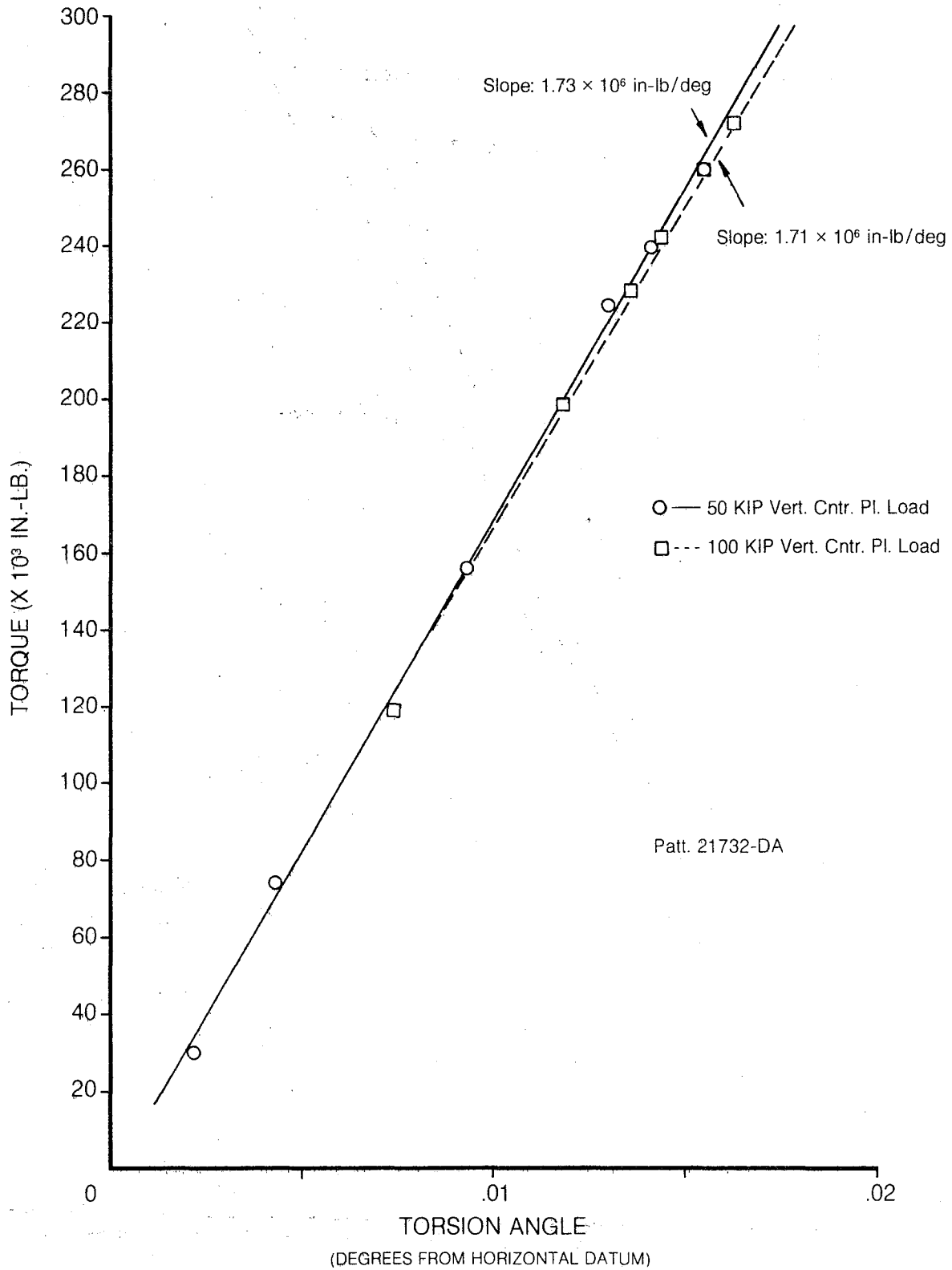


Fig. 41
SIDE FRAME RIGIDITY
 — TRANSVERSE —

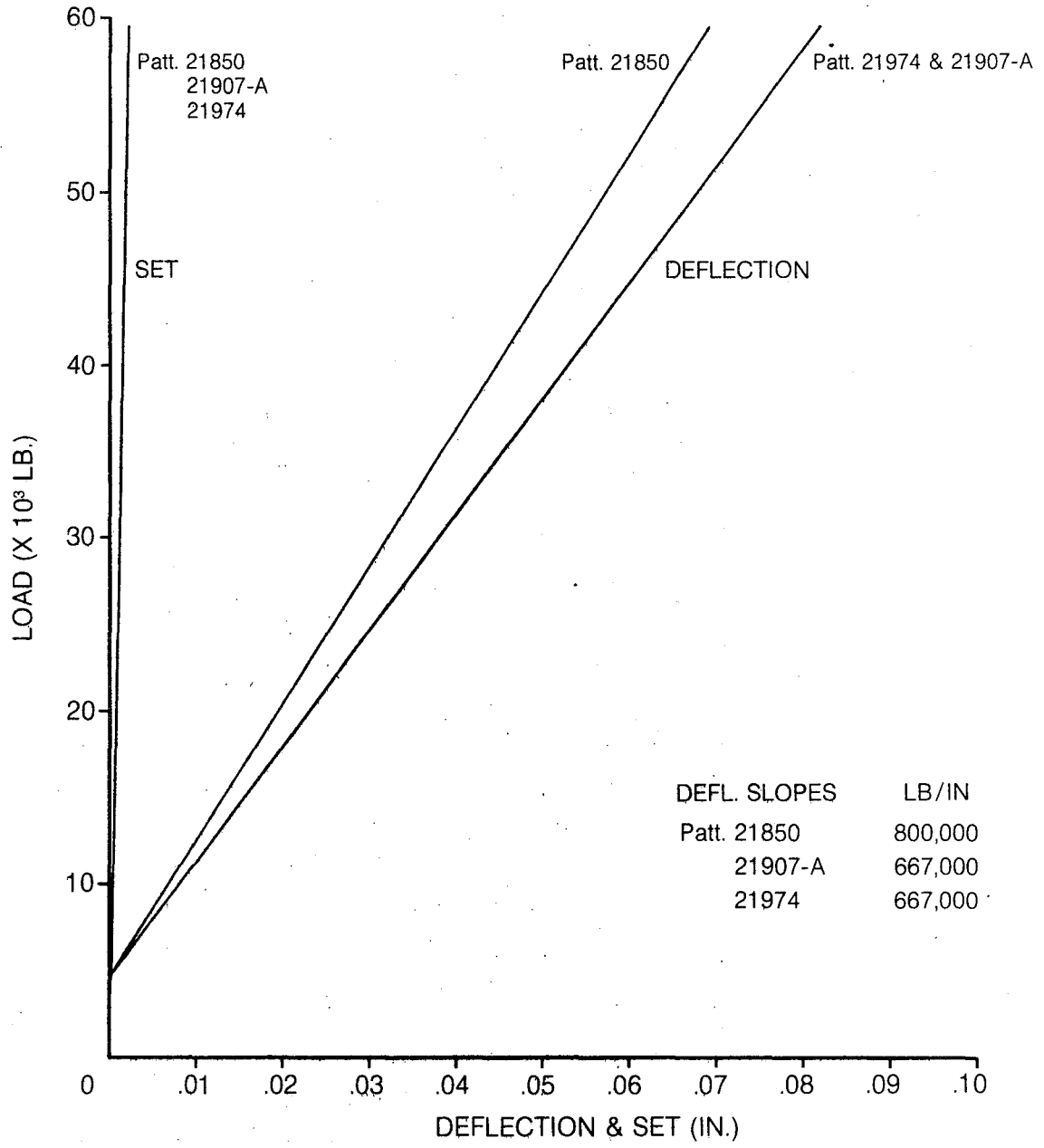
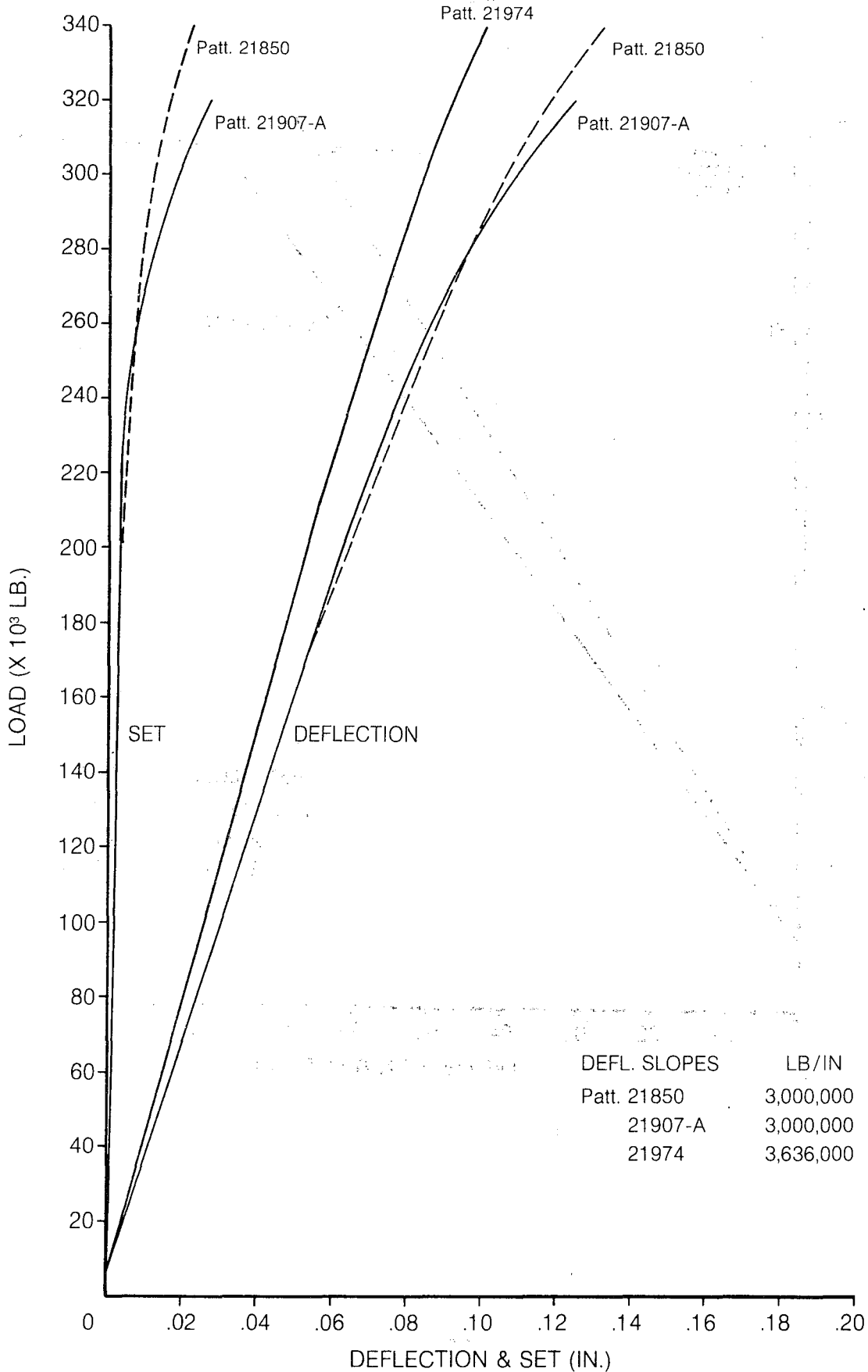


Fig. 42
SIDE FRAME RIGIDITY
— VERTICAL —



tested. The two vertical clamping forces were equally acceptable since they afforded similar results. Considering the very high load rate derived from the test plot, it appears that torsional load rate should be outside concern in most mathematical model situations since, except at solid height, the spring group is incapable of transmitting sufficient torque input for appreciable bolster torsion. Even at spring solid it would take roughly 50,000 lb input action at one wheel to instill a 1° twist in the bolster, assuming loading conditions similar to those in this test.

Other than torsional inputs at spring solid, the only other conceivable rail occurrence under "normal" situations which could provide high twisting loads is that which sometimes accompanies high speed coupling. Occasionally, excess coupling speed can rotate the bolster sufficiently to jam it with the side frame, thus providing a positive twisting interface should additional twisting energy be present. But, this is hardly a ride quality consideration.

TRUCK BOLSTER AND SIDE FRAME DEFLECTION CHARACTERISTICS

6" x 11" RIDE CONTROL COMPONENTS

TRUCK BOLSTERS

PATT. NO.	LOAD RATE (x 10 ⁶ LB/IN)		SET (In. After Lb*)		ELASTIC LIMIT (LB)			
	Trans.	Vert. Side Brg.	Trans.	Vert. Cntr. Pl.	Vert. S.B.	Vert. C.P.		
21732-AJ	1.929	3.333	2.028	.0038 (192,000)	.0176 (240,000)	.0046 (288,000)	375,000	
21732-AW	1.871	3.412	2.037	.0038 "	.0113 "	.0044 "	Not Available	
21732-CE	2.043	4.0	2.30	.0028 "	.0013 "	.0018 "	"	
21732-DA	1.72 x 10 ⁶ In-Lb/Deg. (Torsional)							

SIDE FRAMES

	Vertical		Vertical	
	Transverse	Vertical	Transverse	Vertical
21850	0.8	3.0	.0024 (60,000)	.0046 (225,000)
21907-A	0.667	3.0	.0033 "	.0034 "
21974	0.667	3.636	.0026 "	.0016 "

* GROSS MACHINE LOAD (INCLUDES 5,000 LB. DATUM LOAD).

TORSIONAL RESISTANCE AT A TRUCK
BOLSTER/CAR BODY CENTERPLATE INTERFACE

Test Report - Part IV

American Steel Foundries Participation In
AAR/RPI/FRA Track-Train Dynamics Program

OBJECT

Determine the frictional resistance to torsional relative motion between car body and truck bolster centerplates. Primary test conditions include use of a "worn-in" diameter bolster centerplate with both lubricated and non-lubricated (dry) surface.

CONCLUSIONS AND RECOMMENDATIONS

3.0 (dry) and .41 (lubricated) in-lb/lb. vertical load are torsional friction rates recommended for mathematical uses simulating the conditions of this test. These figures correspond to sliding co-efficients of friction, μ_s , of .624 and .09 for dry and lubricated surfaces, respectively, and do not account for any interaction between the vertical centerplate surfaces. Breakaway (static) friction figures were generally no higher than those for the sliding conditions.

In the process of data acquisition for development of the indicated friction rates, it became clear that, while the "lubricated" information should relate well to service conditions of similar nature, the range of centerplate conditions definable as "dry", compounded by possible surface galling, renders the actual service friction rate subject to considerable variation (perhaps 45%) from the test friction rate given.

TEST SPECIMENS

Test specification for use of a worn-in 14" diameter centerplate was satisfied by mating an on-hand car body centerplate (nominal 13-3/4" outside dia., 3-3/8" dia. king pin hole) and a 100-ton bolster with 15" diameter centerplate. Both of these items were well worn-in from previous on-track test usage and possessed typical smooth and gall-free appearance.

As a secondary test and for general information, a new Patt. 21732-DA truck bolster was also enlisted for use with the previously-mentioned car body centerplate. This bolster had been acquired to serve as the primary specimen in other phases of the Track-Train Dynamics program, but its as-cast centerplate surface, wear-in of which was impractical, disqualified it from primary usage in this test phase.

PROCEDURE AND TEST FIXTURE

Data were acquired through application of the specimens to the fixture illustrated in Figure 43 & 44. The basic function of the apparatus was to turn the car body centerplate relative to the restrained bolster during application

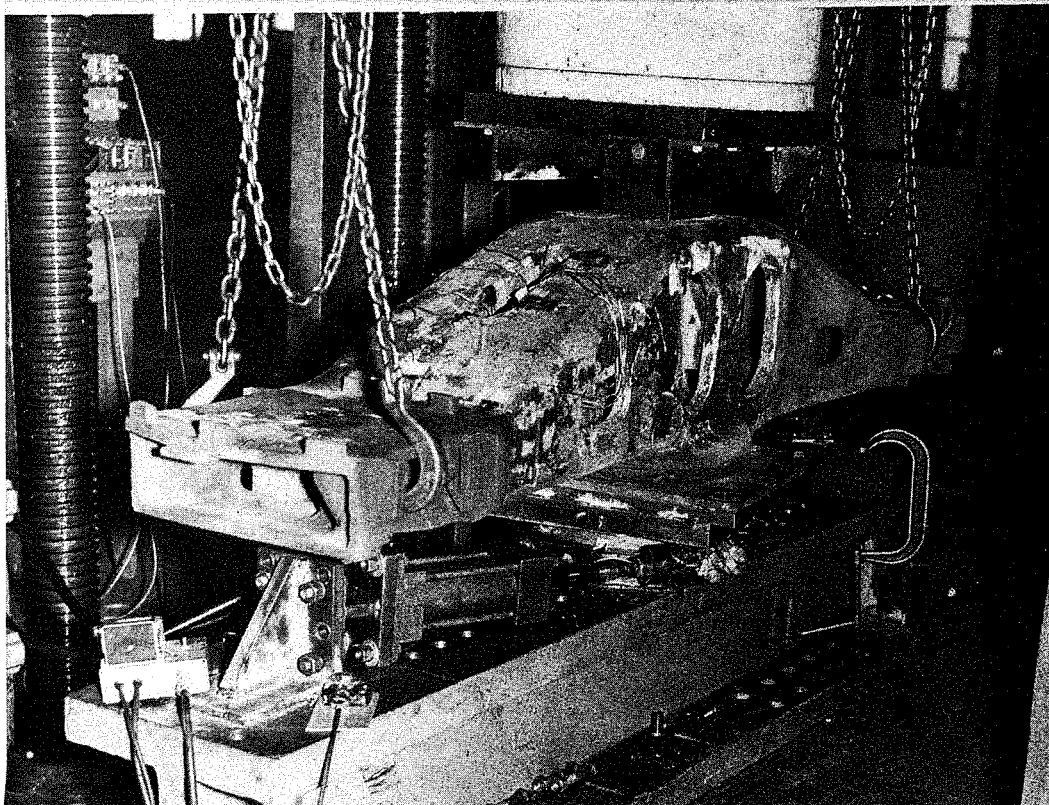


Fig. 43

CENTERPLATE TORSIONAL FRICTION TEST SET-UP

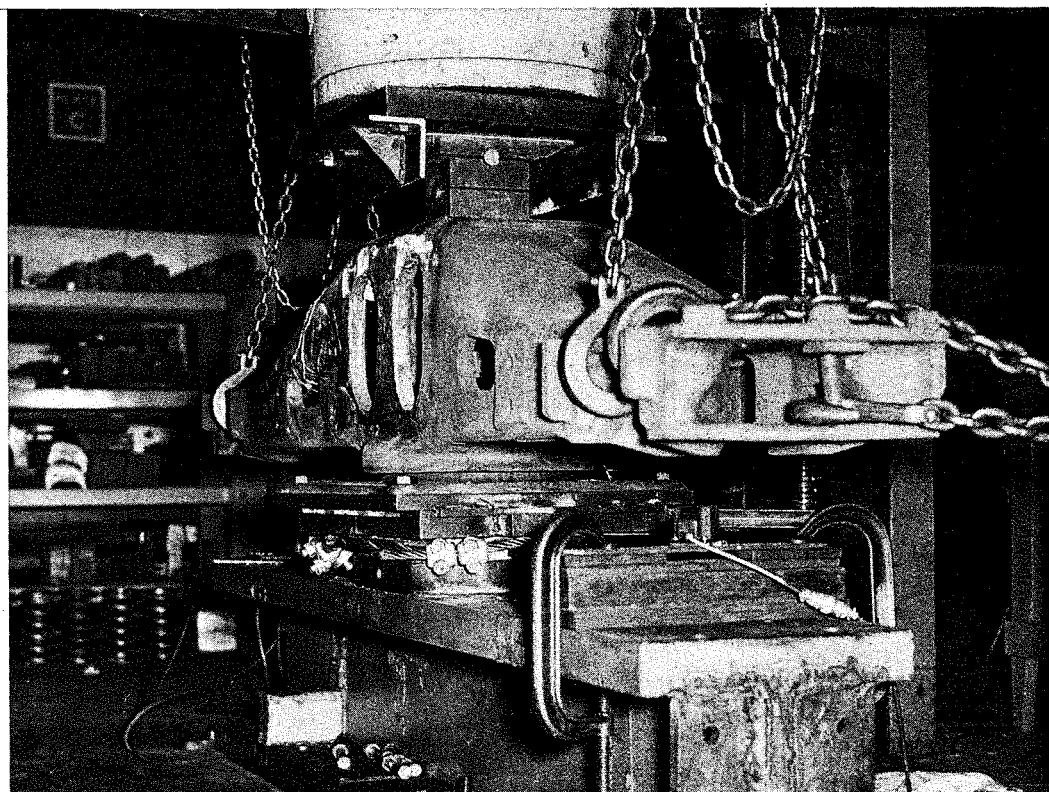


Fig. 44

of a constant vertical centerplate load. The torque required to induce the motion, obtained as a function of applied vertical load, yielded the desired torsional friction rate.

Figure 45 helps to simplify understanding of the fixture operation. As shown, the car body centerplate was bolted to a rotatable platform which was itself isolated from the base plate and I-beam structure by a greased sheet of 1/8" thick teflon. The teflon was used to diminish friction between the turning platform and base plate, and thereby establish frictional resistance at the car body and bolster centerplate interface as the primary resistance to the turning relative motion. A stud and free-turning radial bearing located and retained the platform center (also car body centerplate center) at the base plate center.

Turning force was applied to the car body centerplate/platform assembly by the hydraulic cylinder/cable system acting through a partial sheave. A load cell between the cylinder and cable clevis measured the axial cable load, which was later transformed to torque by multiplication with the known sheave radius. A displacement transducer mounted on the I-beam monitored location and movement of the car body centerplate with respect to the bolster. With an actuator stroke capability of 6", arcuate displacement per test event were in the neighborhood of 20°. An oscillograph recorded the axial load and displacement signals.

Vertical loads were applied to the bolster bottom through a double rocker block to equalize loading and counter possible non-parallelism between test machine and centerplate surfaces. Vertical load magnitudes were chosen on logical steps to provide a range from zero to roughly one-half loaded weight of a 70-ton car. (Dry tests were limited by strength of the cable assembly). The sequence of vertical loading for the dry surface phase generally resorted to use of three widely spaced loads to achieve significant data range before possible galling altered the frictional characteristics. Fill-in points were then conducted as required. Since galling was not a problem with the lubricated centerplate, loads in this phase were simply increased from zero in even increments.

Pre test conditioning of the centerplate surfaces included wire brushing and solvent cleaning to remove all traces of lubricating grease or dirt. Occasionally during the dry surface testing, the centerplate surfaces were separated and any galling removed by grinding. "Moly-kote" served as the grease in the lubricated testing.

Torque data were acquired for both as-cast and worn-in bolsters under both dry and lubricated conditions, with

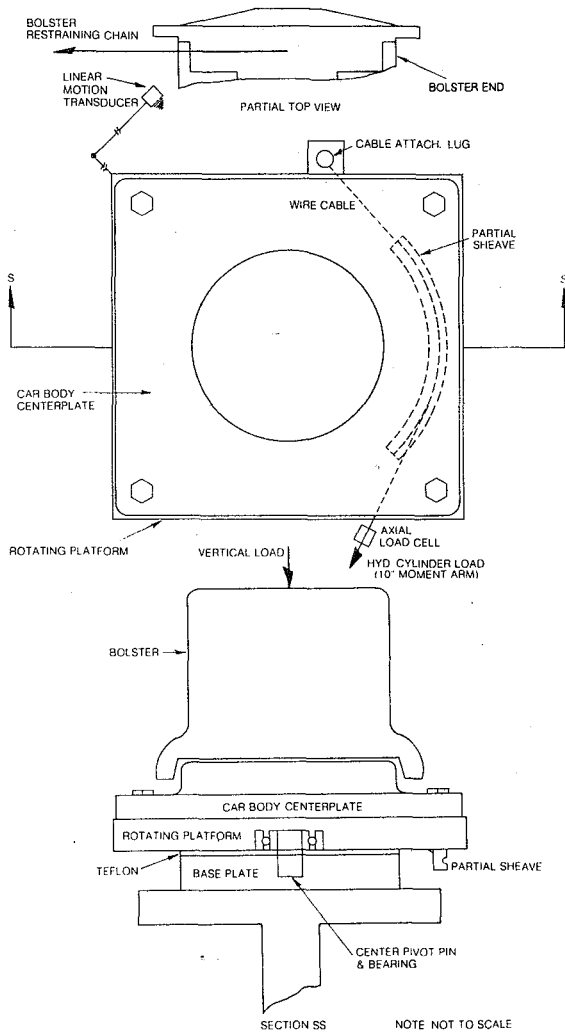


Fig. 45
 CENTERPLATE TORSIONAL
 FRICTION TEST SET-UP

worn-in surface receiving primary consideration. Since the teflon used to reduce friction between the turning car body centerplate assembly and base plate was not actually friction-free, calibration tests were also conducted. These consisted of "lubricating" the centerplate surfaces with another teflon sheef and running the torque tests through a similar gamut of vertical loads. One-half of the applied torque was taken as the teflon friction loss for the centerplate tests, and was appropriately subtracted, proportionately with vertical load, from the measured dry and lubricated data.

Test method consisted simply of zeroing position of the car body centerplate, applying vertical load and then applying cable tension until cylinder run-out, with effort toward

producing a constant and unabrupted motion. Essentially, each data pull or event such as this provided two primary points of information: the break-away (static friction) load, and the sliding motion friction load. The upper sample oscillograph recording in Figure 46 illustrates these points for a data event. Note that the deflection trace was used primarily for reference since specific position is actually irrelevant to friction characteristics.

The measured break-away and sliding loads, when appropriately multiplied by the radius moment arm (10"), supplied the desired torque loads for the particular vertical load and conditions of the test. The data were then applied to a plot with points from other vertical loads to enable graphical (slope) determinations of the friction rates.

Relating the torque/vertical load data to coefficient of friction was accomplished by solving the following formula for

$$T = 2/3 \frac{R_2^3 - R_1^3}{R_2^2 - R_1^2} P,$$

where: P = vertical load
 T = torque input
 = coefficient of friction
 R₁ = 1-11/16" nominal radius of car body center-plate king pin hole
 R₂ = 6-7/8" = nominal outer radius of car body centerplate

RESULTS AND DISCUSSION

Results converge to the torque/vertical load plots of page 69 and the following summarizing table derived therefrom.

	<u>Friction Rate (Sliding)</u> <u>(in-lb/lb vert.)</u>	<u>Sliding</u>
Worn-in Bolster		
(a) lubricated (Moly-kote)	0.41	.09
(b) lubricated (Teflon)	0.41	.09
(c) dry	3.0	.624
As-cast Bolster		
(a) lubricated	0.72	.15
(b) dry	2.5	.520

As might be expected, the lubricated as-cast centerplate was somewhat "stickier" than the greased worn-in surface, whereas the opposite was true for the surfaces in the dry test condition. This logically relates to the many peaks of

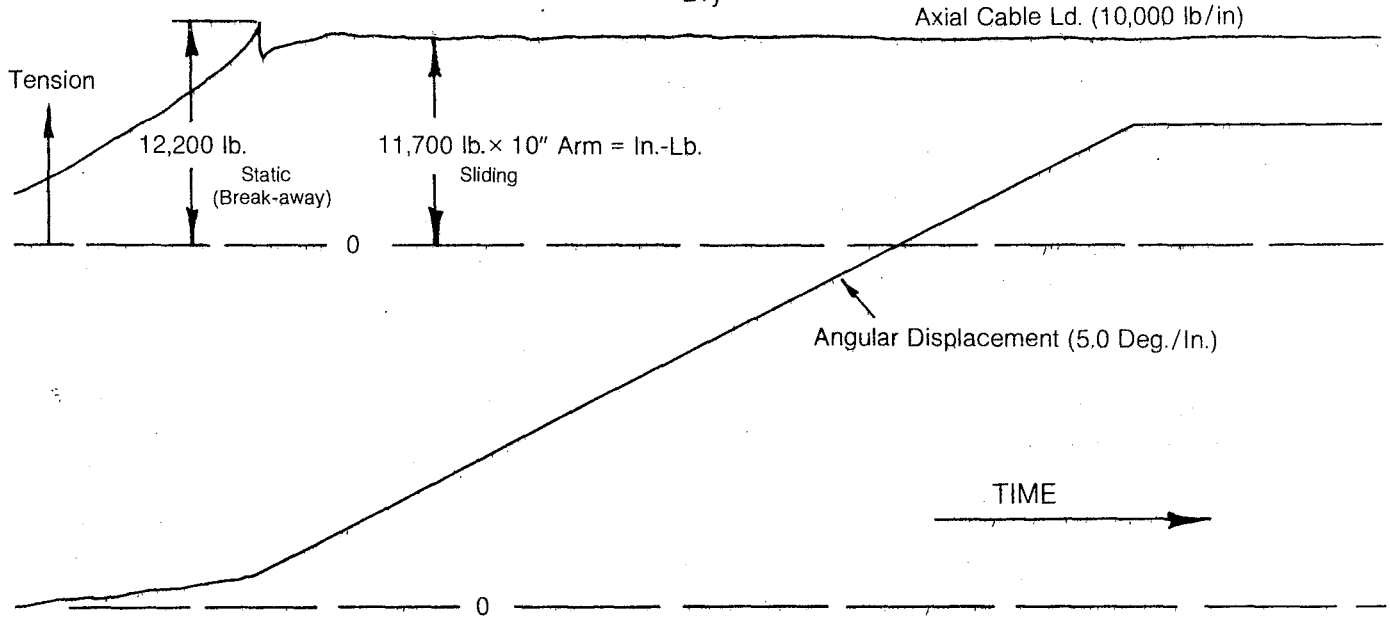
Fig. 46

50,000 LB VERTICAL LD.

13 3/4" Car Body C.P.

Worn-In Bolster

"Dry"

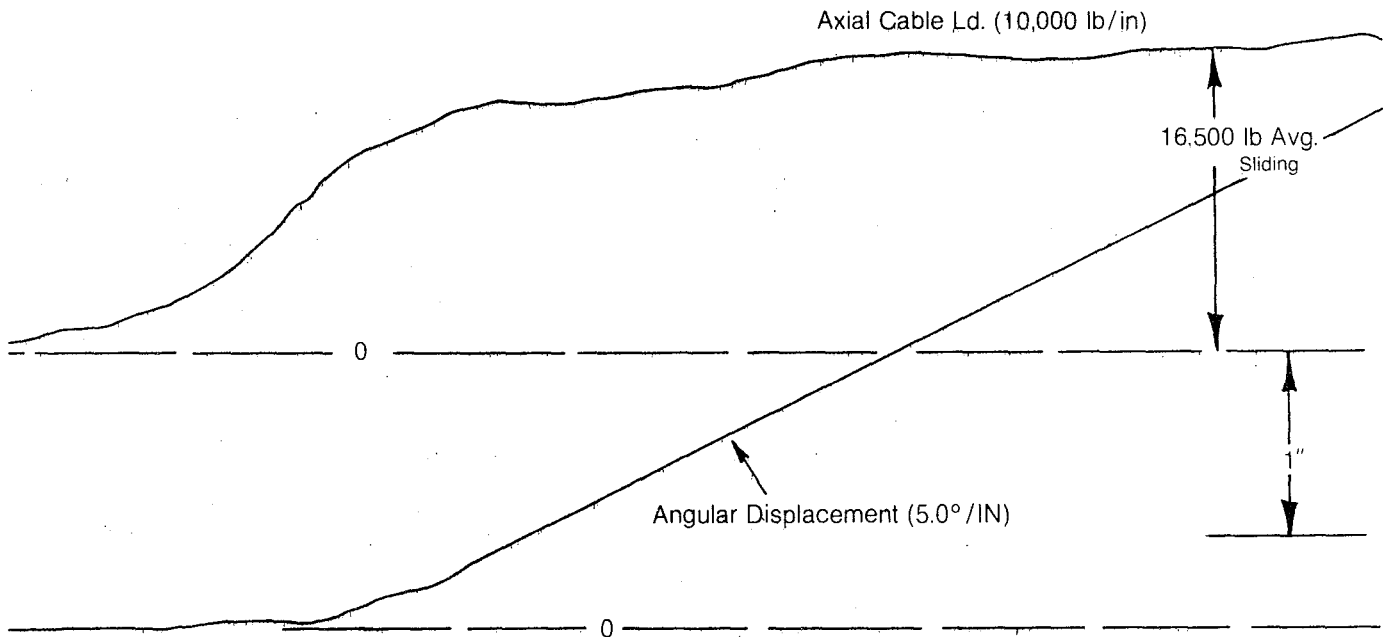


50,000 LB VERTICAL LD.

13 3/4" Car Body C.P.

Worn-In Bolster

"Dry"



the rough as-cast surface which tend to "pierce" lubricant, but offer less adhesion than the flat, smooth surface under dry conditions. In any case, an as-cast surface will wear in quite rapidly under typical service and should therefore require little concern in mathematical simulations. As an aside, note that the Moly-kote grease and the teflon sheet afforded nearly identical friction reduction when applied to the worn-in centerplate.

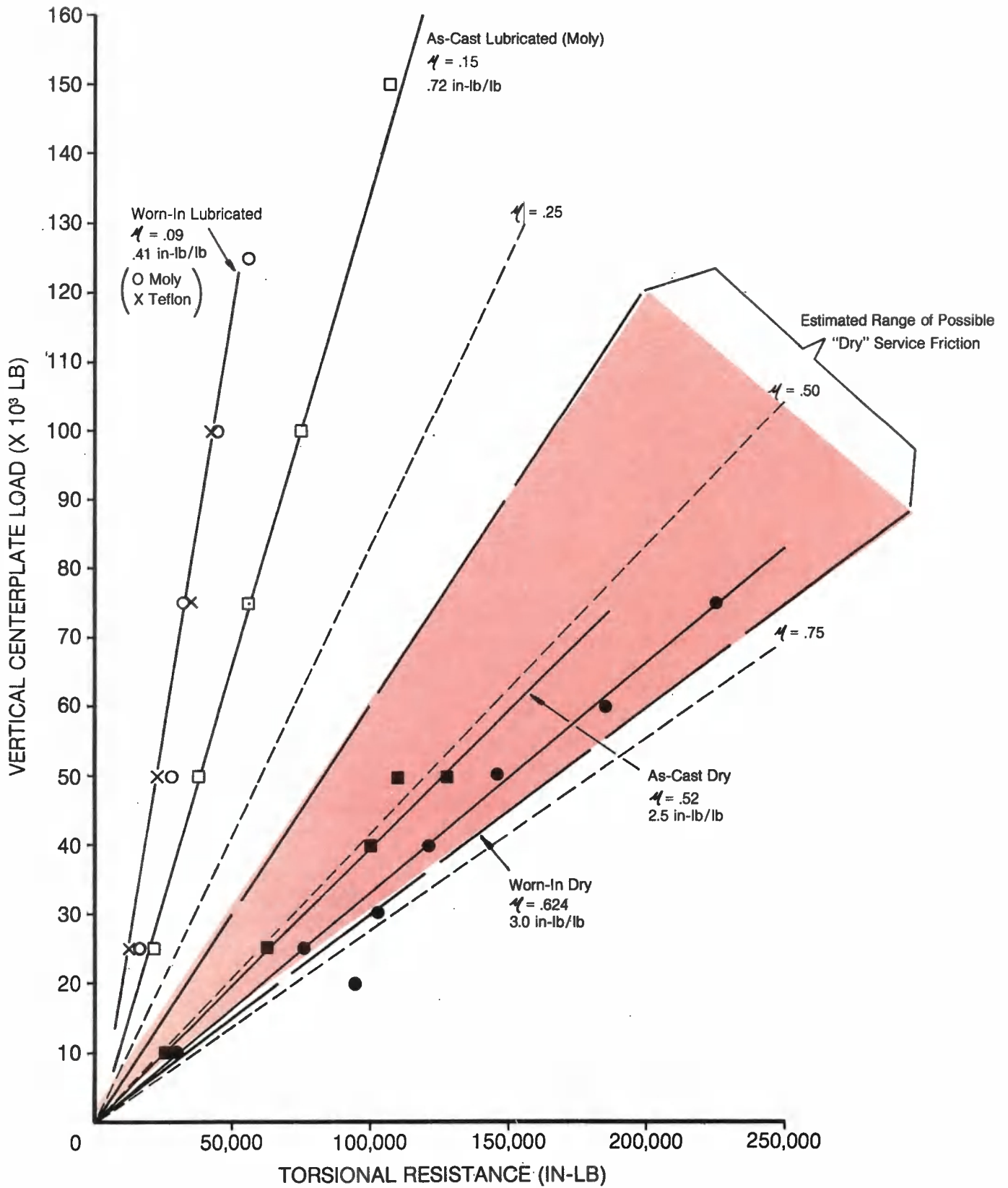
The above table and enclosed data plot offer no information about static friction because test events usually did not exhibit breakaway loads greater than the steady sliding forces, if any were present at all. In fact, the lower oscillograph recording on page 67 illustrates a more typical force curve than that of the nearly ideal upper recording. For instances in which break-away was prominent (less than 10% of the data events) it was on the order of 5 to 15% (8% average) greater than the steady sliding friction force, and was most consistent for the dry, as-cast surface test conditions.

As the plots of Figure 47 indicate, all events related to lubricated test conditions produced very linear and repeatable data. But, as hinted in the Procedure report section, non-lubricated test conditions were very inconsistent, thereby complicating derivation of a representative friction rate. The given data points (reference to worn-in test) do not appear excessively scatter-prone because they were chosen as most representative from the many points scattered about the relative graph area. Criteria for data acceptability was based on relationship with other data and judgment of possible bias from surface galling, which tended to markedly increase turning force. (Since service centerplates are usually gall-free, gall-free data were obviously most desirable for this test). As it turned out, the majority of data points plotted for the worn-in case were taken from a single series of events, primarily because they displayed roughly linear relationship (indication of constant surface conditions), with near gall-free appearance at termination.

The dry testing made it obvious that similar scatter was even more probable under dry service conditions due to the possible presence of dirt and residual lubricant. Realistically, service friction rate for any random condition could span the lubricated and dry rates of this report. However, from a practical model standpoint, the given lubricated rates should be service representative of that condition. The dry test rate for the worn-in centerplate would probably be on the high (sticky) side of average service conditions because of the laboratory-clean surfaces and galling tendency. Based on the data scatter experienced, estimation of the possible range of dry friction rates in service modifies the given 3.0 in-lb/lb test rate by + 10% (3.3 in-lb/lb) to -45% (1.65 in-lb/lb). An average service rate might split the extremes at about 2.5 in-lb/lb.

Fig. 47
CENTERPLATE TORSIONAL FRICTION
14" DIA. TRUCK BOLSTER C.P.

—Data Corrected For Teflon Bearing Friction
 —All Data Relate To Steady Sliding Motion



THEORETICAL CLEARANCES AND RESULTING
POSSIBLE RELATIVE MOTIONS BETWEEN
TRUCK BOLSTER, SIDE FRAME AND AXLE BEARING

Test Report - Part V

American Steel Foundries Participation In
AAR/RPI/FRA Track-Train Dynamics Program

OBJECT

Determine existing clearances and resulting possible relative motions between defined major truck components for use in mathematical model analysis.

CONCLUSIONS

Manufacturing tolerances of side frames and truck bolsters provide a relatively wide range of possible clearances. These, in turn, allow variations in possible component motions that would appear to be significant in any cause and effect study on a mathematical truck model.

SPECIMENS

For the purposes of this study, major truck components are defined as follows:

<u>Components</u>	<u>ASF Piece No.</u>	<u>ASF Drg. No.</u>
Ride Control Truck Arr'g't.		74524
Side Frame	21850-R	74098-K
Truck Bolster	21732-DA	74455-B
Ride Control Spring	3091	54222-D
D-5 Outer Coil	3072	31981-003
D-5 Inner Coil	3073	32506-129
6"x11" Roller Brg.		
Roller Brg. Adapter (Standard AAR)		

PROCEDURE

Brief consideration was given to the idea of assembling the subject test truck and physically measuring the various clearances and relative motions. However, the known variations due to manufacturing tolerances quickly ruled out the physical approach because of the considerable time and cost involved in duplicating the possible variations in hardware.

A theoretical approach was deemed a very satisfactory substitute. The result of the theoretical approach is a series drawing board layouts depicting the possible variations in clearances and resulting motions.

All working layouts were made full scale so a high degree of accuracy in measurements could be maintained. Geometry was used, whenever possible, to determine the relative motions.

However, on several occasions, it was necessary to "scale off" a dimension because of too many unknowns.

The general approach to each layout was to:

- 1) Decide on type motion possible (rotation, etc.)
- 2) Define limits of motion (contact points).
- 3) Construct full scale layout.
 - a) Nominal dimensions
 - b) Maximum dimensions (tolerances)
 - c) Minimum dimensions (tolerances)
- 4) Superimpose desired motion (bolster rotation relative to side frame, etc.) on layout.
- 5) Calculate (or measure) extremes of motions for nominal, maximum and minimum clearances.
- 6) Reduce layout to scale convenient for reporting.

As noted, each layout (except no. 12) is shown under three conditions - nominal dimensions and dimensions imposed by maximum and minimum tolerances.

RESULTS

Sketches, numbered 1 thru 12, (Figures 48-59) show clearance and motions deemed most important for meeting stated objective of this study. Table on page 74 summarized the results of the study. Table shows the maximum, nominal and minimum possible peak-to-peak motions. Angles shown on the sketches are corrected to the decimal system in the tabulation.

Limits of motion ranges occur when minimum tolerances on one component are matched up with maximum tolerances on the paired component. A simple example is the Lateral Bolster Motion Relative to the Side Frame condition shown in sketch no. 2 (Figure 49). Maximum bolster gib width (9-1/2") matched peak-to-peak relative motion of 1-1/16". Reversing the tolerances (minimum bolster gib width and maximum side frame column width) produces a minimum peak-to-peak relative motion of only 11/16". Nominal peak-to-peak motion of this location is 7/8". Thus, the tolerances in this instance can allow motion anywhere from nominal to plus or minus 21%.

Relative range of variation is even greater for several locations. One location that may be of particular interest when studying truck swivel (hunting) is axle yaw inside the side frame pedestal, shown in sketch no. 11 (Figure 58). Maximum yaw with nominal dimensions is calculated to be 5.932° . Maximum and minimum yaw angles (with proper tolerances matches) are 7.184° and 3.447° , respectively. Here, the tolerances can allow yaw angles anywhere from nominal to plus 21% or minus 42%.

Examination of the summary table shows many such "clearance" ranges. Naturally, various clearance ranges can be examined in various combinations. For instance, maximum side frame yaw can be combined with minimum axle yaw. Or, the maximums and minimums can be reversed for a different effect.

Care must be exercised when combining various motions for study. It is possible that maximum limits of motion at one interface would prevent the maximum limits of motion from occurring at a second interface. For instance, side frame rock (roll) relative to the bolster end could not reach the maximum angle because of limits imposed at the axle bearing/side frame pedestal interface.

Note, also, that the possible effects of brake beam interference are noted on the sketches, but not measured. The brake beams were not included in the truck defined by Task #13 for the clearance study and would appear to be of little importance at this time. Although the beams may have some limiting effects on motions, limits would apply only to a rocking side frame near the outer limits of motion.

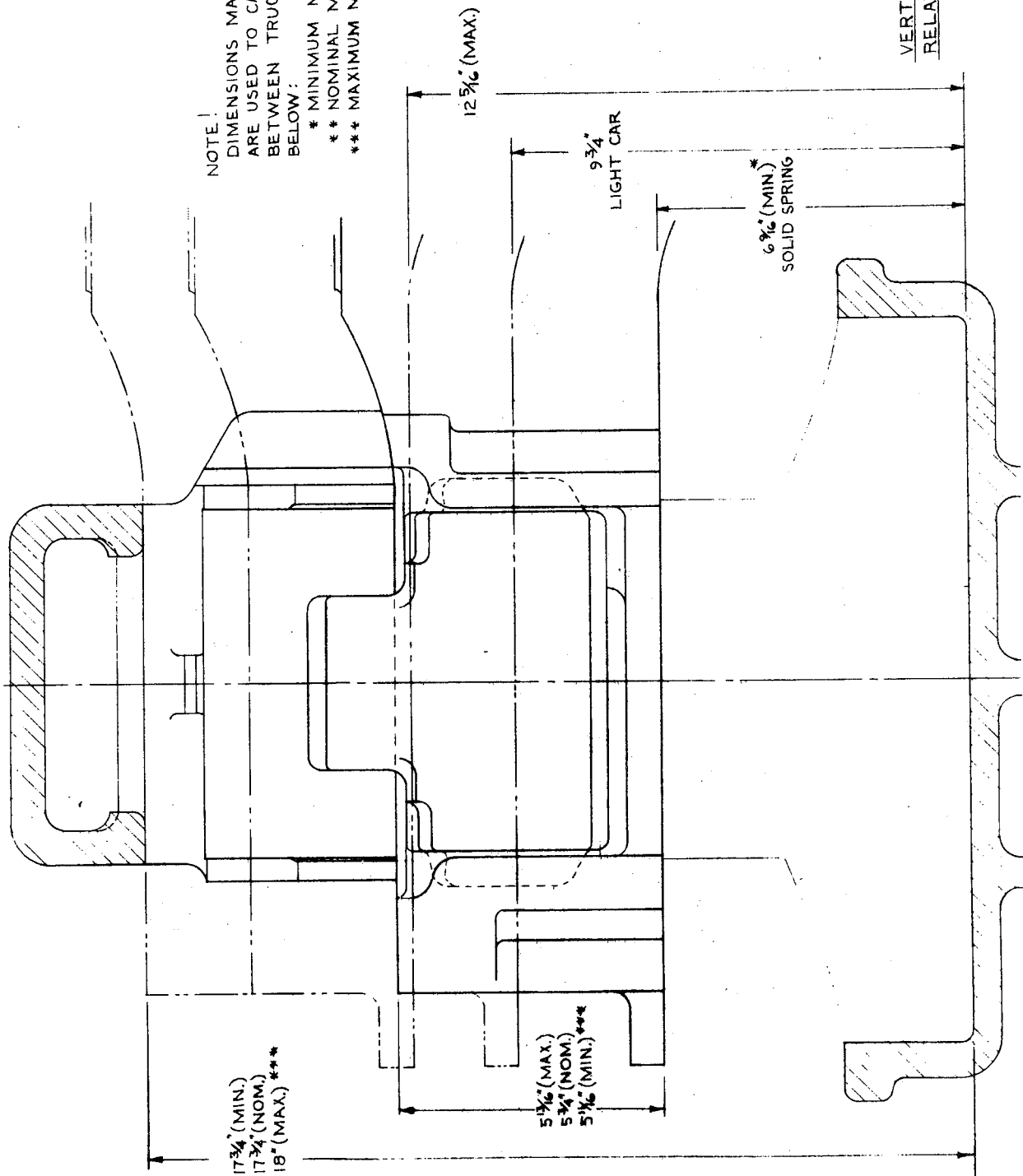
It should be emphasized that all the clearances and motions presented herein are based on "unworn" truck conditions. Although test truck has been defined as a vehicle with 5000 miles service, wear (actual loss of significant metal) is considered negligible.

TABLE OF
TRUCK COMPONENT RELATIVE MOTIONS ("CLEARANCES")

70-TON ASF RIDE CONTROL TRUCK (ASSM. DRG. NO. 74524)
BOLSTER: PATT. NO. 21732-DA, DRG. NO. 74455-B
SODE FRAME: PATT. NO. 21850-R, DRG. NO. 74098-K

SKETCH NO.	SUBJECT	POSSIBLE MOTION (PEAK-PEAK)			REMARKS
		MAXIMUM	NOMINAL	MINIMUM	
1	Vert. Bolster Motion Relative to Side Frame	12-5/16"	TO 6-9/16"	Bolst.-to-S.F. Spring Seat Height	
2	Lateral	"	7/8"	11/16"	Gib-To-Gib
3	Side Frame Longitudinal Mot. Rel. to Bolster	3/8"	3/16"	1/16"	
4	" Pitch	"	4.675°	1.90°	@ 8" Coil Height
5	"	"	4.858°	2.202°	@6-9/16" (Solid) Height
6	" Rock*	"	12.010°	9.954°	Positive Camber
7	"	"	11.866°	-8.637°	Negative Camber
8	" Yaw	"	2.921°	1.167°	
9	Bolster Rock Rel. to Assembled Truck	7.393°	6.940°	6.753°	Level Road Bed
10	Longitudinal Axle Mot. Rel. to S.F. Pedestal	23/32"	7/16"	3/8"	
10	Lateral	"	3/32"	1/16"	
11	Axle Yaw	"	5.932°	3.447°	
12	Side Frame Rock Rel. to Bearing Adapters		15°		

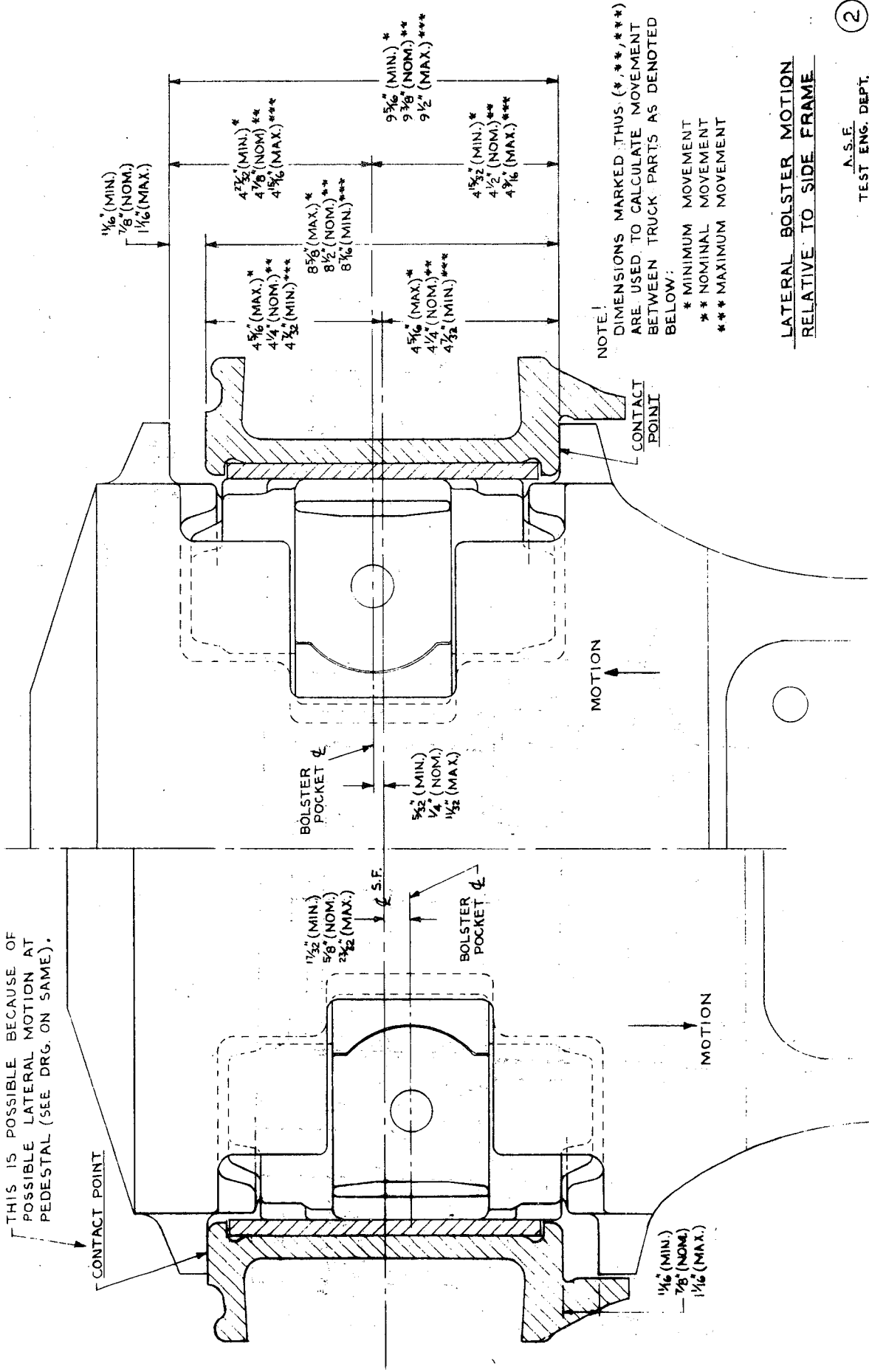
* Not Peak-To-Peak



NOTE!
 DIMENSIONS MARKED THUS (*, **, ***)
 ARE USED TO CALCULATE MOVEMENT
 BETWEEN TRUCK PARTS AS DENOTED
 BELOW:
 * MINIMUM MOVEMENT
 ** NOMINAL MOVEMENT
 *** MAXIMUM MOVEMENT

Fig. 48

THIS IS POSSIBLE BECAUSE OF POSSIBLE LATERAL MOTION AT PEDESTAL (SEE DRG. ON SAME).



LATERAL BOLSTER MOTION
RELATIVE TO SIDE FRAME

A.S.E.
TEST ENG. DEPT.

2

Fig. 49

☉ BOLSTER

☉ SIDE FRAME ☉

NOTE!

DIMENSIONS MARKED THUS (*, **, ***) ARE USED TO CALCULATE MOVEMENT BETWEEN TRUCK PARTS AS DENOTED BELOW:

- * MINIMUM MOVEMENT
- ** NOMINAL MOVEMENT
- *** MAXIMUM MOVEMENT

☉ (MIN.)
☉ (NOM.)
☉ (MAX.)
EQUALS PEAK TO PEAK SIDE FRAME LONGITUDINAL MOTION RELATIVE TO BOLSTER ENDS.

☉ (MIN.)
☉ (NOM.)
☉ (MAX.)

☉ (MIN.) *
☉ (NOM.) **
☉ (MAX.) ***

☉ (MAX.) *
☉ (NOM.) **
☉ (MIN.) ***

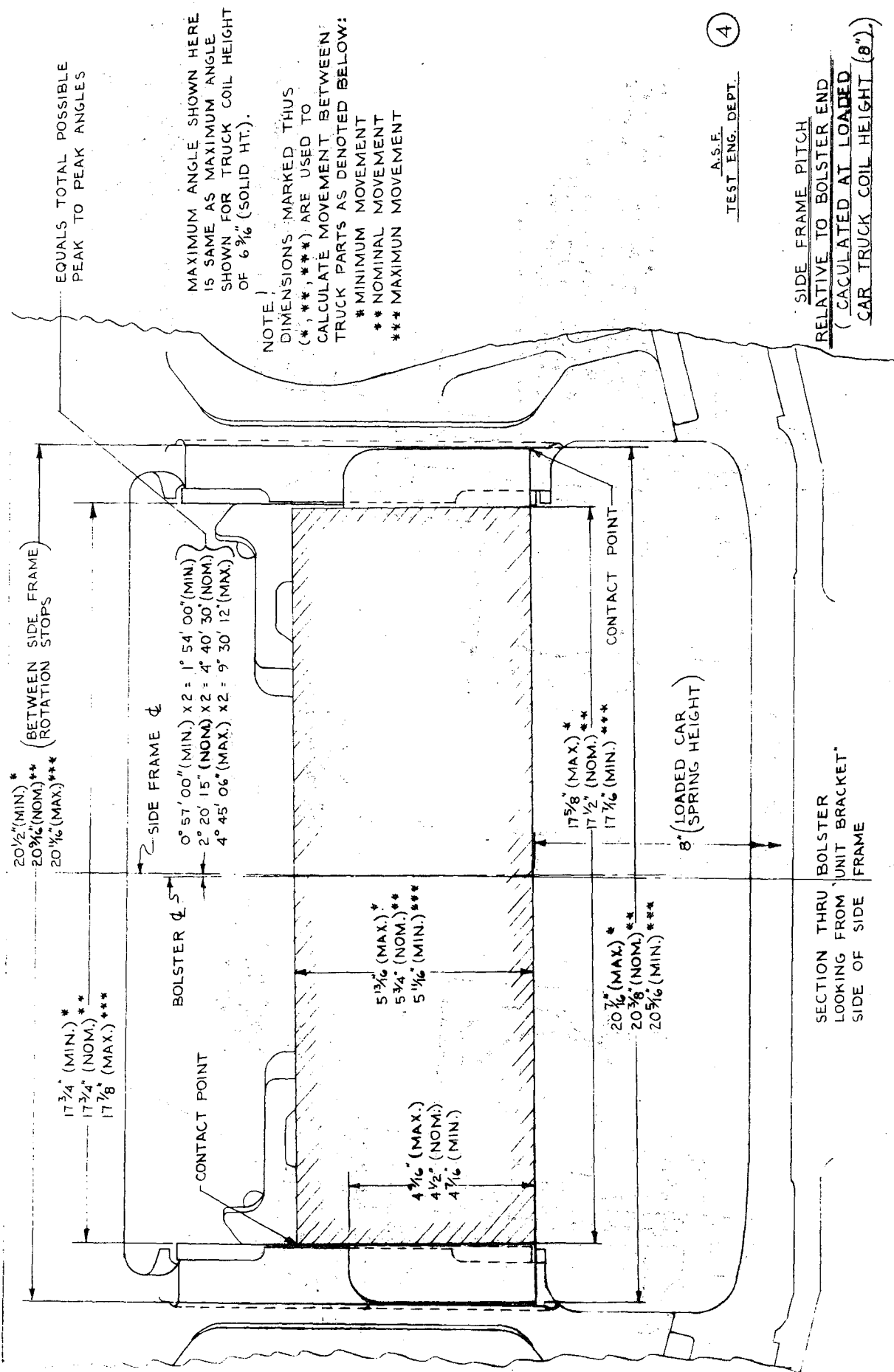
☉ CONTACT POINT

☉ SIDE FRAME LONGITUDINAL MOTION RELATIVE TO BOLSTER ENDS.

A.S.E.
TEST ENG. DEPT.

3

Fig. 50



EQUALS TOTAL POSSIBLE PEAK TO PEAK ANGLES

MAXIMUM ANGLE SHOWN HERE IS SAME AS MAXIMUM ANGLE SHOWN FOR TRUCK COIL HEIGHT OF 6 3/4" (SOLID HT.).

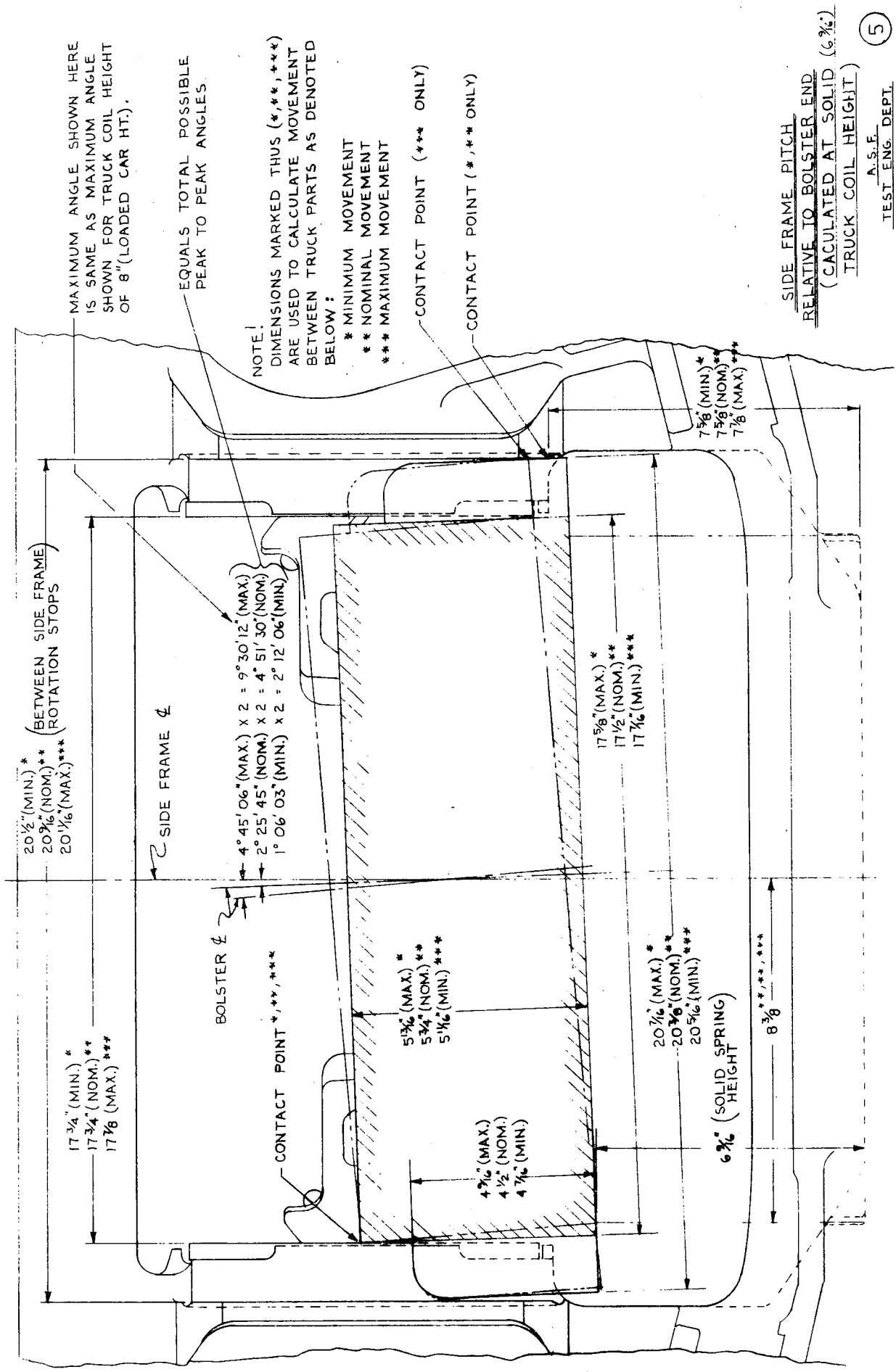
NOTE!
DIMENSIONS MARKED THUS (*, **, ***) ARE USED TO CALCULATE MOVEMENT BETWEEN TRUCK PARTS AS DENOTED BELOW:
* MINIMUM MOVEMENT
** NOMINAL MOVEMENT
*** MAXIMUM MOVEMENT

A.S.E.
TEST ENG. DEPT.
4

SIDE FRAME PITCH
RELATIVE TO BOLSTER END
(CALCULATED AT LOADED
CAR TRUCK COIL HEIGHT (8").

SECTION THRU BOLSTER
LOOKING FROM "UNIT BRACKET"
SIDE OF SIDE FRAME

Fig. 51



MAXIMUM ANGLE SHOWN HERE IS SAME AS MAXIMUM ANGLE SHOWN FOR TRUCK COIL HEIGHT OF 8" (LOADED CAR HT.).

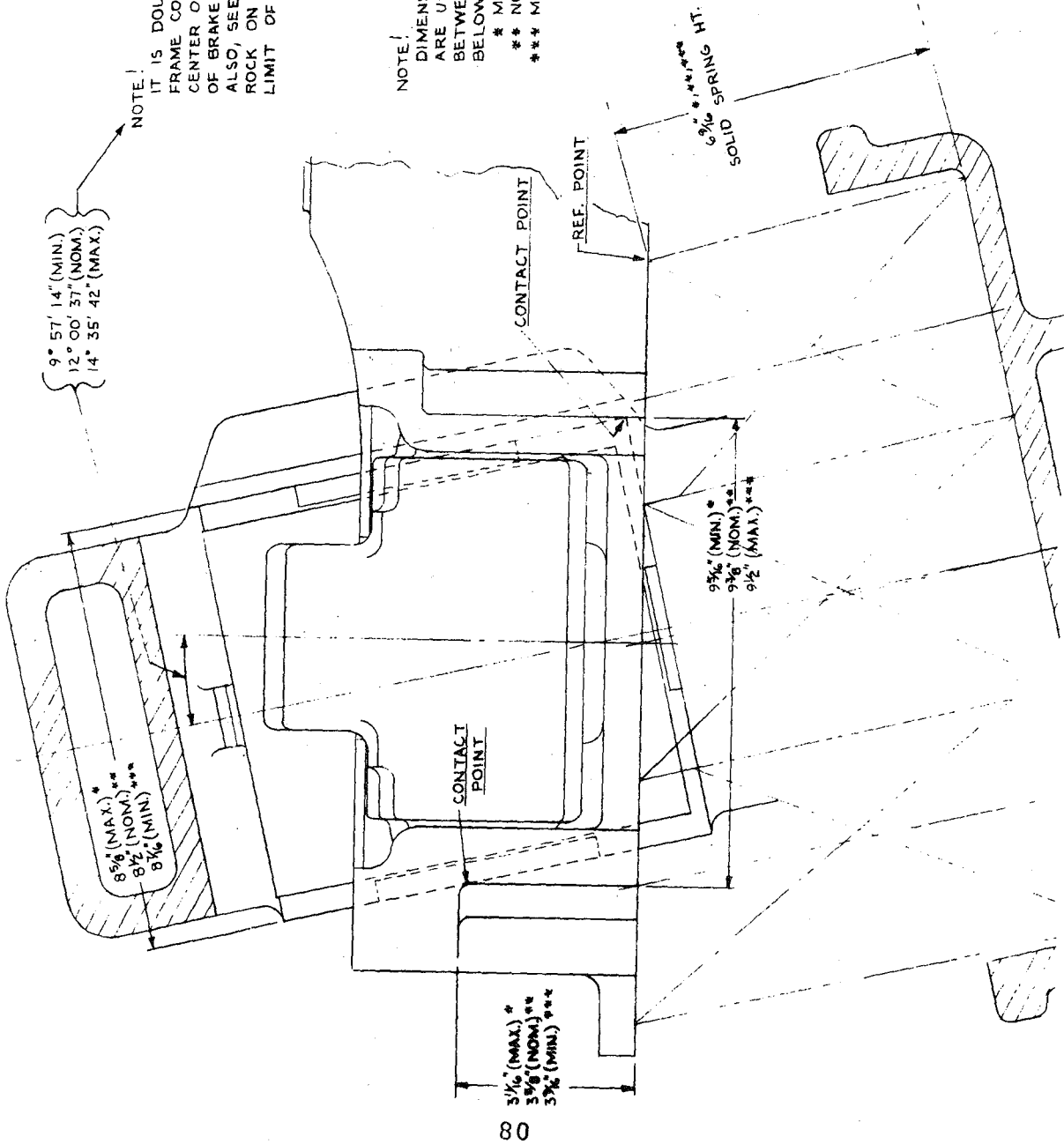
EQUALS TOTAL POSSIBLE PEAK TO PEAK ANGLES.

NOTE!
 DIMENSIONS MARKED THUS (*, **, ***) ARE USED TO CALCULATE MOVEMENT BETWEEN TRUCK PARTS AS DENOTED BELOW:
 * MINIMUM MOVEMENT
 ** NOMINAL MOVEMENT
 *** MAXIMUM MOVEMENT

CONTACT POINT (*** ONLY)

CONTACT POINT (*, ** ONLY)

Fig. 52



9° 57' 14" (MIN.)
 12° 00' 37" (NOM.)
 14° 35' 42" (MAX.)

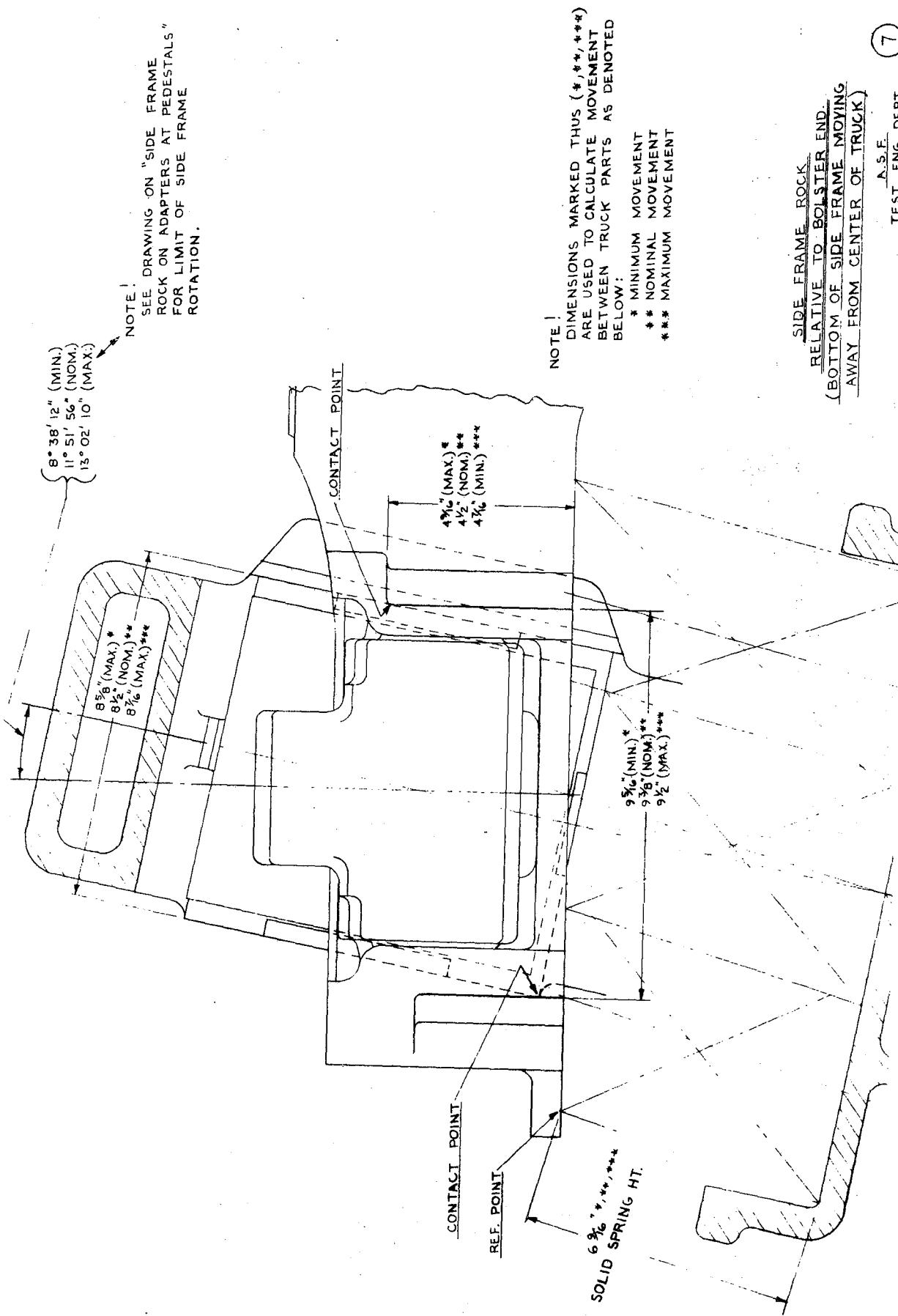
NOTE!
 IT IS DOUBTFUL THAT BOTTOM OF SIDE FRAME COULD BE ROTATED IN TOWARD CENTER OF TRUCK TO THIS DEGREE BECAUSE OF BRAKE BEAMS.
 ALSO, SEE DRAWING ON "SIDE FRAME ROCK ON ADAPTERS AT PEDESTALS" FOR LIMIT OF SIDE FRAME ROTATION.

NOTE!
 DIMENSIONS MARKED THUS (*,**,***) ARE USED TO CALCULATE MOVEMENT BETWEEN TRUCK PARTS AS DENOTE BELOW:
 * MINIMUM MOVEMENT
 ** NOMINAL MOVEMENT
 *** MAXIMUM MOVEMENT

SIDE FRAME ROCK
 RELATIVE TO BOLSTER END
 (BOTTOM OF SIDE FRAME MOVING
 IN TOWARD CENTER OF TRUCK)
 A.S.F.
 TEST ENG. DEPT.

6

Fig. 53



NOTE!
SEE DRAWING ON "SIDE FRAME
ROCK ON ADAPTERS AT PEDESTALS"
FOR LIMIT OF SIDE FRAME
ROTATION.

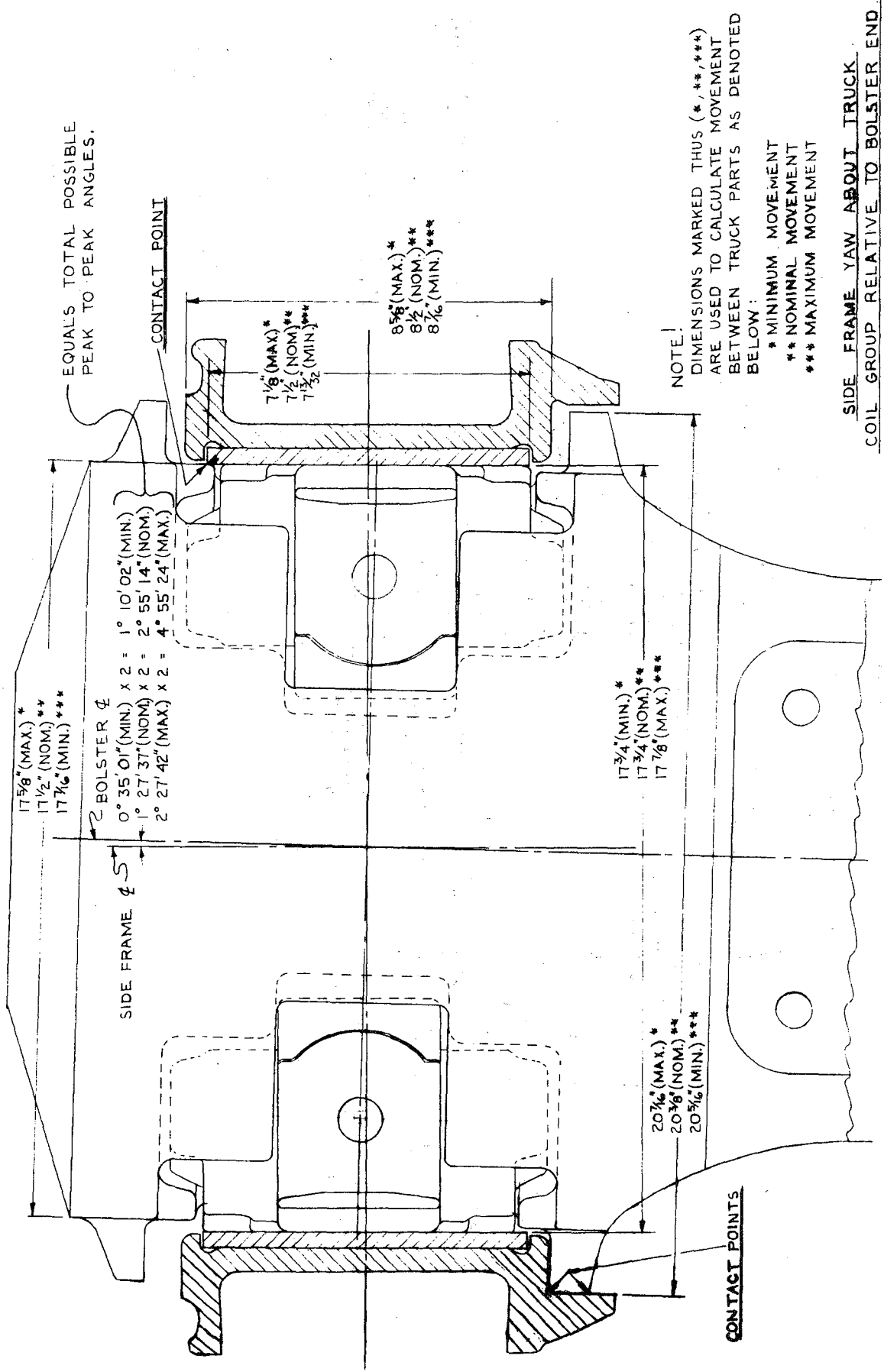
NOTE!
DIMENSIONS MARKED THUS (*,**,***)
ARE USED TO CALCULATE MOVEMENT
BETWEEN TRUCK PARTS AS DENOTED
BELOW:
* MINIMUM MOVEMENT
** NOMINAL MOVEMENT
*** MAXIMUM MOVEMENT

SIDE FRAME ROCK
RELATIVE TO BOLSTER END
(BOTTOM OF SIDE FRAME MOVING
AWAY FROM CENTER OF TRUCK)

7

A.S.F.
TEST ENG. DEPT.

Fig. 54



EQUALS TOTAL POSSIBLE PEAK TO PEAK ANGLES.

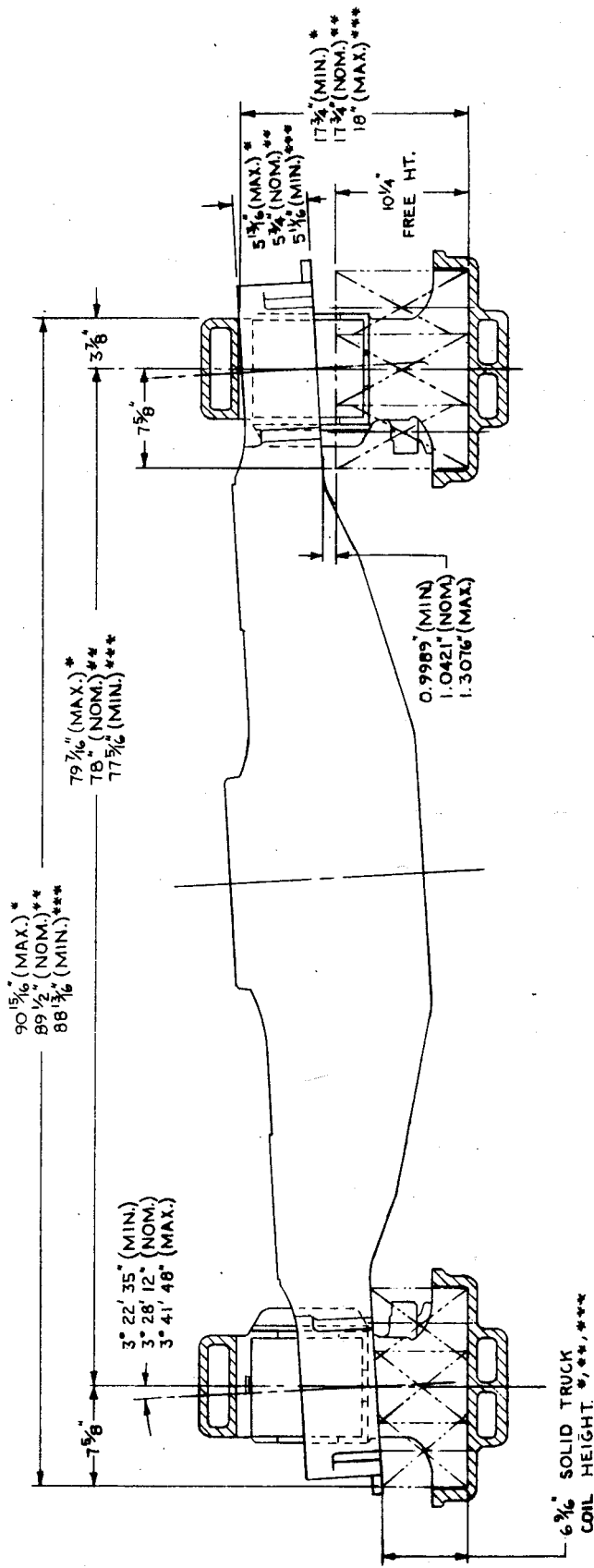
NOTE!
 DIMENSIONS MARKED THUS (*, **, ***) ARE USED TO CALCULATE MOVEMENT BETWEEN TRUCK PARTS AS DENOTED BELOW:
 * MINIMUM MOVEMENT
 ** NOMINAL MOVEMENT
 *** MAXIMUM MOVEMENT

SIDE FRAME YAW ABOUT TRUCK COIL GROUP RELATIVE TO BOLSTER END

8

A.S.E.
 TEST ENG. DEPT.

Fig. 55



NOTE:
 DIMENSIONS MARKED THUS (*, **, ***)
 ARE USED TO CALCULATE MOVEMENT
 BETWEEN TRUCK PARTS AS DENOTED
 BELOW:

- * MINIMUM MOVEMENT
- ** NOMINAL MOVEMENT
- *** MAXIMUM MOVEMENT

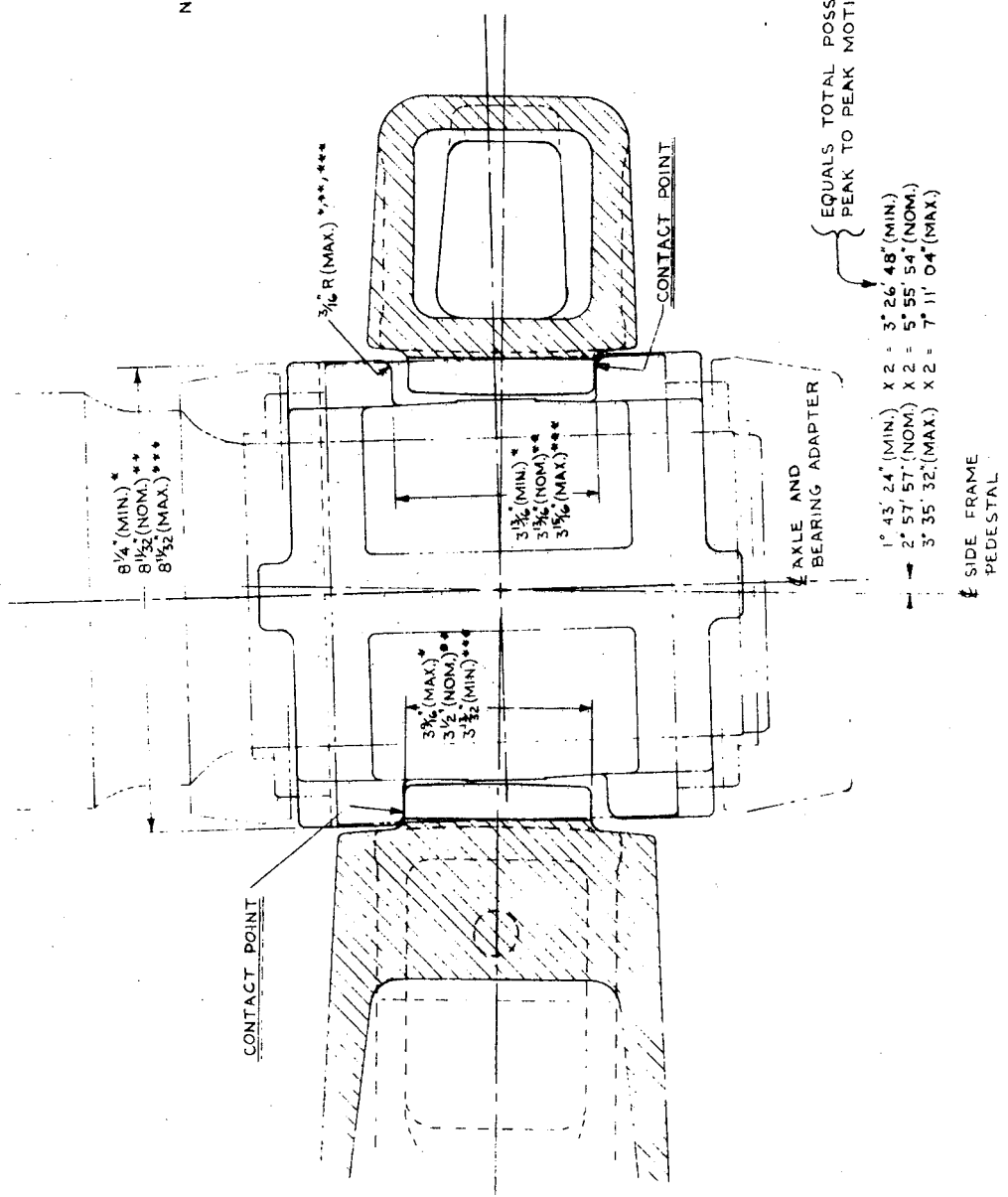
TRUCK BOLSTER ROCK
(ASSEMBLED TRUCK ON
LEVEL ROADBED)

A.S.F.
 TEST ENG. DEPT.

Fig. 56

NOTE!
 DIMENSIONS MARKED THUS (*, **, ***)
 ARE USED TO CALCULATE MOVEMENT
 BETWEEN TRUCK PARTS AS DENOTED
 BELOW:

* MINIMUM MOVEMENT
 ** NOMINAL MOVEMENT
 *** MAXIMUM MOVEMENT



AXLE YAW RELATIVE TO
 SIDE FRAME PEDESTAL

A.S.F.
 TEST ENG. DEPT.

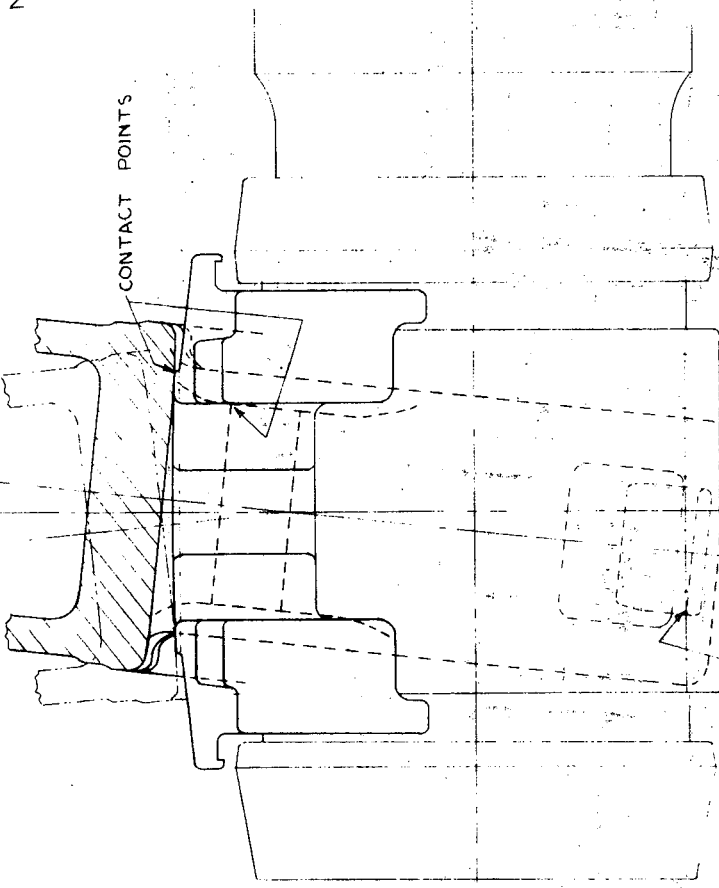
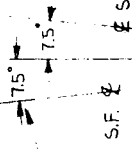
11

Fig. 58

NOTE!

IT IS DOUBTFUL THAT BOTTOM OF SIDE FRAME COULD BE ROTATED IN TOWARD CENTER OF TRUCK TO THIS DEGREE BECAUSE OF BRAKE BEAMS.

15° PEAK TO PEAK
(NEGLECTING BRAKE BEAMS)



CONTACT POINT WHERE TIP OF SIDE FRAME KEY HITS CONTOUR OF ROLLER BEARING CUP.

NOTE!
BECAUSE OF THE MANY CONTOURS OF TRUCK PARTS AT SIDE FRAME PEDESTALS, A FULL SIZE DRAWING WAS MADE USING NOMINAL DIMENSIONS (ONLY) TO FIND ANGLE OF ROCK.

SIDE FRAME ROCK ON ADAPTERS AT PEDESTALS

A.S.E.
TEST. ENG. DEPT.

12

Fig. 59

MASS MOMENT OF INERTIA OF SIDE
FRAME (YAW AND PITCH) AND TRUCK
BOLSTER (YAW AND ROCK)

Test Report - Part VI

American Steel Foundries Participation In
AAR/RPI/FRA Track-Train Dynamics Program

OBJECT

Determine, for the subject castings, the mass moments of inertia relative to the following axes through the respective centers of gravity.

1. Truck Bolster (with and without friction shoes).
 - a) Roll (Rock) axis.
 - b) Yaw axis.
2. Side Frame.
 - a) Pitch axis.
 - b) Yaw axis.

RECOMMENDATIONS

The following values are recommended for use as the mass moments of inertia for typical castings of the type tested.

1. Truck Bolster: Roll and Yaw axes,
178.6 lb-ft-sec²
(with friction shoes)
2. Side Frame: Pitch axis, 83.1 lb-ft-sec²
Yaw axis, 77.6 lb-ft-sec²

TEST SPECIMENS

1. Truck Bolster: Pattern No. 21732-DA
(6"x11"Ride Control)
Drawing No. 74455-B
Serial No. 1887
2. Side Frame: Pattern No. 21850-N
(6"x11"Ride Control)
Drawing No. 72965-H
Serial No. 1861

Original plan called for use of a Pattern No. 21850-R side frame, but the close similarity of the "N" and "R" patterns enabled convenient use of the "on-hand" "N" side frame.

TEST FIXTURE

To the exclusion of the tedious method of increment mass calculation, an experimental procedure was used for determining the desired inertial figures. This consisted of suspending the castings individually on a free pivot and treating the resulting system as a compound pendulum for application

of the following formulas.

Mass Moment of Inertia about

the pivot,

$$I_o = \frac{T^2 WL}{4 \pi^2} \quad \text{for small angles}$$

where: T = period of oscillation

W = weight of specimen.

L = distance from pivot to specimen center of gravity.

From the parallel axis theorem:

Mass Moment of Inertia about

specimen center of gravity,

$$I_{cg} = I_o - \frac{W}{g} L^2$$

with g taken as 32.2 ft/sec²

Figures 60 & 61 respectively illustrate test set-ups with the bolster specimen in the yaw orientation and the side frame in the pitch orientation. As seen, the free pivots consisted of two spherical rod ends (secured to the cross beam) through which a rod, appropriately oriented and welded to the specimen, was passed. This arrangement maintained the castings in the single plane of oscillation perpendicular to the desired inertial axis. Set-ups for attaining bolster roll and side frame yaw inertial specifics used rods welded to the opposite casting ends and perpendicular to the pivot rods illustrated. All pivot rods were affixed at a point corresponding to intersection with imaginary longitudinals through the specimens' centers of gravity.

TEST PROCEDURE

Period of pendulum swing, T, was obtained by angularly displacing the suspended castings and stopwatch timing the motion through a specific number of free cycles; the total time divided by number of cycles yielded T. A number of

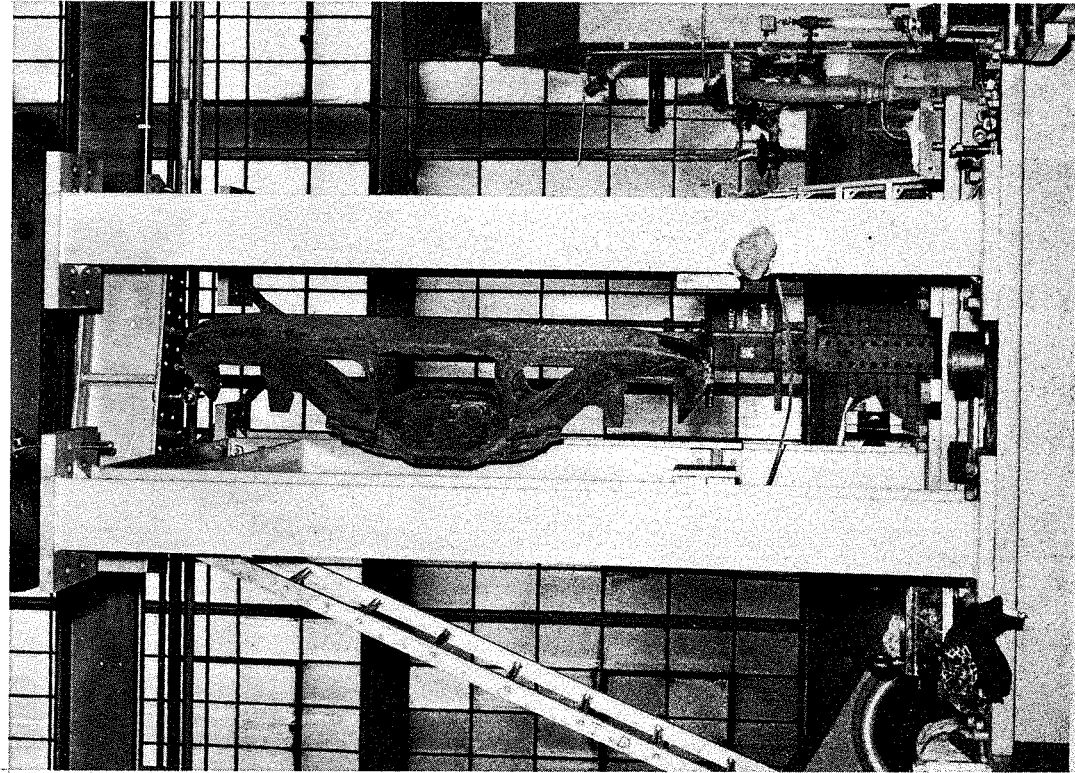


Fig. 61
SIDE FRAME IN PITCH TEST ORIENTATION

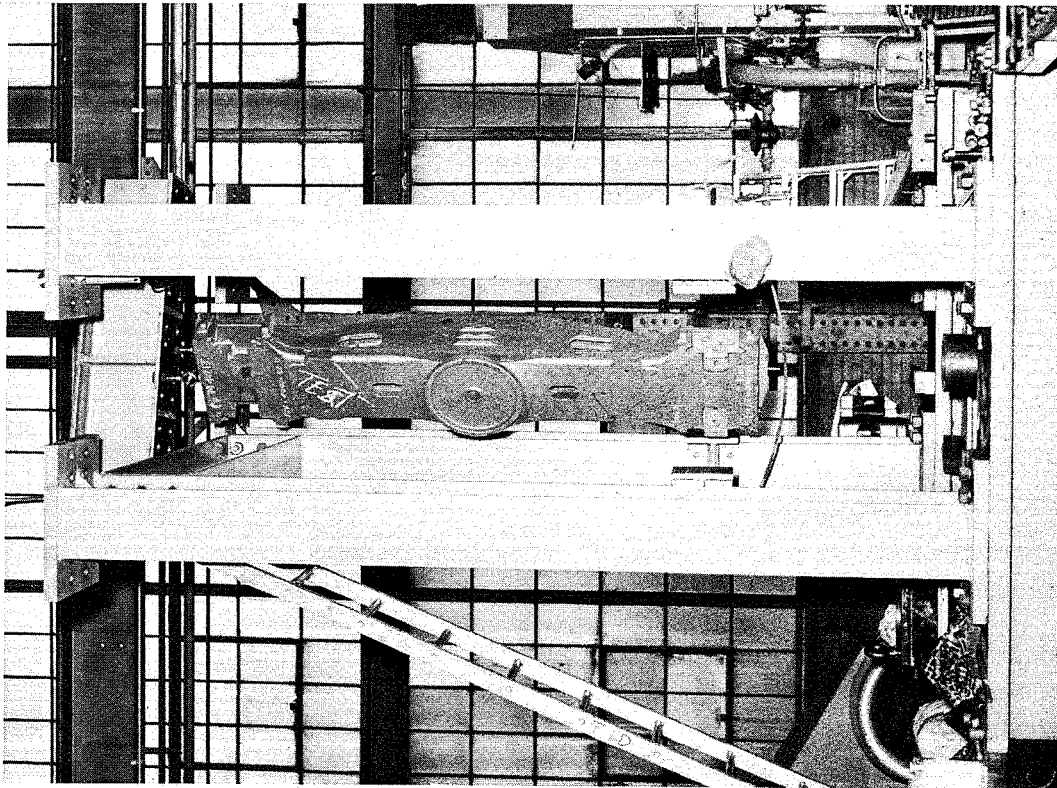


Fig. 60
BOLSTER IN YAW TEST ORIENTATION

initial angular displacements and cyclic counts were tried, but the excellent repeatability afforded by a 15° displacement for 20 cycles rendered this combination suitable for T input to the calculations. (Note that, despite use of the specified combination for formula application, T varied relatively little regardless of displacement or count utilized). The timing procedure was repeated three to five times for attainment of a good average T. Check of T sensitivity to relatively small changes in inertia was provided by testing the bolster with and without friction shoes as well as with various weights affixed at the centerplate.

Weight, W, of the test specimens was determined through simple scale weighing. Pendulum arms, L, were tape measured on the specific specimens and found agreeable with blue print dimensions.

Inertial determinations were made through simple application of the T, W and L figures to the previously noted formulas and, while nearly negligible, corrections were made to account for the small weights of the pivot pins.

RESULTS

The following table discloses the experimental determinations for the test weights indicated:

Test	<u>W(lb)</u>	<u>L(in)</u>	<u>T(sec)</u>	<u>I_o</u> (lb-ft-sec ²)	<u>I_{cg}</u> (lb-ft-sec ²)
<u>Bolster</u>					
<u>Roll axis</u>					
W.frict.shoes	1161*	46.5	2.533	723.5	185.8
W.O. " "	1089	46.5	2.508	664.7	160.6
<u>Yaw axis</u>					
W.frict.shoes	1157*	48.0	2.543	758.1	185.2
W.O. " "	1085	48.0	2.520	698.1	161.0
<u>Side Frame</u>					
<u>Pitch axis</u>	774*	41.625	2.354	373.2	85.5
<u>Yaw axis</u>	772*	43.75	2.360	397.6	79.7

Note: *Slight test weight variations due to differing pivot pin assemblies.

Friction shoe weight: 18 lb. per unit.

(The above I_{cg} values were approximated by assuming weight differential occurrence at the center of gravity only, which would have no effect on period of swing, and then multiplying the experimental values by ratio of desired weight to test weight).

Discussion with ASF manufacturing personnel derived that normal weight is a good figure by which to define a representative casting (weight variations are typically within 10-20 lb.). Hence, the listed I_{cg} (normal) values should be applicable to mathematical considerations of "typical" castings.

It was previously noted that an "N" pattern side frame was tested instead of the "R" pattern requested, but similarity of design and normal weight (758 lb. for the "R" and 752 lb. for the "N" pattern) make the inertial figures satisfactory for either.